

Analysis of a Multi-Aquifer System in the Southern Coastal Plain of Virginia by Trial
and Error Model Calibration to Observed Land Subsidence

Nathan David Roethlisberger

Thesis submitted to the faculty of the Virginia Polytechnic Institute and State University
in partial fulfillment of the requirements for the degree of

Master of Science
In
Geosciences

Thomas J. Burbey
David L. Nelms
Ryan Pollyea
Mark A. Widdowson

December 1, 2021
Blacksburg, VA

Keywords: land subsidence, groundwater modeling, relative sea-level rise, bore-hole
extensometer, aquifer-system, compaction

Copyright (CC-BY – ©)

Analysis of a Multi-Aquifer System in the Southern Coastal Plain of Virginia by Trial and Error Model Calibration to Observed Land Subsidence

Nathan David Roethlisberger

ABSTRACT

The Coastal Plain in the southern Chesapeake Bay area is becoming increasingly susceptible to nuisance flooding as a result of the combination of sea-level rise and land subsidence associated with aquifer compaction from excessive groundwater pumping. Detailed time-series of cumulative compaction data (land subsidence) from the three U.S. Geological Survey deployed extensometers in the regions, along with cyclical piezometer data, reflect the nature of the complex multi-aquifer/aquitard system in the Coastal Plain. Franklin, Virginia and Suffolk, Virginia extensometers were deactivated in 1995 and were reactivated in 2016 along with the addition of a high-sensitivity borehole extensometer in Nansemond, Virginia in collaboration with the Hampton Roads Sanitation District as a part of the Sustainable Water Initiative for Tomorrow (SWIFT). Yearly compaction rates estimated from the reactivated extensometers are -3.3 mm/year, 15.6 mm/year, and -20.7 mm/year in Franklin, Suffolk, and Nansemond, Virginia respectively. One-dimensional vertical compaction modeling is utilized to estimate the total compaction and differentiate which fine-grained confining units or aquifer interbeds are contributing most to total compaction historically and presently. Additionally, properties of the system can be estimated including the elastic specific storage of the aquitards and aquifers and the inelastic storage of the aquitards. The total cumulative change in aquifer system thickness estimated by the MODFLOW subsidence package can be compared to the observed total cumulative change in aquifer system thickness at each site for validation of hypothesis about the dynamics of the aquifer system to known changes in stress. Subsidence rates and aquifer/aquitard properties can be useful for managing and modeling the groundwater in the Coastal Plain of Virginia.

Analysis of a Multi-Aquifer System in the Southern Coastal Plain of Virginia by Trial and Error Model Calibration to Observed Land Subsidence

Nathan David Roethlisberger

GENERAL AUDIENCE ABSTRACT

The Coastal Plain in the southern Chesapeake Bay area is becoming increasingly susceptible to flooding at high tides in low lying areas as a result of the combination of sea-level rise and sinking of the land surface (land subsidence) associated with aquifer compaction from excessive groundwater pumping from buried aquifers. Detailed time-series of land subsidence data from the three U.S. Geological Survey deployed extensometers in the region, along with water level data from nearby wells, reflect the nature of the complex multi-aquifer/aquitard system in the Coastal Plain. Franklin, Virginia and Suffolk, Virginia extensometers were deactivated in 1995 and were reactivated in 2016 along with the addition of a high-sensitivity borehole extensometer in Nansemond, Virginia in collaboration with the Hampton Roads Sanitation District as a part of the Sustainable Water Initiative for Tomorrow (SWIFT). Yearly land subsidence rates estimated from the reactivated extensometers are -3.3 mm/year, 15.6 mm/year, and -20.7 mm/year in Franklin, Suffolk, and Nansemond, Virginia respectively. One-dimensional vertical compaction modeling is utilized to estimate the total sinking of the land surface as well as to differentiate which fine-grained confining units or aquifer interbeds are contributing most to total subsidence historically and presently. Additionally, properties of the system can be estimated including the elastic specific storage of the aquitards and aquifers and the inelastic storage of the aquitards. The total cumulative change in aquifer system thickness estimated by the MODFLOW subsidence package can be compared to the observed total cumulative change in aquifer system thickness at each site for validation of hypothesis about the dynamic changes of the aquifer system with known changes in stress. Subsidence rates, understanding the dynamics of the aquifer system, and aquifer/aquitard properties can be useful for managing groundwater and modeling the aquifer system in the Coastal Plain of Virginia.

Acknowledgments

Completion of this work took far longer than expected and the majority of the lessons learned through this work are beyond the science. I am so grateful for the path I was led into. Those who know me best know that it was Jesus who led me here, and while it is not what I had hoped to accomplish from the start, I find that I have received much more in the strain and obstacles than I imagined. A brief testimony of obstacles includes poverty, food scarcity, housing scarcity, addiction recovery, family issues, COVID-19 isolation, long-haul illness, other persistent illness, anxiety and depression, fear, anger and rebellion. All of these have been overcome not by my efforts, but by the steadfast love and goodness of God towards me. I was given what I did not deserve. When I was unacceptable, I found that He is with me and has made me acceptable. Instead of shame and condemnation, I am given a double portion and He is right in it. My joy and hope with Jesus is my greatest delight from these past three years. Whatever the work, I have to acknowledge and testify of what has happened. I could have finished on time and with ‘glorious’ results but I have received so much more. I am certainly a better modeler by the difficulty and the long hours of trial and error now having learned the effect of almost every variable and approach in simulating land subsidence in aquifer systems.

Tom Burbey has had a massive impact on my life with his patience, mercy, communication, challenges, and encouragement. I have been very blessed to get to know him over these three years and he has been a principally redemptive person in my life. I can truly say his guidance and peace gave me the encouragement to continue through the most difficult years of my life.

I also acknowledge the United States Geological Survey; particularly Dave Nelms, George Harlow, and Kurt McCoy for the opportunity to work with the data, for their kindness and friendship, and for answering any questions with their wealth of knowledge and experience. In addition, I thank Jason Pope, Randy McFarland, and Michelle Sneed, and Stan Leake for giving their time and experience while making sense of the puzzle in the Virginia Coastal Plain. I hope the underlying knowledge I have gained shows in the work. Of course, Richard Winston has been fundamental to figuring out ModelMuse and the CSUB package. Additionally, Scott Bruce at the DEQ was an enormous help in understanding data integrity, avoiding pulling just any water level data without scrutinizing the well construction.

Without Isaac and Audra Barnard I would not have had an adequate place to live or work down the stretch, much less a Juny to befriend and adore. I pray you know the constant blessing our friendship has been. I love you so much and hope to come around still for a good spar. Isaac, your obedience has saved my life and my heart. You know that I am not being dramatic.

Finally, my family deserves a special acknowledgement. Your love and support was a rock to me Mom, Dad, Drew, Bill, Josh. You have seen the fruit in my life because of your sacrifice and love for me. Thank you Steve Van Zandt, Andrew Brown, and Drew Roethlisberger for opening your home to me for a year that was expected to be a few months. David Anderegg, Patrick Lestyan, Josh Hirscher, Zach Kemp, and Bill Fagan, praise God for you! It has been long and hard but this time has been worth every moment! I hope to enjoy reading between these lines in the future and sharing my story shamelessly in the days to come. “Further up and further in.”

Table of Contents

List of Figures	vii
List of Tables	ix
1. Introduction	1
1.1 Key Terms.....	2
1.2 Purpose and Scope.....	3
1.3 Development of Groundwater and Land Subsidence in the Coastal Plain	6
1.4 Relative Sea-Level Rise.....	8
1.5 How Land Subsidence is Measured	9
2. Analytical Approach for Aquifer-System Storage and Compaction.....	12
2.1 Principle of Effective Stress and One-dimensional Vertical Compaction	17
2.1.1 Compressibility and Specific Storage	17
2.1.2 Delayed Drainage of Confining Units	21
2.2 Discussion of Assumptions.....	22
3. Hydrogeology	25
3.1 Previous Geological Work in the Virginia Coastal Plain	25
3.2 Hydrogeology of the Virginia Coastal Plain.....	26
3.3 Hydrogeologic Framework.....	28
3.3.1 Potomac Aquifer	30
3.3.2 Potomac Confining Zone	30
3.3.3 Upper Cenomanian Confining Unit	31
3.3.4 Virginia Beach Aquifer.....	31
3.3.5 Virginia Beach Confining Unit	31
3.3.6 Peedee Aquifer.....	32
3.3.7 Peedee Confining Zone	32
3.3.8 Aquia Aquifer	32
3.3.9 Nanjemoy-Marlboro Clay Confining Unit.....	32
3.3.10 Exmore Clast Confining Unit	33
3.3.11 Exmore Matrix Confining Unit	33
3.3.12 Chickahominy Confining Unit.....	33
3.3.13 Piney Point Aquifer	34
3.3.14 Calvert Confining Unit.....	34
3.3.15 Saint Mary’s Aquifer.....	34

3.3.16 Saint Mary’s Confining Unit	35
3.3.17 Yorktown-Eastover Aquifer	35
3.3.18 Yorktown Confining Unit.....	35
3.3.19 Columbia (Surficial) Aquifer	36
4. Measurements and Analysis of Hydrogeologic Data	37
4.1 Withdrawal Data	37
4.2 Hydraulic Head Data	40
4.3 Geophysical Log Data.....	42
4.4 Extensometer Design and Data.....	44
5. One-Dimensional Simulation of Compaction.....	63
5.1 Numerical Modeling of Aquifer-System Compaction	63
5.2 Modeling Approach.....	64
5.3 Model Input	68
5.4 Boundary Conditions.....	69
5.5 Nansemond Conceptualization	71
5.6 Suffolk Conceptualization	72
5.7 Model Simulation and Calibration	72
6. Discussion of Data and Model Results	78
6.1 Time Constant Uncertainty	78
6.2 Franklin Results	79
6.3 Nansemond Results	82
6.3.1 Analysis of Water-Level and Compaction Observations.....	87
6.3.2 Possible Consolidation of the Potomac Interbeds and Potomac Confining Zone	89
6.3.3 Time Constants and Constraining Vertical Hydraulic Conductivity	89
6.3.4 Coarse Elastic Compaction Overestimation and Model Limitations.....	91
6.4 Suffolk Results.....	92
6.4.1 Analysis of Water-Level and Compaction Observations.....	99
6.4.2 Hydrogeology and Stress History Differences.....	103
7. Conclusions	106
8. Bibliography	110

List of Figures

Figure 1. The study area within the Virginia Coastal Plain.....	5
Figure 2. A map of simulated drawdown in the Virginia Coastal Plain.....	7
Figure 3. A generalized borehole extensometer installation.....	11
Figure 4. The idealized relationship of stress and strain in an unconsolidated fine-grained bed .	24
Figure 5. Generalized geologic cross-section of southeastern Virginia	27
Figure 6. The hydrogeologic framework of the Virginia Coastal Plain	29
Figure 7. Withdrawal rates in the Virginia Coastal Plain from 1900 to 2008	38
Figure 8. The measured change in land surface elevation from 1940 to 1971	39
Figure 9. The synthetic interpolated stress data for the Nansemond model from 1900 to 2020 ..	49
Figure 10. The synthetic interpolated stress data for the Suffolk model from 1900 to 2020	49
Figure 11. The historic water levels of the Middle Potomac Aquifer in Franklin, VA	50
Figure 12. The daily average modern water levels within the surficial Columbia aquifer at the Nansemond site from 2018 to 2020 (USGS Well Identification 59D 40).....	51
Figure 13. The daily average modern water levels within the Piney Point aquifer at the Nansemond site from 2018 to 2020.....	52
Figure 14. Comparison between the stress history in the nested wells at Nansemond and the observed cumulative compaction in 2018.....	53
Figure 15. The daily average modern water level within the Potomac aquifer at the Nansemond site from 2018 to 2020	54
Figure 16. The interpolated modern water levels within the Columbia aquifer at the Suffolk site from 2018 to 2020.....	55
Figure 17. The interpolated modern water levels within the Piney Point aquifer at the Suffolk site from 2018 to 2020.....	56
Figure 18. The interpolated modern water levels within the Potomac aquifer at the Suffolk site from 2018 to 2020.....	57
Figure 19. The observed cumulative compaction at the Franklin and Suffolk sites from 1979 to 1995.....	58
Figure 20. The modern middle Potomac water level (55B 16) and observed cumulative compaction (55B 60) at Franklin, VA.	59
Figure 21. The observed cumulative compaction at the Nansemond site from 2018 to 2020.....	60
Figure 22. The observed cumulative compaction at the Suffolk extensometer site from 2018 to 2020.....	61
Figure 23. The measurement and construction of the borehole extensometer at Nansemond, Virginia	62
Figure 24. The one-dimensional vertical hydrogeology of the Nansemond extensometer site....	65

Figure 25. The one-dimensional vertical hydrogeology of the Suffolk extensometer site	66
Figure 26. The one-dimensional vertical hydrogeology of the Franklin extensometer site	67
Figure 27. A flowchart describing trial and error calibration of each model	77
Figure 28. Photographic evidence of land surface rebound at the Franklin extensometer site	81
Figure 29. Photographic evidence of land surface rebound with the weighted tensioner of the Franklin extensometer site	81
Figure 30. Simulated and observed cumulative compaction at Nansemond from 2018 to 2020.	84
Figure 31. Comparison of simulated compaction at Nansemond	85
Figure 32. The simulated vertical head profile at Nansemond through time.....	86
Figure 33. The simulated and observed cumulative compaction at Suffolk from 1982 to 1995..	95
Figure 34. The simulated and observed cumulative compaction at Suffolk from 2017 to 2020..	96
Figure 35. Comparison of simulated compaction at Suffolk	97
Figure 36. The simulated vertical head profile at Suffolk through time.....	98
Figure 37. A comparison between the Suffolk Piney Point aquifer water levels and the Nansemond Piney Point water levels.....	101
Figure 38. A comparison of the Piney Point aquifer stress history at Nansemond to the observed compaction record at Suffolk 20 kilometers away	102

List of Tables

Table 1. Withdrawals of groundwater for each major aquifer by 2009 in m ³ /d. Table is adapted from Heywood and Pope, 2009.	38
Table 2. Available well information for the Nansemond site. Wells that are not used in the model are denoted by (*) due to similarity in changes in stress while being located within the same aquifer model layer with the same simulated hydrogeologic properties as 59D 35. Wells used in the model are denoted by (+).	41
Table 3. Available well information for the Suffolk site. There is a lack of well data within a mile of the well over the given time frame. These distant wells are also included to predict compaction between the 1982 and 1995 to compare to the study of Pope and Burbey (2004) for additional information.	42
Table 4. The thicknesses of model hydrogeologic layers at Nansemond as determined from geophysical borehole logs. Layers denoted with (*) are layers with specified head.	43
Table 5. Table 5. The thicknesses of model hydrogeologic layers at Suffolk as determined from geophysical borehole logs. Layers denoted with (*) are layers with specified head.	44
Table 6. Initial parameter values for each layer of the Nansemond model. Initial parameter values for each layer of the Nansemond model. Vertical hydraulic conductivities (K' _v) are from McFarland and Bruce (2006), specific storage values are from the calibrated parameters from Pope and Burbey (2004), and the initial preconsolidation stresses are from predevelopment heads estimated by Heywood and Pope (2009).	68
Table 7. Initial parameter values for each layer of the Suffolk model. Vertical hydraulic conductivities (K' _v) are from McFarland and Bruce (2006), specific storage values are from the calibrated parameters from Pope and Burbey (2004), and the initial preconsolidation stresses are from predevelopment heads estimated by Heywood and Pope (2009).	69
Table 8. The final calibrated parameters for the Nansemond model.	82
Table 9. The expected ranges of parameter values at Nansemond from publications (*McFarland and Bruce, 2006) and (**Sneed, 2001).	83
Table 10. The simulated change in specific storage by the Nansemond model.	83
Table 11. The final calibrated parameters for the Suffolk model.	93
Table 12. The expected range of parameters for each Suffolk model layer as published by *McFarland and Bruce (2006) and **Sneed (2001).	94
Table 13. The simulated change in specific storage in the Suffolk model.	94

1. Introduction

Gradual land subsidence, or land surface lowering, is a well-documented occurrence throughout the world, including the United States (Bawden et al., 2012; Eggleston and Pope, 2013; Galloway et al., 1999; Herrera-García et al., 2021; Holdahl and Morrison, 1974; Tolman and Poland, 1940). Human activities are the cause for most land subsidence in the United States. Galloway et al. (1999) estimate up to 80 percent of land subsidence in the United States is due to groundwater withdrawal. Two extreme and deleterious examples of land subsidence in the United States include cases in Galveston and Houston, Texas and the Santa Clara Valley in California.

The Santa Clara Valley was the first region of the United States where land subsidence was attributed to excessive groundwater pumping (Tolman and Poland, 1940). Groundwater pumping in the valley resulted in a maximum subsidence of 4.3 meters between 1910 and 1995 in downtown San Jose (Galloway et al., 1999). Agricultural irrigation and urbanization led to 1.21 meters of land subsidence between 1912 and 1933. The valley is also where the first organized action was taken to effectively mitigate land subsidence by 1969 (Galloway et al., 1999). These mitigation efforts involved a combination of water importation and substantial reductions in groundwater pumping.

Fifty years of pumping caused as much as three meters of land subsidence due to major groundwater and oil extraction in Galveston, Texas. This resulted in increased coastal flooding and the loss of numerous homes to seawater encroachment (Bawden et al., 2012; Galloway et al., 1999; Poland, 1984). New water management practices in Texas have slowed subsidence along the shorelines (Bawden et al., 2012; Galloway et al., 1999).

This study examines the rates of land subsidence in the Southern Virginia Coastal Plain, a region that is generally not known for land subsidence due to the locally high amount of annual precipitation. Consequently, the rates of subsidence are not as great as those in Texas and the Santa Clara Valley. Similar anthropogenic causes of land subsidence are still important for the coastal plain due to its low topography and proximity to the coast making it susceptible to sea level rise (Eggleston and Pope, 2013). Subsidence is important in populated coastal regions

where relative sea-level rise and land subsidence from heavily pumped aquifers can result in infrastructure and ecological damage.

Groundwater withdrawal in the Virginia Coastal Plain was largely for agricultural purposes until the 1940s and increased rapidly in the latter decades of the 20th century when modern pumping technology became widely used with the onset of World War II. Industrial groundwater withdrawals increased from World War II resulting in cones of depression (drawdown) of as much as 60 meters in places by 2003 (Heywood and Pope, 2009).

1.1 Key Terms

This work is interdisciplinary with collaboration and interest from both geoscientists and engineers. For this reason, five terms are selected for clarification as suggested by Helm (1975) that may be interpreted differently by each discipline. These five terms are confining bed, aquitard, subsidence, consolidation, and compaction. These definitions were first referenced in Poland et al (1972) and are summarized here. Aquitard is used in this report to represent a fine-grained, low permeable compressible unit that exhibits largely vertical flow due to the large permeability difference between the aquitard and adjacent aquifer units. An aquitard can be a continuous unit (confining layer) or a thin discontinuous lens within an aquifer (interbed). A fine-grained interbed acts as a doubly draining layer when the adjacent aquifer undergoes a reduction in pore pressure due to pumping. A confining layer is areally extensive and creates a hydraulic obstruction between aquifers usually resulting in the aquifer having different hydraulic head values. Subsidence refers to the areal lowering of the land surface that includes subsurface compaction and consolidation of all material beneath the land surface. In saturated sediments, compaction is often referred to by engineers as one-dimensional consolidation (Helm, 1975). Compaction is used in this report to describe the decrease in thickness of sediment by an increase in vertical compressive stress that may or may not respond elastically to a decrease in vertical compressive stress. Herein, the word consolidation describes the final realignment of fine-grained material in a permanent or non-recoverable way while compaction can describe changes of thickness that are not permanent and may experience some recovery, particularly in coarse-grained units such as aquifers. The word ‘compaction’ is always associated with ‘recoverable’ and ‘non-recoverable’ storage to serve both disciplines.

1.2 Purpose and Scope

This study aims to characterize the historical and modern dynamics of the aquifer-system in the southern Coastal Plain of Virginia by numerical groundwater modeling. The investigation includes analysis of time-series observations of aquifer-system compaction and water level data at Suffolk, Franklin, and Nansemond, VA, over a period spanning the past 120 years. Analysis includes high precision subsidence measurements from extensometers and multiple observation wells at different vertical depths at three sites within the past 3 years. One-dimensional numerical modeling of aquifer system properties is possible by direct observation of aquifer system compaction. The purpose of the modeling effort is to gain greater understanding of the behavior of the complex layered aquifer system and to identify the units most responsible for land subsidence. Numerical modeling can provide temporal updated estimates of aquifer system properties that affect compaction and observed land subsidence for the region as hydraulic head values change over time. These properties include the inelastic and recoverable elastic specific storage of coarse-grained aquifers and the fine-grained confining and interbed units, as well as the vertical hydraulic conductivity of each layer. Importantly, analysis of the aquifer-system by numerical modeling is used to quantify and estimate the dynamics of the aquifer system by trial and error methods. Additionally, the depth location of where compaction is currently occurring within the vertical profile of the aquifer-system is estimated. These estimates and properties can be incorporated in future regional models for the coastal plain of Virginia for groundwater management decisions. Due to time constraints, one-dimensional modeling of aquifer-system parameters is only applied to the Nansemond and Suffolk extensometer locations, neglecting the Franklin extensometer record for a later analysis. Finally, this work aims to begin a foundation for estimating the aquifer-system response to projected injection by SWIFT. A goal for SWIFT includes raising the head pressures in the Potomac aquifer to mitigate land subsidence and salt-water intrusion caused by a reversal of the hydraulic gradient between land based aquifers and the Chesapeake Bay and Atlantic Ocean.

The study area of this research focuses on the southeastern section of the Virginia Coastal Plain (Figure 1). The Virginia Coastal Plain is the Eastern most physiographic province in the state of Virginia. The Virginia Coastal Plain province covers approximately 33,700 square kilometers between latitude 36° 30'' and 39° 00' N and longitude 75° 15' and 77° 30' W.

The Coastal Plain limits are constrained to the west by the north-south oriented Fall Line that divides it from the Piedmont province. The Atlantic Ocean and Chesapeake Bay bound the province to the east. The area for this report is focused more precisely on the southeastern part of the Coastal Plain of Virginia, which represents about 9,970 square kilometers within the 33,700 square kilometers of the greater Virginia Coastal Plain (Figure 1). This southeastern area of the Coastal Plain of Virginia is selected to match to preceding models created by the United States Geological Survey (USGS), Hamilton and Larsson (1988), and Pope and Burbey (2004). Subsidence by water level decrease is expected to be happening throughout the region; however, one-dimensional measurements of aquifer-system compaction are made only at these three sites equipped with borehole extensometers. Despite a lack of widespread regional aquifer-system compaction data, these three sites in Nansemond, Suffolk, and Franklin can be useful for understanding the entire southern coastal plain of Virginia. Compaction is occurring throughout the southern Virginia Coastal Plain due to overall declining groundwater levels in the region. Major urban centers are located to the west in Richmond and Fredericksburg areas and a collective Hampton Roads metropolitan area is located in the southeast. Hampton Roads is made up of 16 counties and cities, including Franklin, Hampton, Newport News, Poquoson, Portsmouth, Chesapeake, Virginia Beach, Williamsburg, and Suffolk. The counties outside the city areas are mostly comprised of rural cropland and forests with small intermittent towns. Residential areas are increasing adjacent to the larger urban centers and along waterfronts (McFarland and Bruce, 2006). The topography of the Coastal Plain is relatively flat and slopes gently toward the east. Major rivers, including the Potomac, Rappahannock, James, Appomattox, Blackwater, Meherrin, Nansemond, Elizabeth, Nottoway, Pamunkey, York, Piankatank, Mattaponi, and North Landing cut across the province and all drain to the Atlantic Ocean. The climate of the area is temperate and humid subtropical. Average annual precipitation is about 102 centimeters and there is heavy vegetation throughout the region with extensive wetland areas in the southeast.

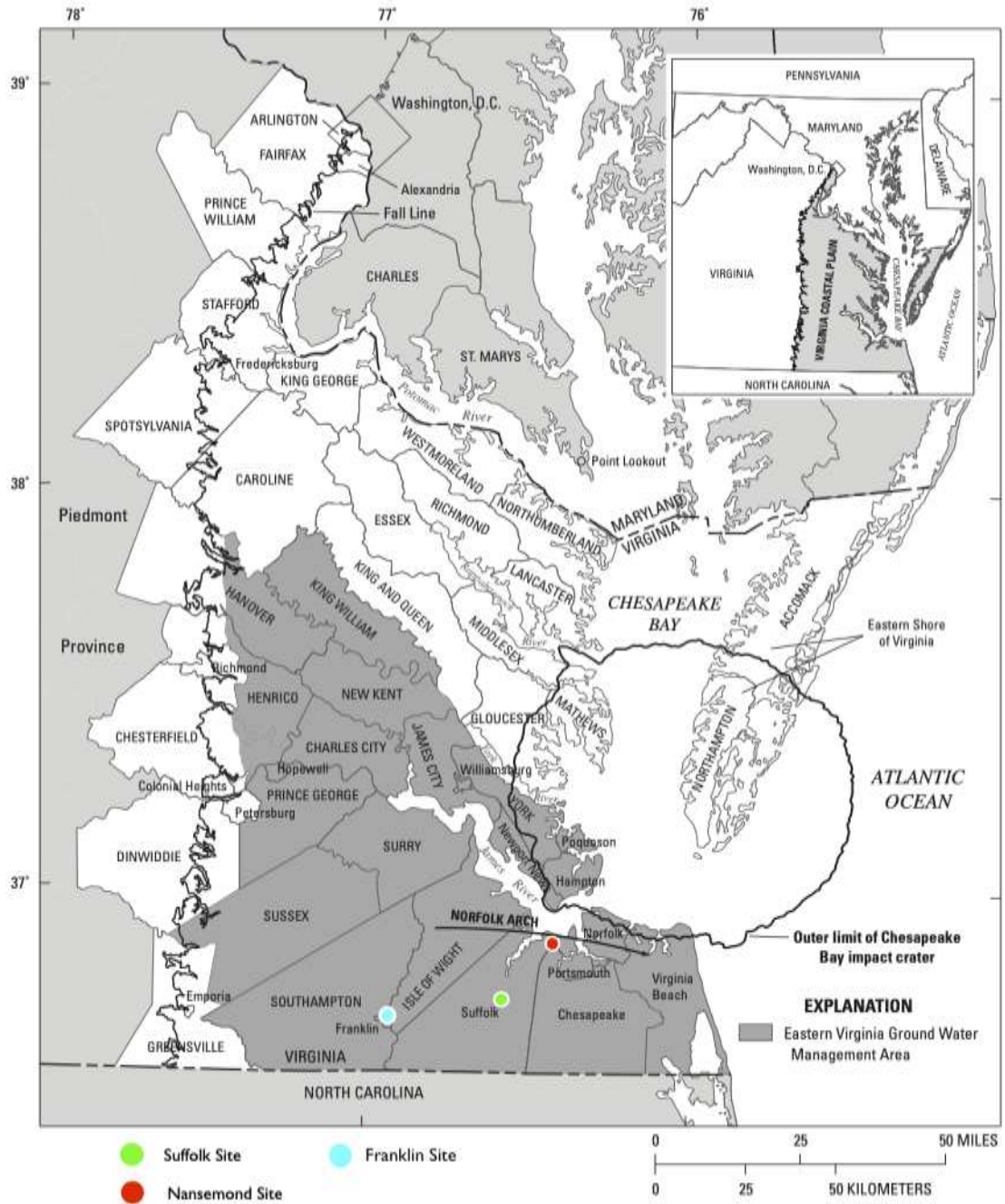


Figure 1. The study area within the Virginia Coastal Plain showing the Eastern Virginia Ground Water Management Area, the approximate location of the Chesapeake Bay impact crater, the Fall Line, the Norfolk Arch, and the two extensometer sites at Nansemond and Suffolk, Virginia. Modified from Heywood and Pope (2009).

1.3 Development of Groundwater and Land Subsidence in the Coastal Plain

In the late 1800's artesian hydraulic head conditions existed in the coastal plain. These conditions allowed for easily accessible groundwater for agriculture and industrial uses. Increased demand for groundwater led to the commencement of pumping in the early 1900's, which has been steadily increasing due to the growing population in the region. This population growth has seen increased pumping from industrial and residential centers to the extent that 7,770 square kilometers in Virginia were eventually protected in the Groundwater Act of 1973 as a Ground Water Management Area. With this designation, extraction of groundwater exceeding 1135 m³/month requires a permit (Hamilton and Larson, 1988).

Water levels in the Lower Potomac in the vicinity of Nansemond, VA, prior to pumping were about 12 to 13 meters above sea level (Hamilton and Larsson, 1988). By 1939, water levels in the Potomac were still close to 6 meters above sea level (Cederstrom, 1945b). Kull and Lacznik (1987) noted that rapid increases in industrial and municipal withdrawals began from Cretaceous aquifers (Potomac Aquifer) near Franklin in the early 1940s through the 1970s before the rate of withdrawal began leveling off. These withdrawals increased in industrial, municipal and agricultural withdrawals beyond Franklin and throughout the region at the same time.

Industrial groundwater withdrawals near Franklin, Virginia represent a major influence on the hydrogeology in the region. An increase in groundwater pumping rates from approximately 19,000 m³/day in the 1930's to almost 132,500 m³/day by the 1990's occurred in the region (Harsh and Lacznik, 1990). Long-term abstraction has now caused water levels to decrease by as much as 61 meters in certain withdrawal centers and as much as 355,800 m³/day has been reported (Hammond and Focazio, 1995; McFarland and Bruce, 2006). The large pumping rates in the area has resulted in two regional cones of depression, which have now migrated into North Carolina and into the northern Virginia Coastal Plain. These cones of depression are represented in Figure 2. The southern cone of depression around Franklin, VA extends towards Suffolk and Nansemond, VA. Additionally, the cone of depression has resulted in a change of flow gradients from a westward direction to an eastward direction, increasing the potential for saltwater intrusion (Harsh and Lacznik, 1990).

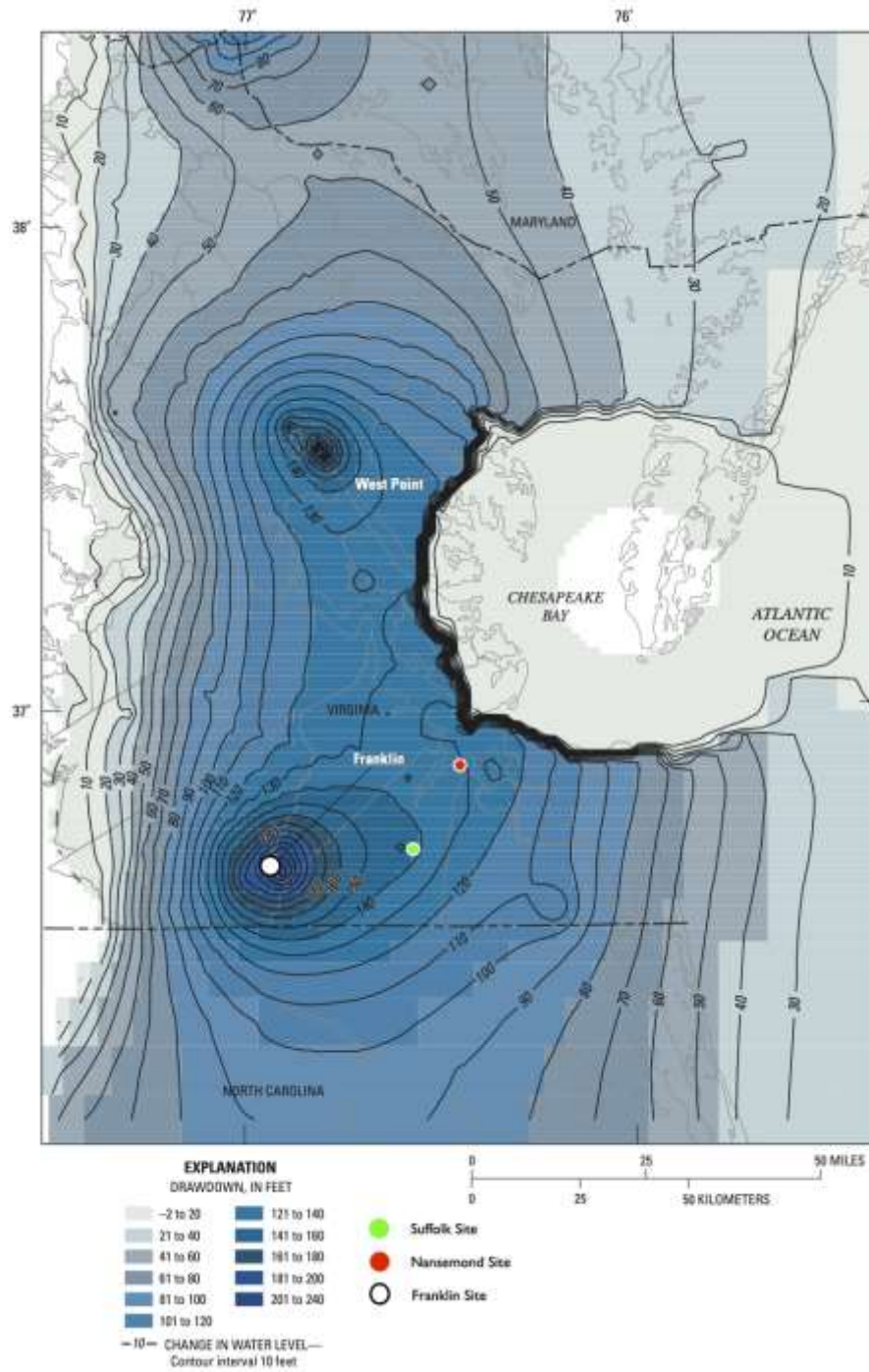


Figure 2. A map of simulated drawdown in the Virginia Coastal Plain modified from Heywood and Pope (2009). Two major cones of depression are identified by three-dimensional modeling of the Virginia Coastal Plain with drawdown data in numerous lateral locations. The cone of depression at Franklin is moving eastwards towards the Suffolk extensometer site.

1.4 Relative Sea-Level Rise

Land subsidence was identified in the Virginia Coastal Plain in the 1970s by a geodetic survey described by Holdahl and Morrison in 1974. These authors noted that relative land subsidence was occurring at an average rate of 2.8 mm/year along releveled lines in the Chesapeake Bay Area from 1940 to 1971. Two of the areas where the fastest rates of land subsidence occurred coincided with the two major industrial groundwater-pumping centers at Franklin and West Point.

Concern about land subsidence in these two areas led the USGS and Virginia Water Control Board to drill boreholes in Franklin, VA and Suffolk, VA in the late 1970s. These boreholes were equipped with pipe extensometers to measure the aquifer-system compaction component of land subsidence as a result of the extensive groundwater pumping in these regions. A forthcoming section of this report will describe in detail the mechanics and application of borehole extensometers as an accurate vertical subsidence-monitoring device. The borehole extensometers installed at Franklin and Suffolk measured and collected land subsidence data until they were decommissioned in 1995. Pope and Burbey (2004) used the time-series compaction records from these extensometers and analyzed the data with time-series observations of well-head data as a proxy for groundwater pumping in the region to determine annual compaction rates over a study-period from 1979 to 1995. Additionally, aquifer system properties were estimated using groundwater model calibration techniques. Pope and Burbey (2004) found that compaction rates from 1979 to 1995 averaged 1.5 mm/year in Franklin, while the Suffolk subsidence averaged 3.7 mm/year from 1982 to 1995. The total estimated compaction in the periods of record were 24.2 mm in Franklin and 50.2 mm in Suffolk. There was greater decline in water levels of the Potomac aquifer in the Suffolk area over the decade, measured at almost 5 meters in Suffolk as opposed to only 2 meters in Franklin (Eggleston and Pope, 2013; Pope and Burbey, 2004). These two borehole extensometers were deactivated in 1995 due to funding decisions.

Current attention regarding land subsidence has resulted in the commencement of the Sustainable Water Initiative For Tomorrow (SWIFT) project by the Hampton Roads Sanitation District in eastern Virginia to address environmental problems in the Chesapeake Bay region including restoration of the bay, sea level rise due to land subsidence, and saltwater intrusion

(Hampton Roads Sanitation District, n.d.). As a part of the SWIFT initiative, the borehole pipe extensometers in Franklin and Suffolk were recommissioned and outfitted with new digital potentiometers for greater precision in land surface change measurement in 2016. Additionally, another pipe extensometer was constructed in Nansemond, VA in close proximity to a test well that is injecting thousands of cubic meters of water a day into the Potomac Aquifer at the SWIFT Demonstration site. In addition to the water quality and bay restoration, the development of the injection well provides a unique opportunity to study the aquifer-system response to the pumping and injection of water at the Nansemond site.

1.5 How Land Subsidence is Measured

Land subsidence can be measured by several different types of instrumentation. Each are capable of achieving different spatial and temporal resolutions. These include, GPS (global position system), InSAR (interferometric synthetic aperture radar), Spirit leveling and borehole extensometers (Eggleston and Pope, 2013). Multiple reliable methods are often used together for a better understanding of how land subsidence is occurring. Locations and rates of land subsidence change with time and so repeatable measurements in different locations are useful for models to forecast future subsidence. The primary instrumentation used in this study is a borehole extensometer that is capable of measuring the continuous temporal changes of aquifer-system thickness from the land surface to the total depth of the extensometer pipe with sub-millimeter resolution.

The general function of a borehole extensometer is to measure one-dimensional vertical compaction or expansion of an aquifer system independent of other crustal or tectonic motions (Galloway et al., 1999). A general extensometer installation is shown in Figure 3. Changes of aquifer system thickness are measured between two points in a well, which are usually at the top and bottom of the aquifer system to determine the total aquifer system compaction. The extensometer pipe is a steel rod under tension that is ideally attached to the formation at its base as well as to a laterally anchored reference table at the surface. It is believed that the extensometers at Franklin and Suffolk are cemented into the bedrock but it is difficult to confirm. The extensometer at Nansemond is not cemented into bedrock but is instead balanced with a fulcrum and resting on the bedrock. The tension on an extensometer rod decreases friction between the extensometer pipe and the well casing it is enclosed in. A compaction recorder either digital

(potentiometer) or analog (steel-tape), can measure the small changes in thickness between the top of the extensometer and the bedrock. This effectively measures specifically the compaction of the mostly unconsolidated sediments of an aquifer system, independently of the movement of the bedrock beneath. Another method of using extensometers is to measure compaction over specific intervals within an aquifer system, such as a single aquifer in a layered aquifer system. The aquifer system compaction is often compared to surface subsidence monitoring to differentiate the portion of aquifer system compaction from total land subsidence (Poland, 1984).

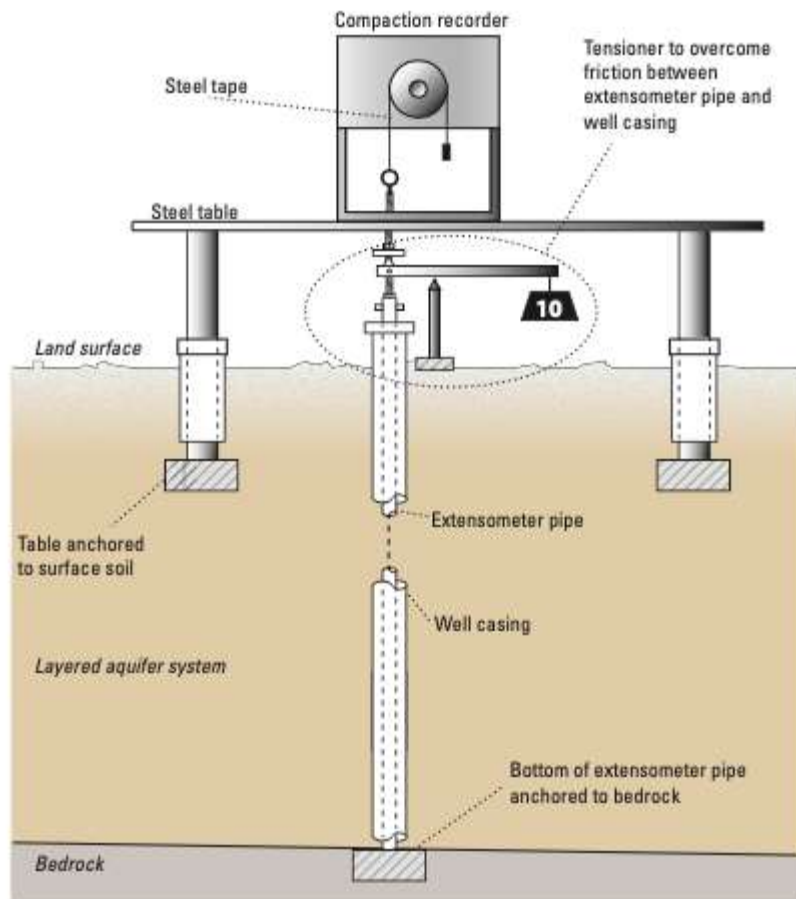


Figure 3. A generalized borehole extensometer installation (Eggleston and Pope, 2013).

2. Analytical Approach for Aquifer-System Storage and Compaction

Aquifer-system compaction from excessive groundwater withdrawal represents the key mechanism for land subsidence in this study. Terzaghi first described the aquifer drainage model in 1925 to describe the time-dependent nature of compaction through individual hydrogeologic units. This analytical modeling principle is described as a one-dimensional (vertical) process whereby decreased pore pressures cause an increase in effective (grain-to-grain stress) of the aquifer system. The loss of fluid (pore) pressure results in this increase in effective stress on the granular matrix or skeleton as it bears more of the weight of the material layers above it. This increase in stress on the aquifer-system skeleton matrix causes deformation through a decrease in porosity (loss in pore space), especially if that matrix is still unconsolidated or only partially consolidated. This deformation has been shown to occur in three dimensions, but the vertical deformation is generally significantly greater than the horizontal component and is much easier to measure. Practically, horizontal displacement can be a result of pumping and seasonal recharge or discharge stresses. These horizontal stresses are usually localized near the pumping wells, in the vicinity of heterogeneities, or at the margins of groundwater basins and result in little change in groundwater storage at regional scales (Hoffmann et al., 2003). In this investigation, the potential horizontal deformation is considered to be negligible and is therefore ignored. The total vertical compaction of the entire aquifer-system is typically equal to the land subsidence measured at the land surface.

The rate of compaction of an aquifer system undergoing a water-level decline is dependent on the compressibility and porosity of the materials, as well as the vertical hydraulic conductivity of the material undergoing deformation and thickness of each unit. The seasonal pattern of groundwater withdrawal can also be significant, resulting in seasonal changes in compaction and recovery. Hence, some compaction can be recoverable, especially in coarse-grained aquifer units, but most compaction is non-recoverable and results from slow, irreversible consolidation of finer grained confining layers or interbeds within an aquifer-system. This process of irreversible compaction is described by the aquitard drainage model, which has become a basis for much research in subsidence by aquifer system compaction (Galloway and Burbey, 2011; Galloway et al., 1999).

Terzaghi's (1948) understanding of the principle of effective stress began the basis of a theoretical relationship between groundwater levels and compaction. Terzaghi's principle of effective stress states that while total stress on an aquifer system does not vary the change in stress between grains in a material (effective stress) is related to the change in pore-fluid pressure (Sneed, 2001). This expression describes the vertical stress on a horizontal plane at any depth below land surface at equilibrium. The relationship is expressed as

$$\sigma_T = \sigma_e + P \quad (1)$$

where T is total stress of the geostatic load [N/m²],

e is the effective stress or the stress between grains [N/m²],

P is the pore-fluid stress [N/m²].

This equation makes seven important assumptions (Hanson, 1988):

1. The aquifer-system properties are homogeneous.
2. Drainage occurs at both horizontal boundaries of aquitards.
3. All flow is within the limits of Darcy's Law (laminar flow).
4. Water and soil grains are incompressible.
5. Compression and flow in fine grained layers are vertical and one-dimensional.
6. Compaction is small, and vertically averaged hydraulic conductivity, K'_v, and specific storage, S'_s, remain constant.
7. There is a hysteretic relationship between the change in void ratio and the change in effective stress, meaning that there is a non-linear stress-strain relationship between the void ratio and the change in effective stress.

Effective stress is the primary stress to consider in dealing with aquifer-system compaction and land subsidence. Helm (1975) rearranged Terzaghi's equation to solve for effective stress:

$$\sigma_e = \sigma_T - P \quad (2)$$

This equation shows more clearly that effective stress increases with increasing total stress (overburden) and/or by the removal of fluid that decreases the pore-fluid stress (Helm,

1975). Hanson (1988) provides a means of separating the different components of the stress terms that show that stresses must be considered differently when fluids are removed from confined or unconfined aquifers. The separated components are given by Hanson (1988) to be:

$$\sigma_T = \int_0^{z_w} S n p_w g dz + \int_{z_w}^z n p_w g dz + \int_0^{z_w} (1 - n) G p_w g dz \quad (3)$$

Where z_w is the depth to the water table from land surface [meters],

S is the degree of saturation above the water table [dimensionless],

n is the average porosity,

p_w is the density of water [kg/m^3],

z is the depth below land surface [meters],

and G is the specific gravity of solids in an aquifer system.

The three terms for the components of geostatic stress in a vertical column include the weight of the water above the water table, the weight of water below the water table, and the weight of the sediment (Hanson 1988). The pore water pressure contribution of effective stress that causes an outward buoyant force is given by Hanson (1988) as

$$P = - \int_{z_w}^z p_w g dz \quad (4)$$

Pore-fluid pressure can be expressed as an equivalent hydraulic head (h) if it is assumed that there is constant gravity and a uniform incompressible fluid. With typical conditions, a meter of water is equal to a pressure of 9780.8 Pascal (Sneed and Galloway, 2000):

$$h = \frac{P}{p_w g} \quad (5)$$

By this expression, change in hydraulic head is directly proportional to change in pore-fluid pressure. Other stresses are in terms of mass, length, and time as $\text{ML}^{-1}\text{T}^{-2}$ while hydraulic

head is in units of L (length). However, they are interchangeable with constant fluid density and gravity assumptions (Sneed and Galloway, 2000).

The rise and fall of the water level in an unconfined aquifer changes the gravitational stress as the water mass is removed or added and the pore-water stress (P) increases or decreases in the aquifer. The gravitational stress that is due to the mass of the overlying matter in a system referred to as the total stress (T) in this report. In an unconfined aquifer, a water table decline results in a decline in total stress, which would cause a decline in effective stress; however, the decline in the water table reduces pore pressure in the unconfined aquifer and leads to an increase in effective stress (Lofgren, 1968). The effective stress change in an unconfined system is expressed as a change in weight per unit area (Epstein, 1987):

$$\Delta\sigma_e = \Delta w = \Delta h(\gamma_m - \gamma_b) \quad (6)$$

Where Δh is the change in water table height [meters],

γ_m is the unsaturated unit weight of sediment above depth z ,

γ_b is the buoyant unit weight of sediments above depth z .

The resulting increase in effective stress in an unconfined system can cause elastic or recoverable compaction but it may also result in a small amount of non-recoverable compaction in fine-grained interbeds within the unconfined system. The discussion of stress in an unconfined system is small enough to be considered negligible and is included here for completeness. This study involves an analysis of the stress changes over time in the confined units of the Southern Virginia Coastal Plain.

Changes in effective stress are almost certainly proportional to changes in fluid pressure variations in a confined aquifer. Lowering hydraulic head in a confined aquifer system does not change total (gravitational) stress because lowering head does not result in dewatering of the aquifer. Effective stress is inversely proportional to pore water pressure (Helm, 1975; Poland et al., 1972). Total stress on the system is unchanged so stress migrates to the skeleton of the grains from the water in the pores as pore pressure is reduced. This can be expressed by:

$$\Delta\sigma_e = -\Delta P \quad (7)$$

The increase of effective stress in an aquifer physically results in compaction of the sediment with small reductions in porosity as the skeleton of the grains gets compressed and rearranged. The individual grains are negligibly compressed in comparison to the compression of the grains together as a granular skeleton (Helm, 1975). Compaction in an aquifer will respond almost instantly to decline in fluid pressure and may recover rapidly with an increase in fluid pressure. Additionally, this compaction of a coarse-grained aquifer is normally comparatively small because coarse, angular sediment grains cannot be put in more compact arrangements (Poland et al., 1972).

In fine-grained confining beds or aquitards adjacent to an aquifer experiencing a head decline, the pore water stress decrease and the subsequent effective stress increase is dissipated slowly from the fine-grained unit outward toward the adjacent coarse grained unit (Hanson, 1989). Pore fluid pressure equilibrates in a confining unit or aquitard as quickly as water can diffuse from the unit, which is dependent on its vertical hydraulic conductivity (Lofgren 1968). Fine-grained units have a low vertical hydraulic conductivity and comparatively high specific storage that causes the vertical leakage of water and subsequent lowering of pore pressures to be slower than the response of pore pressures in the adjacent aquifer but also yields greater potential compaction than the adjacent aquifers (Poland et al., 1972). It follows that the compaction of these fine-grained beds will only occur as the pore pressures in the fine-grained units decline towards the pore pressures in the aquifer (Poland et al., 1972). The majority of the compaction that ensues in fine-grained beds is irrecoverable due to the irreversible rearrangement of clay particles (Lofgren, 1968). This rearrangement of the grains in clay-dominated units is important in relation to their typically higher porosities and explains why the majority of compaction in an aquifer system occurs in these fine-grained units (Lofgren, 1968).

2.1 Principle of Effective Stress and One-dimensional Vertical Compaction

2.1.1 Compressibility and Specific Storage

The relation between head decrease (stress) and compaction (strain) is important in understanding aquifer system compaction. Jacob (1940, 1950) and Cooper (1966) suggest that the specific storage of a geological unit is best quantified by the ratio of strain over stress. More completely, specific storage represents the quantity of water per unit volume of a saturated aquifer or aquitard that is stored or released from storage due to the compressibility of the granular skeleton and pore water per unit change in head (Fetter, 2018). The expression is:

$$S_s = \rho_w g (\alpha + n\beta) \quad (8)$$

Where ρ_w is the density of water [kg/m^3],

g is the acceleration due to gravity [m/s^2]

α is the compressibility of the aquifer matrix [m^2/N],

n is the porosity [dimensionless],

β is the compressibility of water [m^2/N].

The compressibility of water (β) is assumed to be negligible in comparison to compressibility of an aquifer matrix (α) in the unconsolidated to semi-consolidated aquifer systems and the specific storage equation above can be simplified to:

$$S_{sk}^* = -\alpha \rho_w g \quad (9)$$

S_{sk}^* is the portion of the specific storage that is a result of the expansion or compression of the granular aquifer skeleton, referred to as the skeletal specific storage (Sneed and Galloway, 2000). An asterisk designates that this is the total specific storage of the overall aquifer system, both aquifers and confining units. The compressibility of the aquifer matrix is the key term that

relates stress and strain. The coefficient of compressibility (α) is the empirical relation between a change of (pore) space and a change in effective stress (Hanson, 1988).

$$\alpha^* = \frac{-\Delta e}{-\Delta\sigma_e} \quad (10)$$

In this relationship, e is the average void ratio or the volume of pore space per volume of solids. When deformation is considered to be vertical as in an aquifer or a confining unit the loss of void space can be rewritten in terms of thickness. The resulting expression is given by Helm (1975) to be the relation between vertical strain and the change in the average void ratio (e):

$$\frac{\Delta b}{b_0} = \frac{-\Delta e}{1+e} \quad (11)$$

Where Δb is the vertical compaction [L],

b is the initial layer unit thickness [L],

$\frac{\Delta b}{b_0}$ is the mean vertical strain, and

Δe is the average change in void ratio in the vertical direction.

The expression of change in vertical thickness and void space is important because the change in vertical thickness is the strain that is measured. As previously shown, change in effective stress can be represented as the change in pore pressure, expressed as hydraulic head. The result of having two measurable parameters to characterize the stress and strain relationship is the expression developed by Hanson (1988) with strain and stress in terms of specific storage:

$$S^*_{sk} = \rho g \frac{\frac{\Delta b}{b_0}}{\Delta\sigma_e} \quad (12)$$

There is a major distinction in the difference in the behavior of the coarse-grained aquifer material and of the fine-grained confining unit or interbed material. This distinction is necessary for a complete understanding of how an aquifer system behaves. A basis for most subsidence research is the recognition that there is a short-term, recoverable, elastic response of coarse-

grained aquifer material and a delayed, non-recoverable, inelastic response of fine-grained confining or interbed material (Sneed and Galloway, 2000).

When the stress on an aquifer system is less than the past maximum stress it has previously experienced the system will respond to any changes in water level by compaction or expansion elastically and almost instantaneously. Another way to observe this conditional response of the system is that groundwater levels are higher than the past maximum stress level, or previous known drawdown. The past maximum stress is also termed as the preconsolidation stress. If the stress on the aquifer system is greater than the past maximum stress the system will experience inelastic compaction that is non-recoverable and often of greater magnitude. This concept is expressed by representing the skeletal specific storage as recoverable and non-recoverable components, or S_{ske} and S_{skv} respectfully. Sneed and Galloway (2000) expresses the elastic and inelastic skeletal specific storage components of the skeletal specific storage as:

$$S^*_{sk} = \{S^*_{ske} = \alpha^*_{ke}\rho g \text{ when } \sigma_e < \sigma_{e(max)}, S^*_{skv} = \alpha^*_{kv}\rho g \text{ when } \sigma_e > \sigma_{e(max)}\} \quad (13)$$

Where an ‘e’ subscript describes the recoverable or elastic component and a ‘v’ subscript describes the non-recoverable or inelastic, which is sometimes referred to as the virgin compressibility. The asterisk (*) again indicates that these specific storage values are averaged across the total aquifer system. The distinction between the fine-grained confining beds or interbeds and the coarse-grained aquifers indicates that the response of the two different layer types should be characterized separately. Specific storage of a confining bed or interbed is given by Sneed and Galloway (2000) to be:

$$S'_{sk} = \{S'_{ske} = \alpha'_{ke}\rho g \text{ when } \sigma_e < \sigma_{e(max)}, S'_{skv} = \alpha'_{kv}\rho g \text{ when } \sigma_e > \sigma_{e(max)}\} \quad (14)$$

The notation to express parameter values for confining units or interbeds is typically a prime (‘). Thus, α' is the compressibility of a fine-grained confining bed or interbed only. For stress on a confining bed that is less than the past maximum stress (ground water levels are higher than the preconsolidation stress) the water released from storage (S'_{ske}) comes from the recoverable strain of the fine-grained skeleton by the reduction of pore pressure (Sneed and Galloway, 2000). When the stress is greater than past maximum stress levels (ground water

levels are below the preconsolidation stress) the water released from storage (S'_{skv}) comes from non-recoverable deformation of the fine-grained skeleton because of rearrangement and reorientation of clay particles. The non-recoverable component of skeletal specific storage (S'_{skv}) was found by Hanson (1988) to be thirty to several hundred times larger than the elastic component of skeletal specific storage in a typical aquifer system of unconsolidated to consolidated sediments. For this reason, the non-recoverable component of skeletal specific storage is the primary contributor to compaction of an aquifer system with severe drawdowns beyond the preconsolidation stress.

The specific storage of an aquifer (S_{sk}) is indicated by the absence of a prime (‘) that is associated with fine-grained parameters. Inelastic specific skeletal compressibility is negligible in aquifers and (α_{kv}) approaches zero because there is negligible reorientation of the grains in aquifer units. Skeletal specific storage of aquifer units can be expressed as the recoverable component of specific storage (Sneed and Galloway, 2000):

$$S_{sk} = S_{ke} = \alpha_{ke}\rho g \quad (15)$$

The elastic component of skeletal specific storage, S_{ke} , is usually an order of magnitude smaller than the elastic skeletal specific storage in a confining bed, S'_{ske} (Hanson, 1988). Once again, the greater non-recoverable compaction of fine-grained confining units and interbeds primarily contributes to the overall compaction of the aquifer system with drawdown due to excessive pumping. While coarse-grained aquifer units have small and noticeable elastic compaction they do not usually have significant permanent compaction. For this reason, the study of aquifer system compaction primarily includes study of strain in fine-grained confining units and interbeds as they encounter changes in stress.

The empirical relation of strain and stress in a confining or interbed unit for this study draws from the laboratory consolidometer tests on confining units from Helm (1975). The idealized stress and strain behavior of a compacting fine-grained aquitard or confining unit is provided graphically in Figure 4, (adapted from Helm, 1975). When a confining unit undergoes a change in stress (drawdown) that is greater than its preconsolidation stress, a non-recoverable compaction or strain is the result along the curve from (A) to (B). A recovery of the water levels

will decrease stress, causing the strain to decrease along the curve from (B) to (C) and a subsequent expansion of void space (S'_{ske}). Pore fluid stress changes from point (C) that are less than what was previously experienced results in re-compaction along the dashed line labeled (1) from (C) to (B). The compaction that occurs within this range of stresses can be reversible and expansion can occur in the confining unit or aquitard (Helm, 1975; Riley, 1969). Additional non-recoverable compaction will occur when the stress exceeds point (B) again until the fine-grained material is consolidated.

It is important to note that S'_{skv} and S'_{ske} are not constant. The compressibility and S'_{sk} values at any exact stress or water level are given by the slope of the tangent to the compaction curve at that particular point (Helm, 1975). The dashed lines from (A) to (B) and (C) to (B) in Figure 3 are the mean compaction and storage values over the range of stresses. These linear approximations are used because the actual values of compressibility and S'_{sk} are not usually measured in the field. The linear approximations are reasonably accurate under the range of stress and strain that are typically found in compacting aquifer systems (Hanson, 1988).

2.1.2 Delayed Drainage of Confining Units

The theory of hydrodynamic consolidation, or delayed drainage of confining units, is a part of Terzaghi's (1925) aquitard drainage model. The aquitard drainage model describes the delayed drainage of an aquitard when hydraulic heads are lowered in adjacent aquifers while compaction continues within the slowly draining aquitards and fine-grained interbeds long after heads in the aquifers have been lowered (Sneed and Galloway, 2000). A one-dimensional diffusion equation for groundwater flow describes the drainage process:

$$\frac{d^2h}{dz^2} = \left(\frac{S'_{sk}}{K'_v}\right) \frac{dh}{dt} \quad (16)$$

K'_v is the vertical hydraulic conductivity of the fine-grained confining unit or interbed and the ratio $\frac{S'_{sk}}{K'_v}$ is the inverse of the hydraulic diffusivity (K'_v/S'_{sk}) of the aquitard. The equilibrium of pore-pressure stress (hydraulic head) is almost instantaneous in an aquifer but pressure diffusion occurs slowly in the fine-grained units. Riley (1969) finds that the time constant (τ) for compaction of a doubly draining aquitard after an instant change in step-load is defined as:

$$\tau = \frac{S'_{skv}(\frac{b_0}{2})^2}{K'_v} \quad (17)$$

The time constant is the time for an aquitard to reach 93 percent of the ultimate compaction following a step increase in applied load (Sneed and Galloway, 2000). This step increase in applied load is described by Sneed and Galloway (2000) as the instantaneous step decrease in hydraulic head in adjacent aquifer units and is related to the volume of water that has to flow out of the aquitard to produce consolidation as well as the impedance to the flow of that water. This expression defines the time for the fine-grained unit to reach equilibrium and varies directly with the specific storage and the square of the half-thickness (mid-plane) of the confining unit and inversely with the vertical hydraulic conductivity of the fine-grained unit (Riley, 1969). As an example of time constants for this study on the Virginia Coastal Plain, Helm (1975) simulated compaction at 15 extensometer sites in the Santa Clara and San Joaquin Valleys while Ireland and others (1984) estimated that time constants of the fine-grained units varied from 5 to 1,350 years, and averaging 159 years. The concept of hydrodynamic consolidation describes both the time-dependence of stress in a fine-grained confining unit or interbed and of its strain response to that stress, often referred to as the residual compaction. The term for the fine-grained interbeds where the time constant is much greater than the time steps used in a simulation is ‘delay beds’ (Hoffman and others, 2003).

2.2 Discussion of Assumptions

The theory of hydrodynamic consolidation and the aquitard drainage model are based on the important assumption that there is only vertical strain. This assumption has been the subject of study and consideration since Jacob (1940) definition of the storage coefficient assumed that volume reduction from compaction is only in the vertical direction. Burbey (2001) describes how assuming only vertical strain is known to be invalid in some situations and can result in an overestimation of vertical strain. Horizontal displacement is often neglected because it is thought to be small in many investigations but it may prove to be significant, particularly in conditions with regions of large radial flow to a pumping center (Burbey, 2001).

Additionally, the equations governing only vertical compaction are simpler and more manageable for numerical computation and field measurements. For ease of numerical

computation and field measurements, the assumption of purely vertical strain is assumed in this study though the limitations of this assumption should be noted.

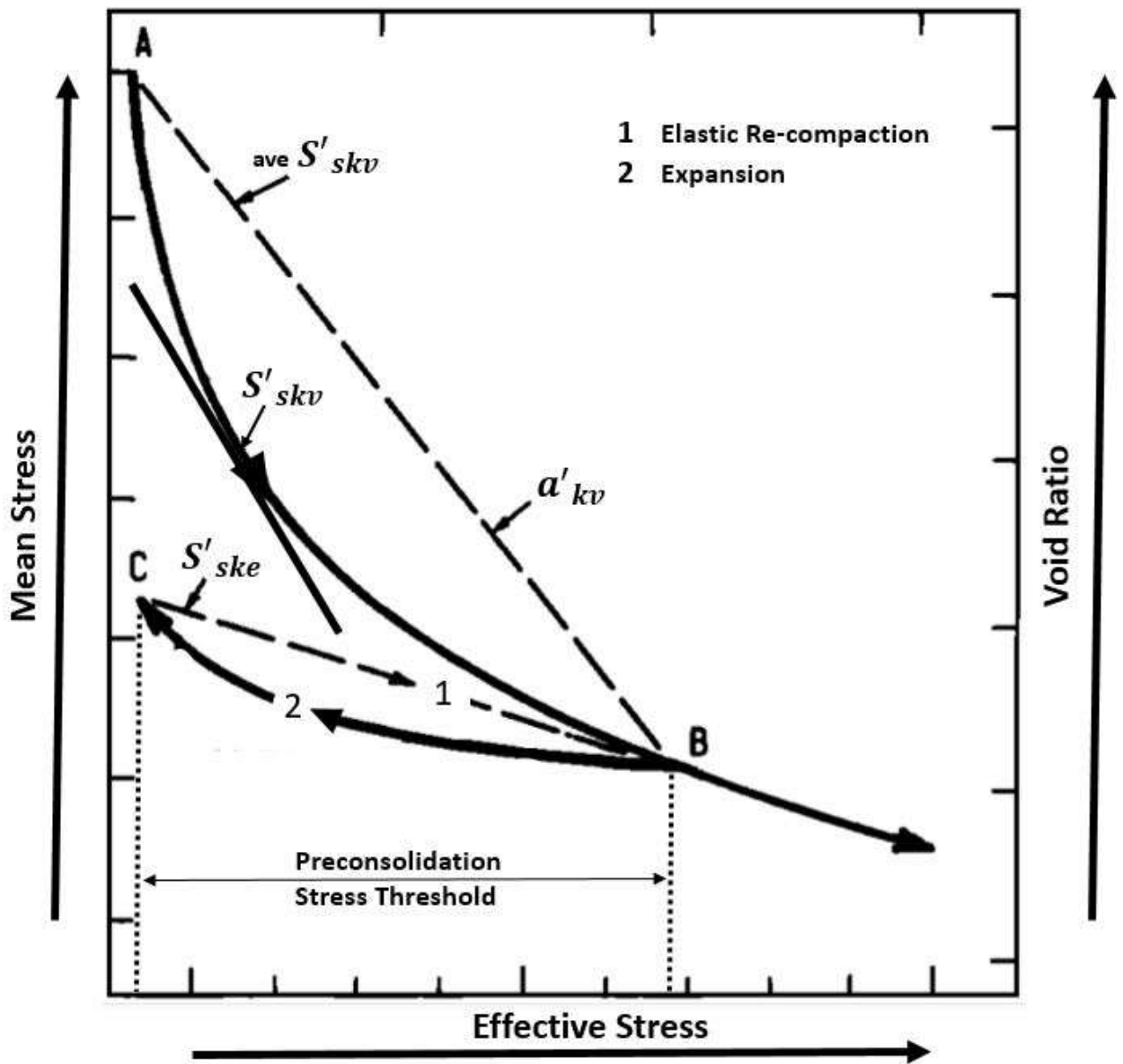


Figure 4. The idealized relationship of stress and strain in an unconsolidated fine-grained bed adapted from Helm, (1975). As stress increases beyond the past maximum stress (preconsolidation stress threshold) inelastic compaction results in a decrease of void ratio, a small portion of which is recoverable should the stress return below the past maximum stress.

3. Hydrogeology

3.1 Previous Geological Work in the Virginia Coastal Plain

A century of published work is available on the geology and hydrogeology of the Virginia Coastal Plain. Clark and Miller (1912) presents a regional geologic framework and Sanford (1913) gives an assessment of groundwater resources within that geologic framework. D.J. Cederstrom of the United States Geological Survey (USGS) was the first investigator to make major contributions to the modern understanding of the Virginia Coastal Plain. He compiled multiple fundamental reports that modern work has used in the later part of the century. Cederstrom's reports are recognized as the earliest relevant work to modern understanding of the Virginia Coastal Plain hydrogeology (Cederstrom, 1939; Cederstrom, 1941; Cederstrom, 1945b; Cederstrom, 1945a; Cederstrom, 1957; McFarland and Bruce, 2006). Cederstrom (1939) described groundwater conditions in southeastern Virginia counties of Sussex, Southampton, and Isle of Wight counties, which was followed by a summary of groundwater conditions south of the James River (Cederstrom, 1941). Cederstrom (1945, 1957) describes the hydrogeology of southeastern Virginia (1945) and the York-James Peninsula (1957).

Significant studies following Cederstrom focus on more regional geologic refinement of the Virginia Coastal Plain. Brown and others (1972) present an analysis of the Atlantic Coastal Plain of which the Virginia Coastal Plain is part and encompasses an area extending from Long Island, New York southward through North Carolina. This work includes a stratigraphic correlation of all sedimentary sections in the region. Teifke (1973) reports the general geology, stratigraphy, structure, and depositional history of the Virginia Coastal Plain but excludes the Eastern Shore. Teifke (1973) did not interpret ground water conditions alongside the geology but the discussion developed the geologic understanding that was necessary for further research to characterize the aquifer-system (McFarland and Bruce, 2006). Finally, Powars and Bruce (1999) described the Chesapeake Bay impact crater, which has important implications for conceptualizing aquifer system continuity in the Virginia Coastal Plain.

3.2 Hydrogeology of the Virginia Coastal Plain

The Coastal Plain in Virginia is ultimately a sedimentary wedge of unconsolidated to semi-consolidated gravels, sands, silts, and clays with variable amounts of shells (Meng and Harsh, 1988). This geologic province represents an eastward thickening wedge that is regionally extensive. A general cross-section is included in Figure 5. The Cretaceous, Tertiary, and Quaternary age sediments uncomfortably lie atop consolidated basement bedrock (McFarland and Bruce, 2006). While the units dip eastward and southward, the dip of each unit decreases upwards from the bedrock. The units strike approximately parallel to the Fall Line that runs north to south along the western boundary of the geologic province (Meng and Harsh, 1988). The oldest depositional units dip at approximately 7.8 meters per kilometer along the basement surface while the youngest units dip just over half of a meter per kilometer (Meng and Harsh, 1988).

The depositional and erosional history of the Virginia Coastal Plain is key to understanding the arrangement of hydrostratigraphic units and subsequent response of the aquifer-system to changes in effective stress. Meng and Harsh (1988) best describe a more detailed depositional history if there is a need for a more complete understanding. For this report, the general deposition and erosional history will suffice. Meng and Harsh (1988) describes the depositional history as a thick wedge of alluvial sediments that are overlain by thinner sequences of marine sediments which are a result of numerous transgressions and regressions with varying time periods of erosion. The earliest and lowermost Cretaceous sediments of the primary Potomac aquifer were deposited by fluvial-deltaic plains along a continental margin as the coast propagated seaward. This thick sequence of deposition is followed by alternating series of transgressions and regressions by the Atlantic Ocean to the east as sea-level rises and falls (McFarland and Bruce, 2006). The thick sequence of nonmarine deposits of Cretaceous age is overlain by thinner marine sequences of Tertiary age. Above the Tertiary sediments is a thin layer of Quaternary flat terrace and flood-plain deposits (Meng and Harsh, 1988). Finally, Coastal Plain sediments in Virginia are affected by an asteroid or comet impact near the mouth of the Chesapeake Bay. The impact crater is over 80 km in diameter and was formed within preexisting sediments, now buried about 300 meters below present day land surface (Powars and Bruce, 1999).

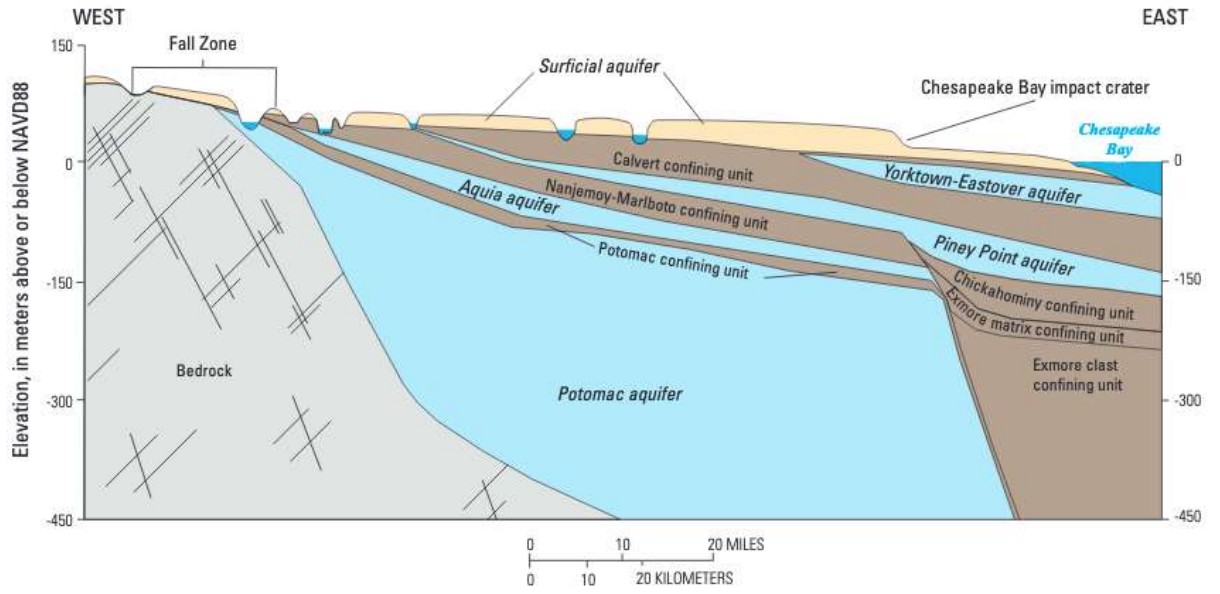


Figure 5. Generalized geologic cross-section of southeastern Virginia (McFarland and Bruce, 2006).

3.3 Hydrogeologic Framework

Nineteen hydrogeologic units have been interpreted by geophysical logs and boreholes in the Virginia Coastal Plain (McFarland and Bruce, 2006). These hydrogeologic units are described from oldest to youngest from the most recent efforts of McFarland and Bruce (2006). The recent discovery of the impact crater by Powars and Bruce (1999) is included in this current understanding of the framework. These hydrologic units are described by their lithologic and hydrologic properties rather than their stratigraphic properties. A hydrogeologic unit can have several geologic formations within its boundaries and a single geologic formation can have multiple lithologic differences resulting in hydrogeologic boundaries of aquifers and confining units. It is not uncommon for a hydrogeologic unit to have combinations or divisions of geologic formations (Meng and Harsh, 1988). Names of hydrogeologic units are still based on the names of the geologic formations that are associated with the unit. For example, the Nanjemoy-Marlboro clay confining unit is hydrogeologically described as the combination of the Marlboro Clay and the Nanjemoy Formations (Meng and Harsh, 1988).

Detailed descriptions of each hydrogeologic unit is beyond the scope of this report and McFarland and Bruce (2006) provide further explanation for how these hydrogeologic units are defined. This summary includes lithologic and stratigraphic information of each of the 19 hydrogeologic units including current understanding of their depositional environments, hydrogeologic properties, depth, extent, and orientation, and relevant information on potential for water supply of each unit. Multiple additional reports describe the Virginia Coastal Plain's hydrogeologic framework (Hamilton and Larson, 1988; Harsh and Laczniak, 1990; Heywood, 2003; Meng and Harsh, 1988). Figure 6 shows the modern stratigraphic correlations of the hydrologic units. None of the aquifers or confining units laterally extend across the entire Virginia Coastal Plain. There are lateral variations in lithology that are significant even in the scale of this report. The positions and thicknesses of aquifer and confining units are complex and are described by McFarland and Bruce (2006) as having a "complex overlapping patchwork configuration." Groundwater in the Coastal Plain is recharged by precipitation infiltration. The basement rock is generally conceptualized as an underlying impermeable boundary layer (McFarland and Bruce (2006).

ERATHM/ ERA	PERIOD	SERIES/ EPOCH	GEOLOGIC UNIT Powers and Bruce, 1999; Powers, 2000	HYDROGEOLOGIC UNIT McFarland and Bruce, 2006		
Cenozoic	Quaternary	Holocene	undifferentiated	surficial aquifer		
		Pleistocene				
	Tertiary	Pliocene	late	Bacons Castle	Yorktown confining zone	
				Chowan River		
			early	Yorktown	Yorktown confining zone	
				Eastover	Yorktown-Eastover aquifer	
		Miocene	late	St. Marys	St. Marys confining unit	
				Calvert	St. Marys aquifer	
			middle	Calvert	Calvert confining unit	
				Old Church	Piney Point aquifer	
		early	Delmarva Beds			
			Eocene	late		Chickahominy
		Exmore tsunami-breccia				Exmore matrix confining unit
		middle		megablock beds	Exmore clast confining unit *	
				Piney Point	Potomac confining zone	
		Paleocene	late	Text Nanjemoy	Potomac aquifer	
	Marlboro Clay			Piney Point aquifer		
	early		Aquia	Nanjemoy-Marlboro confining unit		
			Brightseat	Aquia aquifer		
	Mesozoic	Cretaceous	Late	clayey silty sand	Peedee confining zone *	
organic-rich clay				Peedee		
glaucinite quartz sand				aquifer *		
red beds				Virginia Beach confining zone *		
Early			glaucinitic sand	Virginia Beach aquifer		
			upper Cenomanian beds	Upper Cenomanian confining unit *		
			Potomac	Potomac confining zone		
Jurassic		Undifferentiated	Undifferentiated	Potomac aquifer		
					Triassic	
						Basement
Paleozoic						
Proterozoic						

* Denotes that unit is not found in the area of study.

Figure 6. The hydrogeologic framework of the Virginia Coastal Plain (modified from Heywood and Pope, 2009; McFarland and Bruce, 2006). Units that are not in the study area are recognized and the vertical arrows note where major hydrologic associations are known to cross-stratigraphic boundaries.

3.3.1 Potomac Aquifer

The Potomac aquifer is the largest and deepest aquifer within the entire system as well as the most utilized source of groundwater in the Virginia Coastal Plain. The aquifer extends across the entire coastal plain with the exception of the interior of the impact crater. The Potomac aquifer is hundreds of meters thick and is the lowermost stratigraphic layer within the area of the coastal plain. The Potomac aquifer supplies water to towns and cities, residential properties, and major industries. An expected increase in development of the aquifer is ongoing as demands grow in the nearby metropolitan area of Hampton Roads.

The Potomac aquifer was previously subdivided into three distinct aquifers: upper, middle, and lower, with associated intervening confining units. USGS studies in the 1980s subdivided the Potomac aquifer and designated separate aquifers in order to accommodate the simulation of vertical flow in early groundwater flow models. More recently, the Potomac aquifer has been interpreted to act more as a single aquifer due to the discontinuous nature of the fine-grained interbeds within the Potomac aquifer and similar head values extending through the entire thickness of the unit (McFarland and Bruce, 2006). Borehole data and geophysical logs indicate that confining units are not single fine-grained interbeds but are of sufficient density to function hydraulically as regional barriers to flow among discrete and vertically separated volumes of Potomac Formation sediments (McFarland and Bruce, 2006). The range of thickness of the aquifer is 365 to 610 meters. The Potomac aquifer is overlain across almost all of its extent by the Potomac confining unit. Due to the thickness, extent, and coarse-grained texture, the Potomac aquifer dominates the hydrogeology of the Virginia Coastal Plain. The majority of the groundwater of the Coastal Plain flows through and is stored in the Potomac aquifer. Common yields of major water supply wells completed in the central and southeastern parts of the Potomac aquifer are between 550 m³/day and 2700 m³/day, with some yields in James City County as great as 163,000 m³/day (McFarland and Bruce, 2006). Permeameter data from sands within the Potomac aquifer provide hydraulic conductivities that range over four orders of magnitude from 7.62×10^{-6} to 0.853 m/day.

3.3.2 Potomac Confining Zone

The Potomac confining zone is identified extensively across the entire Virginia Coastal Plain except for the inner portion of the Chesapeake Bay impact crater. It represents a local barrier to

ground-water flow across its extent. The Potomac Confining Zone has a range of thickness typically no more than 10 meters found at depths as great as 600 meters. The Potomac Confining Zone is located stratigraphically above the Potomac aquifer and represents a transition to overlying hydrogeologic units (McFarland and Bruce, 2006).

The fine-grained interbeds of the Potomac confining zone lie along the top of the Potomac Formation and can locally impede vertical leakage between the Potomac Aquifer below and the hydrogeologic units above. There is not a distinct confining zone identified as a hydraulic barrier overlying the Potomac aquifer from previous interpretations of the hydrostratigraphy (McFarland and Bruce, 2006). Published permeameter data suggest that the vertical hydraulic conductivity is small and ranges between 1.11×10^{-5} and 9.14×10^{-5} m/day.

3.3.3 Upper Cenomanian Confining Unit

The Upper Cenomanian Confining Unit is an aquitard above the Potomac Confining Zone. It has a thickness of approximately 60 meters. The only permeameter data for acquiring vertical hydraulic conductivity values are from within the Chesapeake Bay Impact Crater and no published values exist for it (McFarland and Bruce, 2006). The Upper Cenomanian Confining Unit is not within either of the sites for this study and is not discussed further in this report.

3.3.4 Virginia Beach Aquifer

The Virginia Beach Aquifer is limited regionally but is an important source of water in the Virginia Coastal Plain. The thickness of the Virginia Beach Aquifer approaches approximately 21 meters at its maximum extent. Water wells yield 55 to 273 m³/day (McFarland and Bruce, 2006). Published values for the horizontal hydraulic conductivity of the aquifer range from 7.89 m/day (Harsh and Laczniak, 1990) to 13.2 m/day (Hamilton and Larson, 1988).

3.3.5 Virginia Beach Confining Unit

The Virginia Beach Confining Unit acts as an aquitard and is also limited in its areal extent. It is found primarily in the southern part of the Virginia Coastal Plain from the city of Virginia Beach extending as far west as Franklin and Southampton Counties. The aquitard reaches a thickness of 24 meters (McFarland and Bruce, 2006). The published values of vertical hydraulic conductivity come from laboratory analysis of a sediment core that yielded a value of

1.58×10^{-5} m/day (Laczniak and Meng, 1988). Other hydraulic conductivity estimates derived from groundwater model calibration values range from 1.05×10^{-5} to 2.24×10^{-5} m/day.

3.3.6 Peedee Aquifer

The Peedee aquifer is limited to the southern parts of Chesapeake and Virginia Beach and is unused as a source of water in the Virginia Coastal Plain. This heterogeneous aquifer has a thickness typically less than 10 meters and contains interbedded fine-grained interbeds (McFarland and Bruce, 2006). The thickest extent of this aquifer is 26.5 meters and only a single published value exists for horizontal hydraulic conductivity (7.1 m/day) coming from a ground water model calibration (Harsh and Laczniak, 1990).

3.3.7 Peedee Confining Zone

The Peedee Confining Zone is areally limited, like the Peedee Aquifer, to the southern parts of Chesapeake and Virginia Beach areas. The confining zone reaches a thickness of 28.3 meters and published vertical hydraulic conductivity values range from 2.11×10^{-5} m/day (Harsh and Laczniak, 1990) to 2.37×10^{-5} m/day (Hamilton and Larson, 1988).

3.3.8 Aquia Aquifer

The Aquia Aquifer is extensive throughout the Coastal Plain of Virginia but is only sparingly used as a ground-water resource. Its greatest thickness is 46 meters, but is more commonly less than about 15 meters. The published horizontal hydraulic conductivity values range between two orders of magnitude (0.549 m/day to 91.7 m/day).

3.3.9 Nanjemoy-Marlboro Clay Confining Unit

The Nanjemoy-Marlboro Clay is widespread, thick, and impedes groundwater flow regionally throughout the entire Virginia Coastal Plain. The greatest thickness of the Nanjemoy-Marlboro Clay is nearly 46 meters and can provide some leakage from the overlying Piney Point aquifer to the underlying Aquia aquifer. Published values of the vertical hydraulic conductivity of the Nanjemoy-Marlboro confining unit from laboratory tests range from 6.7×10^{-7} m/day (Harsh and Laczniak, 1990) to 1.1×10^{-5} (Laczniak and Meng, 1988). Additional published values from ground water model calibration are estimated to be 1.06×10^{-5} (McFarland, 1999) to 1.98×10^{-5} m/day (Hamilton and Larson, 1988). The greater vertical hydraulic conductivity

values from the groundwater model calibration are more useful at the regional scale (McFarland and Bruce, 2006).

3.3.10 Exmore Clast Confining Unit

The Exmore clast confining unit is limited to the Chesapeake Bay impact crater area and impedes groundwater flow locally. The Exmore clast confining unit is comprised mostly of boulder-size clasts of other older formations with a fining-upwards sequence that is topped with pebble-sized clasts that make it distinct from the overlying Exmore matrix confining unit. The unit is thickest in the center of the crater at approximately 1,417 meters. Permeameter samples range three orders of magnitude, from 1.83×10^{-5} m/day to 1.65×10^{-2} m/day (McFarland and Bruce, 2006). The Exmore clast-confining unit is not located within the study area of this report.

3.3.11 Exmore Matrix Confining Unit

The Exmore matrix confining unit is limited to the Chesapeake Bay impact crater area and extends south into the cities of Hampton, Newport News, and Norfolk, the counties of Middlesex, Gloucester, and York, the lower Chesapeake Bay. The Exmore matrix confining unit differs from the Exmore clast confining unit in that it consists of pebble to cobble-sized clasts of older geologic formations that are suspended in a finer grained matrix in the upper part of a tsunami-breccia. Maximum thickness of the unit is approximately 61 meters. Vertical hydraulic conductivity values range between 5.49×10^{-5} m/day and 1.04×10^{-3} m/day (McFarland and Bruce, 2006).

3.3.12 Chickahominy Confining Unit

The Chickahominy Confining Unit is a local confining unit within the Chesapeake Bay impact crater and extends south into the cities of Hampton, Newport News, and Norfolk and the counties of Middlesex, Gloucester, and York. The Chickahominy is comprised of dense and very fine-grained silt and clay that reaches up to 61 meters in thickness. Published vertical hydraulic conductivities from three permeameter samples yield values from 9.45×10^{-6} m/day to 3.35×10^{-3} m/day (McFarland and Bruce, 2006).

3.3.13 Piney Point Aquifer

The Piney Point aquifer is a widespread unit covering much of the Virginia Coastal Plain with the exception of the southern half of the Fall Zone. The aquifer is not found in the area west of Franklin and south of the James River. The Piney Point aquifer yields public water for small towns and low population rural areas of the Virginia Coastal Plain. In 2002, the Piney Point aquifer produced almost 5 percent of all ground water pumped from the Coastal Plain, or about 257,000 m³/d) (McFarland and Bruce, 2006). The aquifer is composed of medium to coarse quartz, calcified, phosphatic and calcified sands and reaches a thickness of 46 meters but is generally less than 15 meters in the area south of the James River (McFarland and Bruce, 2006). Published values of horizontal hydraulic conductivity are estimated from groundwater model calibration and range from 0.45 m/day to 214 m/day (Hamilton and Larson, 1988).

3.3.14 Calvert Confining Unit

The Calvert Confining Unit is a widespread regional confining unit that is found throughout the Virginia Coastal Plain with the exception of the area west of Suffolk and south of the James River. The confining unit is composed of silt, clay, and fine-grained quartz sands and ranges in thickness from 30 to 60 meters in the Northern Chesapeake Bay but thins to about 10 meters south of the James River. Vertical hydraulic conductivity values are estimated from permeameter samples and range from 1.74×10^{-5} m/day to 1.83×10^{-2} m/day (McFarland and Bruce, 2006).

3.3.15 Saint Mary's Aquifer

The Saint Mary's aquifer is limited in areal extent in the Virginia Coastal Plain and is used sparingly as a ground water resource for private water supply in rural Suffolk. The aquifer is segregated into two parts: a thicker section (up to 60 m) to the north, and a thinner section (10-20 m) in the south, in the vicinity of Suffolk. The aquifer is composed mostly of marine fine to coarse grained quartz sands and is fairly homogenous (McFarland and Bruce, 2006). Ground water production wells use less than one percent of groundwater usage in the Virginia Coastal Plain at a rate of about 227 m³/day. One value of horizontal hydraulic conductivity is published from a ground water model calibration to be 4.5 m/d (Harsh and Laczniaik, 1990).

3.3.16 Saint Mary's Confining Unit

The Saint Mary's confining unit is widespread and regional aquitard unit across the entire Virginia Coastal Plain. The composition of the lower Saint Mary's confining unit is silty clay and the upper Saint Mary's is composed of fine-grained quartz sands with silts and clays. The confining unit varies in thickness from 35 to 91 meters. Published vertical hydraulic conductivities obtained from laboratory analyses of sediment cores range from 8.5×10^{-7} m/day (Harsh and Lacznia, 1990) to 1.26×10^{-4} m/day (Lacznia and Meng, 1988).

3.3.17 Yorktown-Eastover Aquifer

The Yorktown-Eastover aquifer is widespread in the Virginia Coastal Plain except for the northwest part of the study area. This aquifer is the second greatest source of groundwater in the study area with public and private wells withdrawing 13 percent of groundwater supply at a rate of 77,280 m³/day in 2002 (McFarland and Bruce, 2006). In the northern Virginia Coastal Plain the aquifer is composed of glauconitic, phosphatic, and fossiliferous quartz sands interbedded with silts and clays and the southern part has more fossiliferous sands. The thickness of the aquifer ranges between 15 meters and 76 meters but is generally less than 15 meters in the Southern Virginia Coastal Plain. Published vertical hydraulic conductivity values from three permeameter samples range from 1.89×10^{-4} m/day to 6.71×10^{-4} m/day (McFarland and Bruce, 2006).

3.3.18 Yorktown Confining Unit

The Yorktown confining zone is a widespread confining unit that extends across the Virginia Coastal Plain with the exception of the northwest part of the study area. The confining unit is composed of silt and clay with interbedded sands. The thickness of the unit ranges from less than 15 meters to as much as 30 meters (McFarland and Bruce, 2006). Published values of vertical hydraulic conductivity are determined from sediment core analyses that provided values ranging from 3.96×10^{-6} m/day ((Richardson, 1994)) to 1.19×10^{-3} m/day (Harsh and Lacznia, 1990). Hamilton and Larson (1988) derived a value of 2.63×10^{-4} m/day from groundwater model calibration.

3.3.19 Columbia (Surficial) Aquifer

The surficial aquifer is widespread in the Virginia Coastal Plain and covers the land surface as the topmost hydrogeologic unit. The aquifer is composed of sands and gravels with interbedded silt and clay. The thickness of the surficial aquifer can exceed 10 meters. The aquifer yields as much as 55 m³/day and by 2002 it produced about four percent of the total groundwater supply to primarily domestic or agricultural wells at a rate of 26,360 m³/day (McFarland and Bruce, 2006). A single permeameter sample estimated a vertical hydraulic conductivity of 1.37×10^{-2} m/day (McFarland and Bruce, 2006).

4. Measurements and Analysis of Hydrogeologic Data

Analysis of land subsidence due to groundwater withdrawal and subsequent aquifer-system compaction requires the collection of multiple types of data. Aquifer-system compaction data is most useful in conjunction with ground-water head change data for evaluating storage parameters in the aquifer system. This work utilizes time-series analysis of both of these data types in the vertical dimension at two extensometer sites. Because groundwater well data are related to withdrawal, groundwater withdrawal data in the region are also compiled for analysis in this investigation.

4.1 Withdrawal Data

Accurate groundwater withdrawal measurements are difficult to quantify in the Coastal Plain aquifers of Virginia. Requirements for reporting withdrawal vary regionally and by designated groundwater use. Agricultural and private domestic withdrawals are difficult to acquire. However, large industrial and municipal withdrawals are better monitored, especially in the groundwater management areas. Fortunately, withdrawal data are not necessary for this study for simulating one-dimensional compaction that relates aquifer system compaction to changes in hydraulic head. However, withdrawal data are useful for making comparisons of measured compaction data to pumping data. Table 1 shows the estimated groundwater withdrawals by aquifer in 2009. Heywood and Pope (2009) estimates that 77% of the withdrawal in the Coastal Plain is from the Potomac aquifer. Importantly, this shows that withdrawal is not evenly distributed between aquifers in the region. The rates of groundwater withdrawal are represented graphically in Figure 7. Additionally, the measured change in land surface elevation in the Coastal Plain from 1940 to 1971 by Hodahl and Morrison (1974) in Figure 8 coincide with the simulated drawdown in Figure 2. Comparison of elevation data and drawdown data shows that the resulting land surface decline as a result of groundwater withdrawal is not evenly distributed in the region.

Aquifer	Domestic (m³/day)	Reported (m³/day)	Total (m³/day)	Percent of Total
Surficial	23,640	409	24,094	5
Yorktown-Eastover	49,098	2,319	51,371	10
Saint Marys	227	0	227	<< 1
Piney Point	8,638	20,912	29,550	5
Aquia	12,729	2,182	15,002	3
Peedee	0	0	0	0
Virginia Beach	409	364	773	< 1
Potomac	34,096	377,325	411,421	77
Total	128,654	400,056	531,893	100

Table 1. Withdrawals of groundwater for each major aquifer by 2009 in m³/d. Table is adapted from Heywood and Pope, 2009.

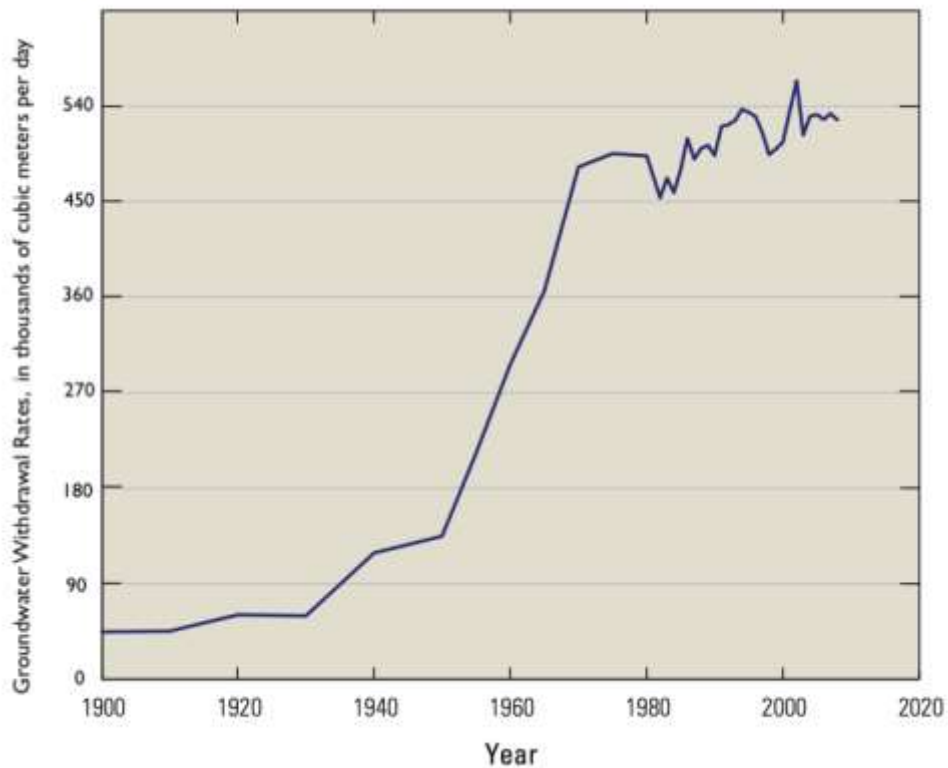


Figure 7. Withdrawal rates in the Virginia Coastal Plain from 1900 to 2008 (Modified from Eggleston and Pope (2013) and Heywood and Pope (2009)).

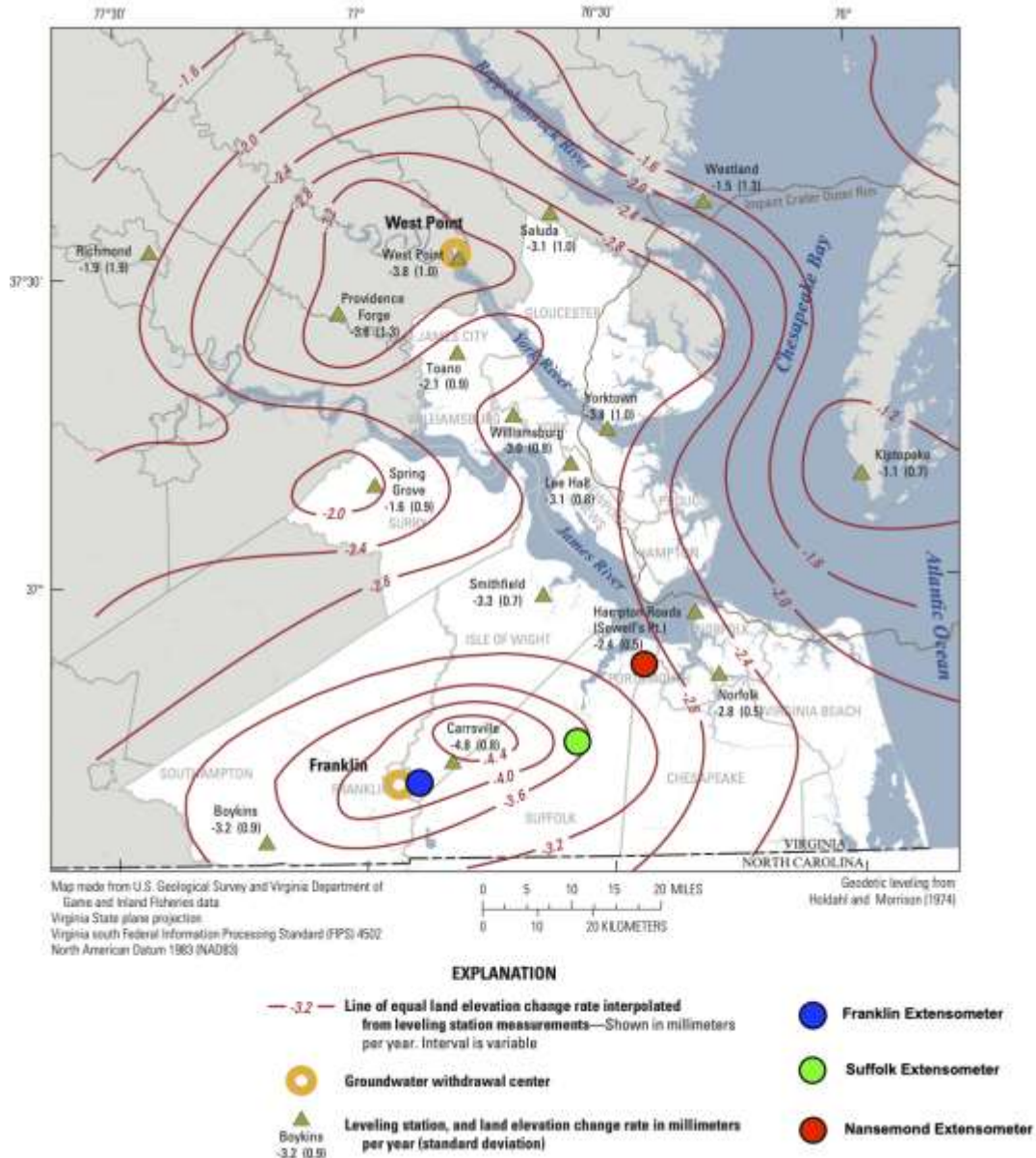


Figure 8. The measured change in land surface elevation from 1940 to 1971 by Hodahl and Morrison (1974). Adapted from Eggleston and Pope (2013) and Hodahl and Morrison (1974). Contours represent lines of equal rate of land elevation change. A negative rate indicates land subsidence. The locations of the leveling stations, groundwater withdrawal centers and extensometer sites are also included. The two cones of drawdown are seen around Franklin and West Point, Virginia.

4.2 Hydraulic Head Data

Analysis of hydraulic head data in the immediate area of Nansemond and Suffolk is a key component of this study. Time-series water level records are the proxy for stress changes within each model layer they are screened within. The water level records that are chosen are assumed to be a proxy for the withdrawal that is occurring in each aquifer in which the well is screened.

Previous interpretations of geologic and geophysical data indicate four important aquifers at Nansemond and five aquifers at Suffolk. Ideally, water-level data would be included in each of these aquifers from pre-development to present. Data availability is not ideal, but all available and relevant water level records are compiled near the two sites over the history of measurement (pre-development in 1900 to present). An examination of the USGS National Water Information System (NWIS) database returned adequate well data for the study. There are no wells with data throughout the complete history of head decline and at Suffolk there is only one well in the immediate vicinity of the extensometer site. These are significant problems at Suffolk especially as the wells are used in conjunction with extensometer data. Proximity and duration are desirable but distant wells from the same aquifer and range of depth are used where available. Figures 9, 10, and 11 show the available long-term water records for Nansemond, Suffolk, and Franklin respectively. One modern water level record remains in commission near the Franklin extensometer. While Franklin is not modeled in this report there is sufficient information from well 55B 16 to see a significant water recovery in the modern period. At all three sites there is a long period of steady head decline since the 1940s, particularly in the Potomac aquifer.

Four ground water records are utilized for the sites at Nansemond and Suffolk while only one is used for the Franklin site. At Nansemond there is one well for the Potomac aquifer, one for the Piney Point aquifer, and one for the surficial aquifer. Additionally, a specified head is input above the Yorktown-Eastover aquifer using the observations of Heywood and Pope (2009) that estimate 0 to 1 meter of drawdown at most in the Virginia Coastal Plain for the Yorktown-Eastover aquifer by 2003. Therefore, an interpolated water record with 1 meter decline in head is included. Pope and Burbey (2004) also utilized a constant head value though there are no nearby well screened within the Yorktown-Eastover aquifer. Wells are acknowledged in this report by their USGS local identifiers. Wells 59D 34, 59D 35, and 59D 36 are all within the Potomac aquifer however, 59D 35 is the water record used in Nansemond for the Potomac aquifer as the stress changes are nearly identical in 59D 36 and 59D35. It is also worth noting that these three

wells are nested and 59D 34 screen in salty water and requires conversion to a freshwater head due to the density differences that affect head values. The depth and time-series water signal of 59D 34 is significantly different from the other two wells in the Potomac aquifer suggesting that there is little short term connection between the lowest portion of the Potomac and the middle and upper Potomac. The water level time-series data for 59D 35 and 59D 36 are so similar to the subsidence signal at Nansemond that their signal was prioritized. Figures 12, 13, and 14 show the available stress history for Nansemond within the Colombia aquifer, Piney Point aquifer, and Potomac aquifer respectively. Figure 15 shows the comparison between the nested wells within the Potomac aquifer at the Nansemond site and the observed cumulative compaction.

Table 2 shows the well information for the Nansemond site. Predevelopment heads are estimates by Heywood and Pope (2009) to begin the records at each well. A single head measurement is used from 1940 and 1982 from the historic well data used from the nearby Suffolk site in 1982-1995 from Pope and Burbey (2004). Linear interpolation is necessary between available head data.

USGS Local Well ID	Well Elevation (meters AMSL)	Screen Interval (meters below land surface)	Aquifer Designation	Distance from Extensometer (meters)	Time- Frame
59D 34*	5.08	541	Potomac	7	2018-2020
59D 35 ⁺	5.08	283	Potomac	7	2018-2020
59D 36*	5.08	152	Potomac	13	2018-2020
59D 37 ⁺	5.08	116	Piney Point	13.5	2018-2020
59D 40 ⁺	5.08	8	Columbia	4.8	2018-2020

Table 2. Available well information for the Nansemond site. Wells that are not used in the model are denoted by (*) due to similarity in changes in stress while being located within the same aquifer model layer with the same simulated hydrogeologic properties as 59D 35. Wells used in the model are denoted by (+).

Well information for the Suffolk site is presented in Table 3. One water level is used in the Potomac aquifer, one screened within the Piney Point, and one well screened within the surficial Columbia aquifer. Predevelopment heads are also estimates by Heywood and Pope (2009). A specified head decline of 1 meter over the model period is also used for the Yorktown-Eastover aquifer though there is no nearby well screened within it. Well data for this site compiled previously by Pope and Burbey (2004) is reconstructed with the addition of the modern water levels. Linear interpolation of heads is needed between predevelopment heads to the data used by Pope and Burbey (2004) from 1982 to 1995. Head data is similar to Pope and Burbey (2004) but only 58C 56 was chosen for the Potomac aquifer due to its proximity to the Suffolk extensometer. Figures 16, 17, and 18 show the modern stress history of the Suffolk site in the Columbia aquifer, Piney Point aquifer, and the middle Potomac aquifer respectively.

USGS Local Well ID	Well Elevation (meters AMSL)	Screen Interval Depth (meters)	Aquifer Designation	Distance to Extensometer (meters)	Time frame
58B 268	11	4-6	Columbia	4914	1982-1995, 2018-2020
58B 269	11	107-110	Piney Point/Aquia	4914	1982-1995, 2018-2020
58C 56	3	170-173	Middle Potomac	0	1983-1995, 2018-2020

Table 3. Available well information for the Suffolk site. There is a lack of well data within a mile of the well over the given time frame. These distant wells are also included to predict compaction between the 1982 and 1995 to compare to the study of Pope and Burbey (2004) for additional information.

4.3 Geophysical Log Data

Thicknesses of layers is critical for estimating compaction, particularly with fine-grained material. USGS staff used borehole geophysical log data from the Suffolk and Nansemond locations to supplement geologic recognition of geologic and hydrogeologic units at each site.

This study depends on the interpretations of Pope and Burbey (2004) for the Franklin and Suffolk sites and as well as the USGS borehole log at the site of the Hampton Roads Sanitation District Nansemond Wastewater Treatment Facility test injection well 59D 39 (David Nelms, personal communication, U.S. Geological Survey, 2019). Geophysical log interpretation techniques are available in the USGS report on borehole geophysics (Keys, 1990). Geophysical log interpretation is beyond the scope of this report, which is dependent upon the interpretations for layer thicknesses. Tables 4 and 5 include the model input thicknesses by layer for Nansemond, Suffolk, and Franklin respectively.

Model Hydrogeologic Layer	Thickness (meters)	Fine-Grained Sediment Thickness (meters)	Aquifer Sediment Thickness (meters)	Model Unit
Columbia Aquifer (*)	4.57	----	4.57	1
Yorktown-Eastover Confining Unit	4.57	4.57	----	2,3,4
Yorktown-Eastover Aquifer (*)	0.30	----	----	5
Yorktown-Eastover Aquifer	58.52	2.7	55.82	6
Saint Mary's Confining Unit	36.88	34.13	----	7,8,9
Calvert Confining Unit	7.92	7.92	----	10,11,12
Piney Point (*)	0.30	----	----	13
Piney Point Aquifer	4.57	----	4.57	14
Chickahominy Confining Unit	7.62	7.62	----	15,16,17
Exmore Matrix Confining Unit	13.72	13.72	----	18,19,20
Potomac Clay	6.10	6.10	----	21,22,23
Potomac Aquifer (*)	0.30	----	----	24
Potomac Aquifer	424.08	122.98	301.10	25
Total	569.08	199.74	366.06	

Table 4. The thicknesses of model hydrogeologic layers at Nansemond as determined from geophysical borehole logs. Layers denoted with (*) are layers with specified head.

Model Hydrogeologic Layer	Thickness (meters)	Fine-Grained Sediment Thickness (meters)	Coarse Sediment Thickness (meters)	Model Unit
Columbia Aquifer (*)	9.14	----	9.14	1
Yorktown-Eastover Confining Unit	4.57	4.57	----	2,3,4
Yorktown-Eastover Aquifer (*)	0.30	----	----	5
Yorktown-Eastover Aquifer	26.21	3.93	22.28	6
Saint Mary's Confining Unit	11.89	11.89	----	7,8,9
Calvert Confining Unit	9.14	9.14	----	10,11,12
Piney Point (*)	0.30	----	----	13
Piney Point Aquifer	9.14	----	9.14	14
Nanjemoy-Marlboro Confining Unit	15.24	15.24	----	15,16,17
Aquia Aquifer	3.04	----	3.04	18
Piney Point/Aquia (*)	0.30	----	----	19
Potomac Clay	22.87	22.87	----	20,21,22
Potomac Aquifer	403.66	30.6	373.06	23
Potomac Aquifer (*)	0.30	----	----	24
Total	515.51	98.24	417.27	

Table 5. Table 5. The thicknesses of model hydrogeologic layers at Suffolk as determined from geophysical borehole logs. Layers denoted with (*) are layers with specified head.

4.4 Extensometer Design and Data

The design of the bore-hole extensometers is important to ensure that data collection for changes in aquifer system thickness are accurate. The two extensometers that were previously decommissioned in Suffolk and Franklin in 1995 were recommissioned in 2017 along with the installation of an additional third extensometer in Nansemond as a part of the Hampton Roads Sanitation District (HRSD) Sustainable Water Initiative For Tomorrow (SWIFT). This initiative has multiple goals in water quality, Chesapeake Bay restoration, and mitigating land subsidence with relative sea-level rise. An extensometer at Franklin (55B 60) was first installed by the

Virginia's State Water Control Board (SWCB) and instrumented by the USGS in 1979. The historic subsidence records from 1982 to 1995 at Franklin and Suffolk are represented in Figure 19. The modern extensometer record at Franklin is in Figure 20. The extensometer at Suffolk (58C 52) was installed by SWCB at Elephant Fork in Suffolk in June of 1982. These two sites were maintained by the USGS, which collected continuous compaction data for the total aquifer system thickness until 1995 when the extensometers were defunded. The Suffolk extensometer record from 2016 to 2020 is shown in Figure 21. Pope (2002) gives the construction details from internal USGS memos and reports for the extensometers in Franklin and Suffolk.

All three extensometers penetrate the entire aquifer system down to the granitic basement. The Suffolk extensometer well has an elevation of 3.44 meters above mean sea level with a depth of 487 meters below land surface or about 483 meters below sea level datum (Pope, 2002). There is a 10.16 cm diameter steel well casing for each hole from surface to bedrock that is connected by joints and threaded couplings. A 3-meter section of screen occurs 1.5 meters from the bottom of the steel casing. Well cuttings fill the annular space of the well with the exception of the top 6 meters that is grouted with cement. The extensometer pipe is between 3 and 5 cm in diameter within the steel well casing. The extensometer pipe cements in the bedrock at the bottom of the well and extends to the land surface for a stable reference thickness to measure changes of total thickness of the aquifer system. A reference platform at land surface is constructed of steel plates around the well and is mounted on three 3 cm steel legs. These legs are approximately 6 meters below the land surface within 10 cm plastic pipes that are in auger holes as deep as the water table at the time of their installation. The platform design minimizes the effects of temperature and moisture differences at the land surface that can better isolate and measure expansion and compaction of the aquifer system. The reference pipe attaches to a counterweighted lever to place the extensometer pipe in tension and to decrease friction between the reference pipe and the well casing. Contact between the reference pipe and the well casing is the greatest contributor to measurement error in a borehole extensometer (Pope, 2002). Vertical movement of the top of the tensioned reference pipe occurs within the steel well casing relative to the steel reference platform that is equal to the compaction or expansion of the aquifer system between the bedrock and the base of the platform.

The compaction and expansion were measured accurately by an analog strip-chart steel recorder in Suffolk from 1984 to 1995 but with more limited resolution than the Penny and Giles

MLS and SLS series linear position sensor (potentiometer) that was installed in 2016. The new potentiometer mounts on the reference platform that attaches to the top of the reference extensometer pipe. Pipe extensometers such as these have been successfully to measure compaction at numerous sites (Poland, 1984; Pope and Burbey, 2004; Sneed, 2001). Hanson (1988) describes the borehole extensometer technique as one of the most accurate and precise means for measuring compaction, with a resolution of 3.0×10^{-4} meters. Poland et al, (1984) describes the effective depth of a borehole extensometer to reach between 750 to 1000 meters under certain favorable conditions. Both sites are within the effective depth.

The Franklin extensometer construction is the same as the Suffolk extensometer apart from its depth. The well elevation is 8.8 meters and is 263 meters in depth from land surface or 255 meters in depth from sea level. It is important to note that this is almost half of the depth of the Suffolk extensometer.

The Nansemond borehole extensometer was built in 2016 at the Nansemond Wastewater Injection Facility as a part of SWIFT testing. The extensometer has an elevation of 5 meters above mean sea level and is the deepest of all the extensometers in the region at 597 meters in depth. Figure 22 shows the modern cumulative compaction from the Nansemond extensometer. The Nansemond borehole extensometer setup is in Figure 23. The borehole diameter is 30.48 cm and contains 17.78 cm diameter steel well casing that extends from land surface down to 608 m and is set in a cement plug that extends from 597 m to the bottom of the borehole at 609 m. The well casing is connected with threaded couplings. The annular space of the borehole above the cement plug is filled with bentonite grout. Four slip joints are welded into the casing string to reduce damage or deformation of the well casing with changes in aquifer-system thickness. Each slip joint is 1.06-m when compressed and have a 76.2-centimeter stroke. The two bottom slip joints are fully compressed, allowing for expansion in the aquifer system with anticipated injection of water. The slip joint second from the land surface is half-extended (38.1 cm), allowing for both compaction and expansion. The topmost slip joint is fully-extended (76.2 cm) allowing for compaction (Figure 23).

The surficial sediment is loose enough that there are further additions to the extensometer to decouple the steel well casing from any lateral motion. Outside of the 30.48 cm borehole steel well casing there is a 50.80 cm wide borehole with a 35.56 cm welded steel casing. The top 6 meters are drilled to a width of 76.2 cm and a third steel casing 61 cm in diameter rests on the

outside of the second. The outermost steel cases rest on cement and bentonite grout fills the annular spaces between the boreholes and the steel casings.

The extensometer is constructed with 5-cm diameter steel pipe that is contained within the 7-cm steel casing and has a 3.5-cm diameter, 1.9-cm thick steel plate attached at the bottom that sets on the cement plug that extends from 597 meters to the bottom of the borehole at 609 meters. The 5-cm steel extensometer pipe extends out of the well casing and fastens to a threaded rod that in turn fastens to a fulcrum arm that is independently supported by a 10.2-cm square steel post that is welded to the wellhead. Counterweights are attached to the end of the fulcrum arm which keeps the extensometer rod in tension with a balance between the weight of the extensometer pipe.

A lower reference plate attaches to the threaded rod extension on the extensometer rod below of the fulcrum. A Penny and Giles SLS and MLS linear positioning sensor (potentiometer) mounts on the side of the lower reference plate and to the side of an upper reference plate that extends down on a thread rod that is connected to the instrument table. The instrument table is anchored by three piers that are 7.62-cm steel pipe within 15.24-cm PVC pipe installed in 25-cm diameter boreholes drilled down to 20.4 m.

A Starrett 25-441J dial gauge mounted on a threaded rod that extends down from the instrument table sets on the lower reference plate. This is an analog measurement of relative changes in distance between the instrument table and the reference plate for quality assurance in comparison with the linear potentiometer. Additionally, a GPS receiver is attached to the bedrock via the threaded steel rod attached to the borehole extensometer. Isostatic adjustment of the continental crust is measured alongside the aquifer component of land subsidence but analysis of this data is outside of the scope of this study.

Measurements from the modern linear potentiometers are digitally stored in six-minute intervals. This high sampling rate has the potential to identify numerous natural frequencies within the extensometer record. These frequencies include deformations associated with lunar and solar tides that can be compared to tidal gauges to determine the delay between the tidal signals in the surface water of the Chesapeake Bay and the nearby Nansemond River. However, this report does not perform frequency analysis and averages the six-minute intervals into daily average time steps. Measurements from the Suffolk extensometer utilized in Pope and Burbey

(2004) are done with a steel tape compaction recorder that had to be digitized later. Each record reveals the cumulative compaction and rate of compaction of the total aquifer system at each site.

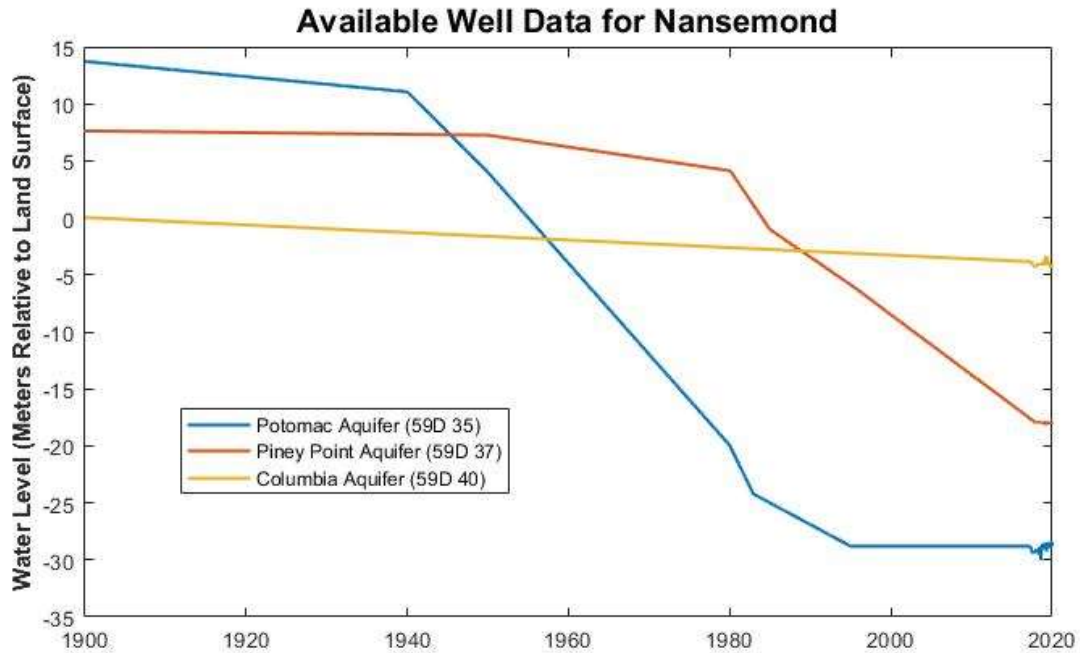


Figure 9. The synthetic interpolated stress data for the Nansemond model from 1900 to 2020 for the Quaternary, Tertiary, and Cretaceous sediments.

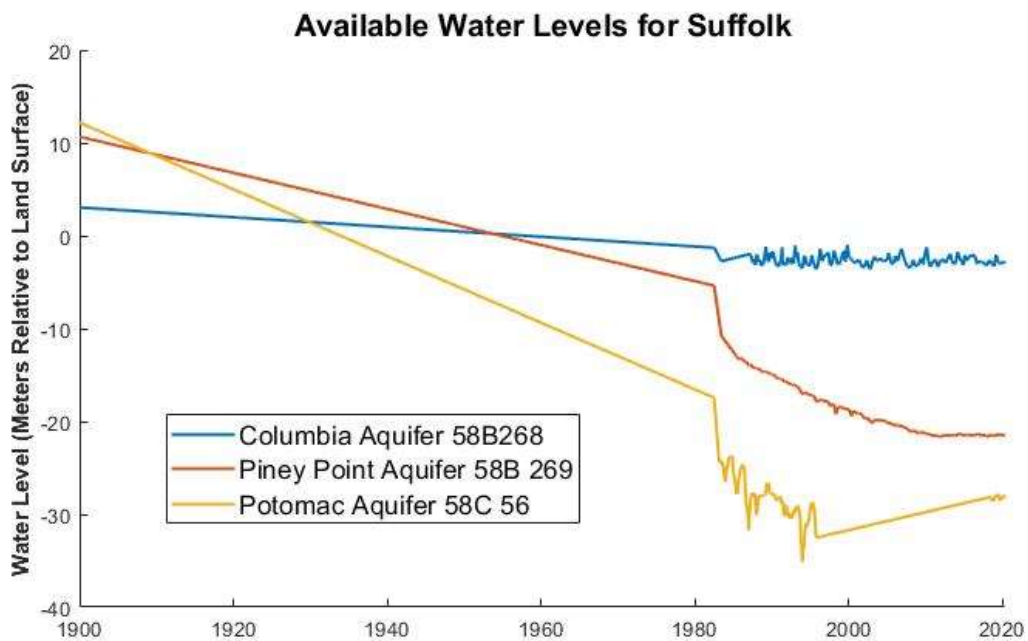


Figure 10. The synthetic interpolated stress data for the Suffolk model from 1900 to 2020 for the Quaternary, Tertiary, and Cretaceous sediments.

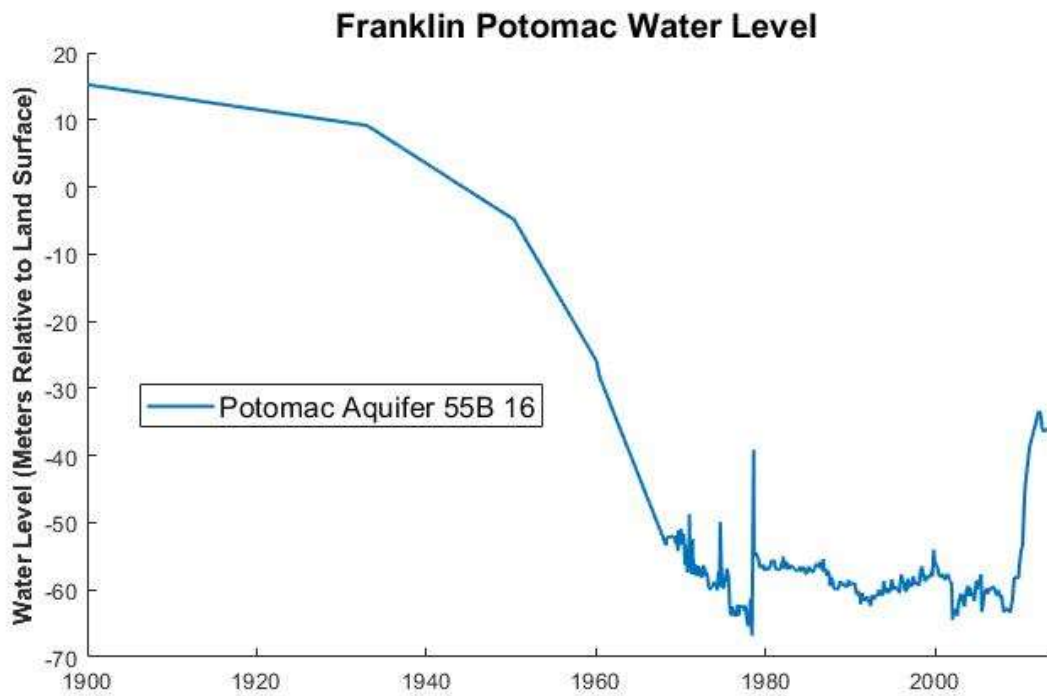


Figure 11. The historic water levels of the Middle Potomac Aquifer in Franklin, VA at well 58B 16. There is early withdrawal around 1933 that increases until the 1980s. Withdrawal stops for a few years in 2008 and there is over 30 meters of rapid head increase in the next several years.

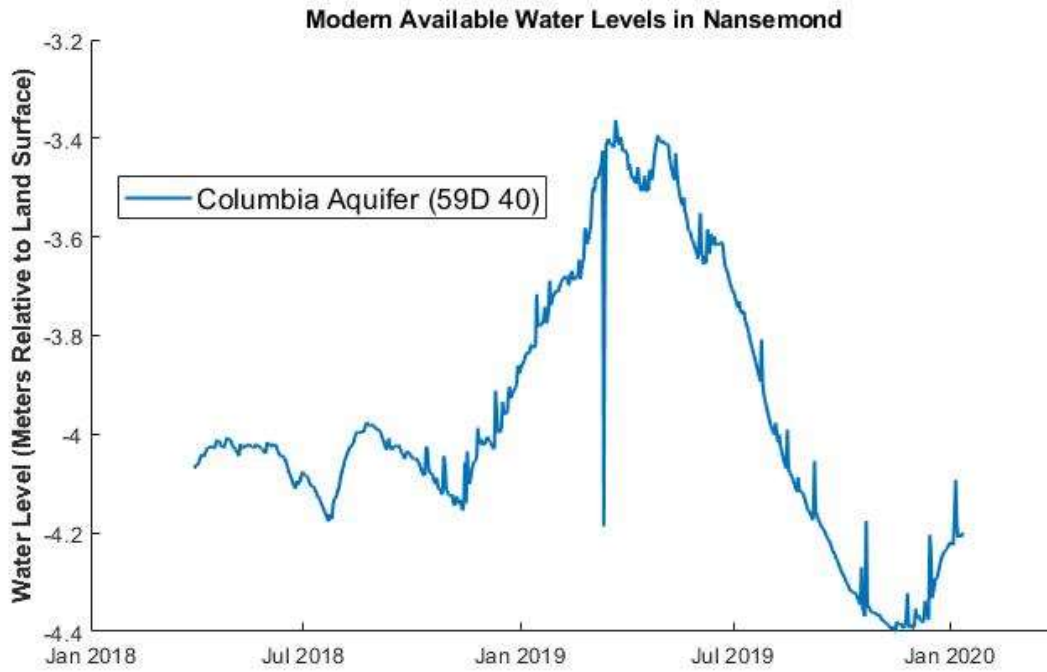


Figure 12. The daily average modern water levels within the surficial Columbia aquifer at the Nansemond site from 2018 to 2020 (USGS Well Identification 59D 40).

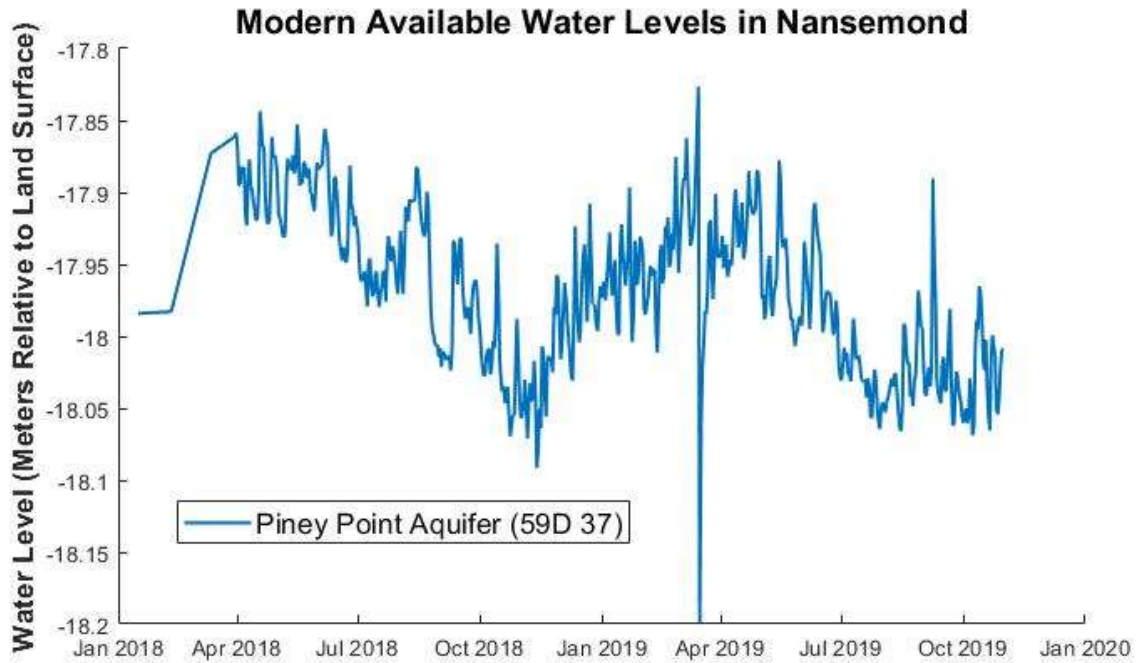


Figure 13. The daily average modern water levels within the Piney Point aquifer at the Nansemond site from 2018 to 2020 (USGS Well Identification 59D 37).

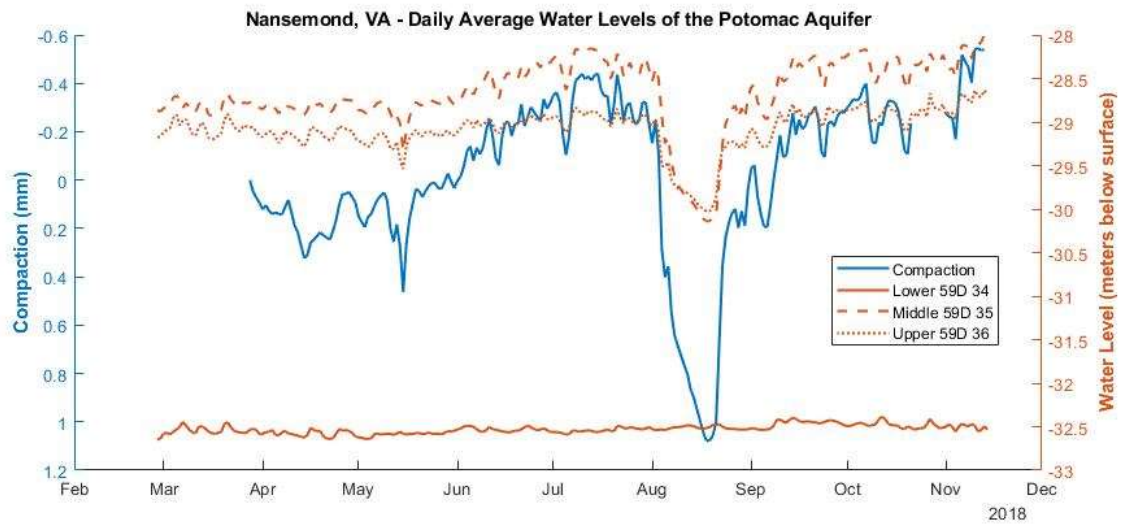


Figure 14. Comparison between the stress history in the nested wells at Nansemond and the observed cumulative compaction in 2018. Wells 59D 35 and 59D 36 are similar enough that only 59D 35 is used for model simplicity.

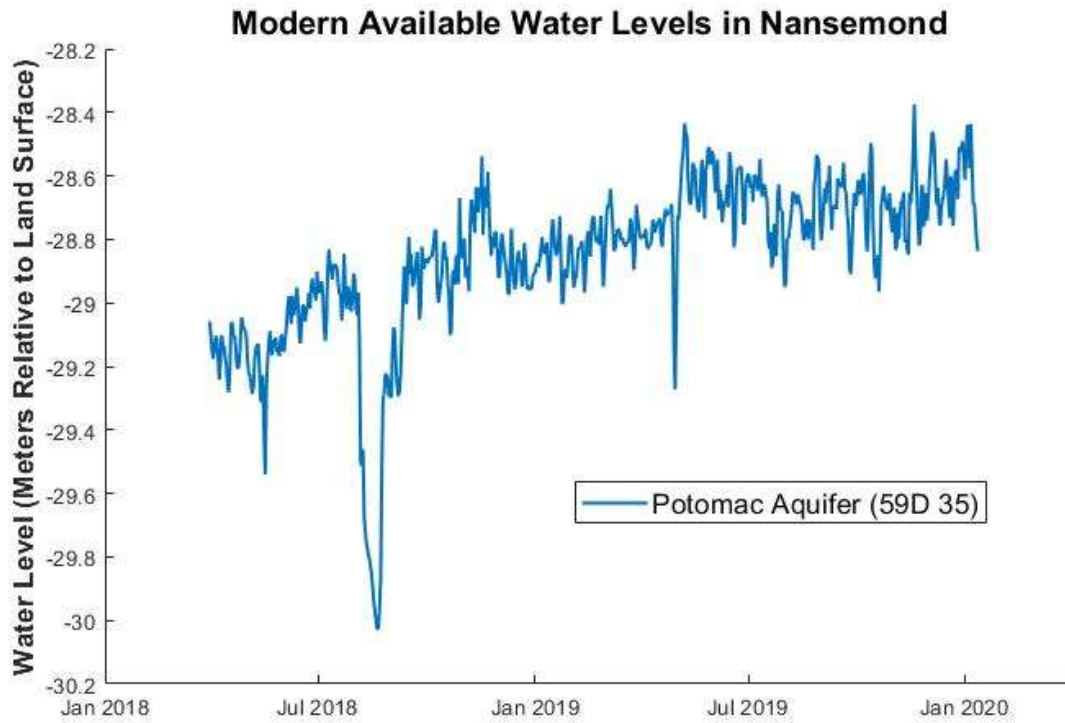


Figure 15. The daily average modern water level within the Potomac aquifer at the Nansemond site from 2018 to 2020 (USGS Well Identification 59D 35).

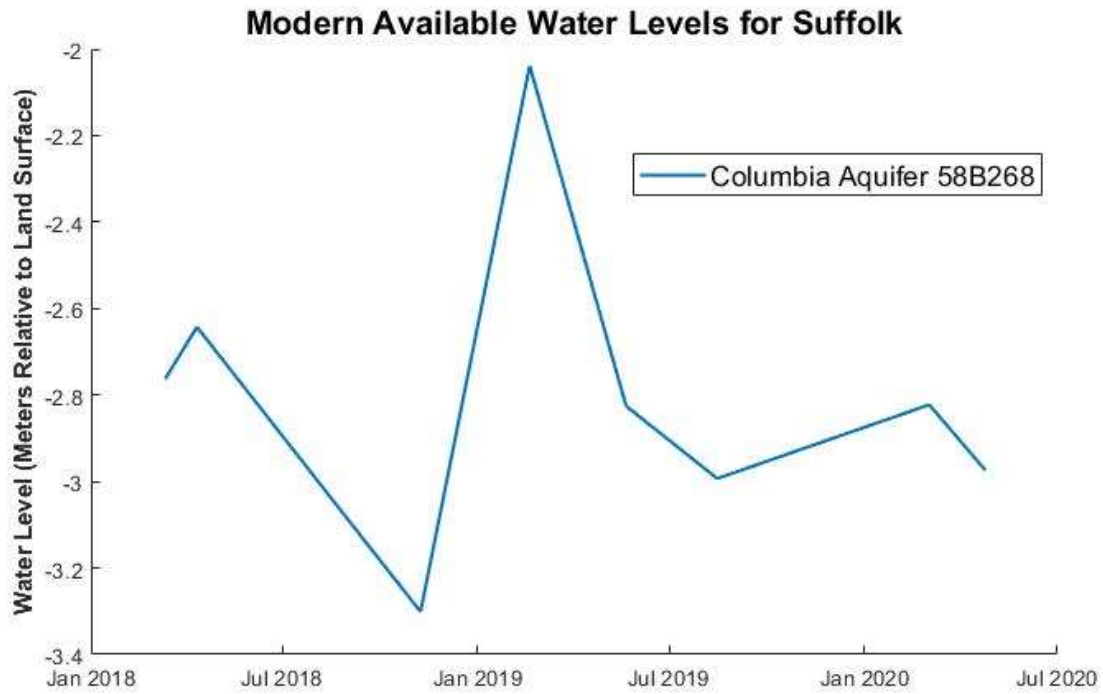


Figure 16. The interpolated modern water levels within the Columbia aquifer at the Suffolk site from 2018 to 2020 (USGS Well Identification 58B 268).

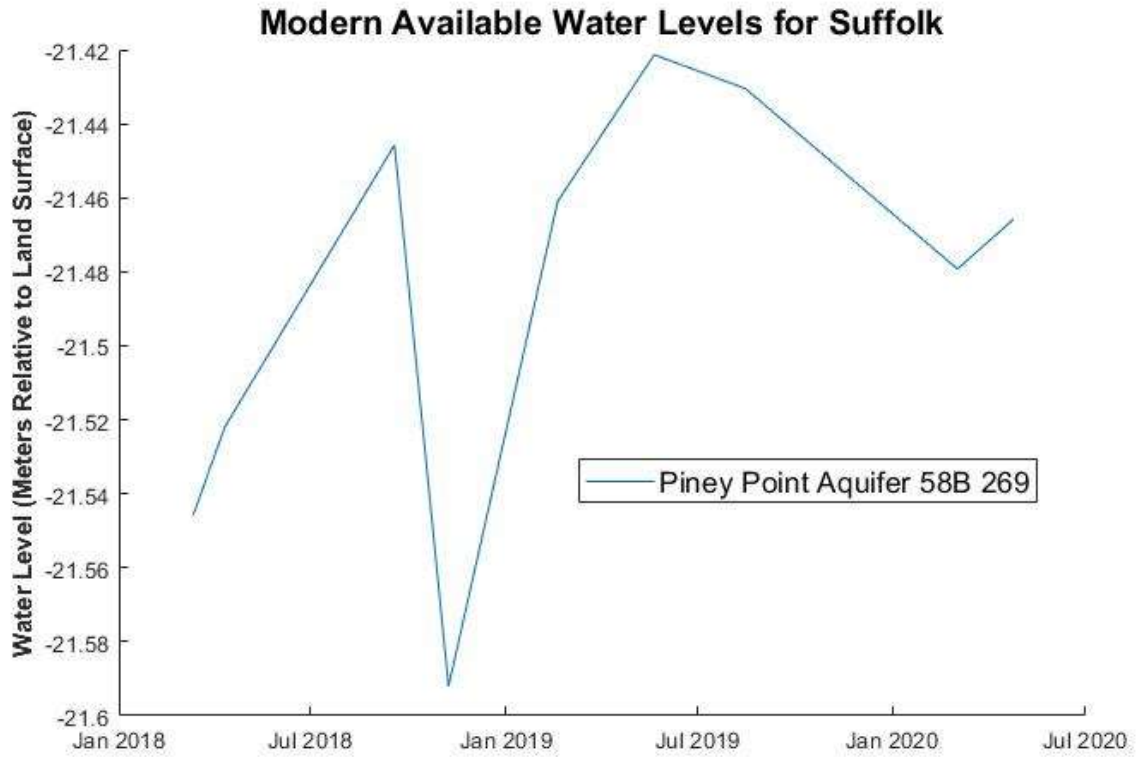


Figure 17. The interpolated modern water levels within the Piney Point aquifer at the Suffolk site from 2018 to 2020 (USGS Well Identification 58B 269).

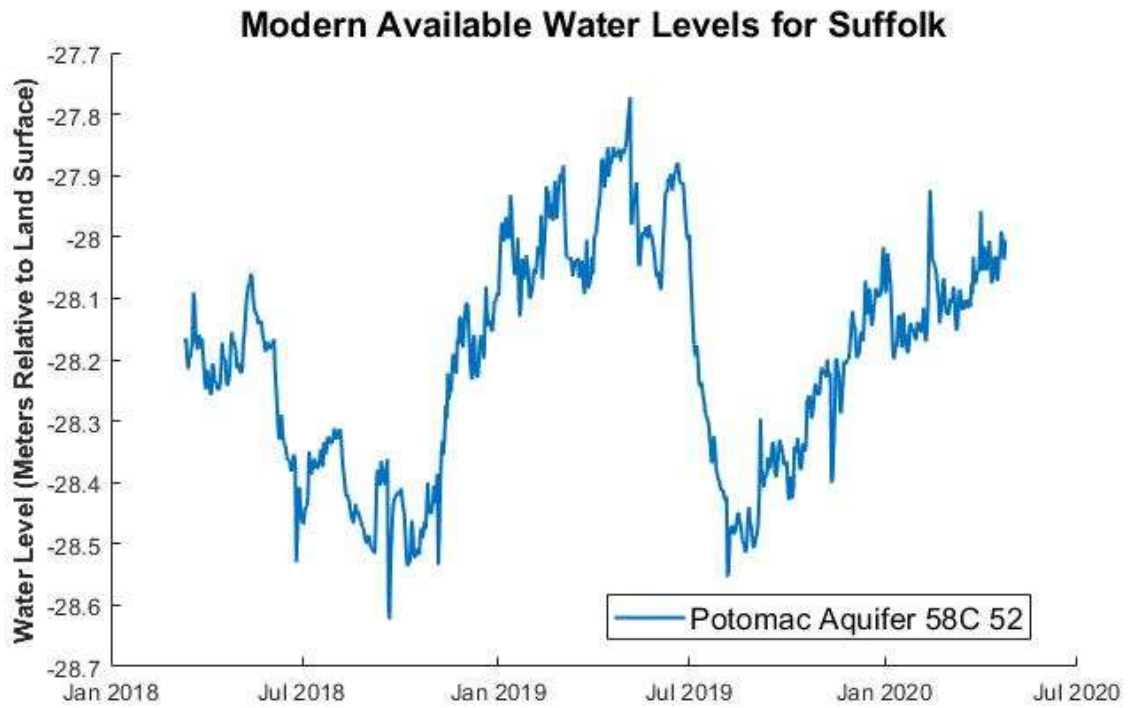


Figure 18. The interpolated modern water levels within the Potomac aquifer at the Suffolk site from 2018 to 2020 (USGS Well Identification 58C 56).

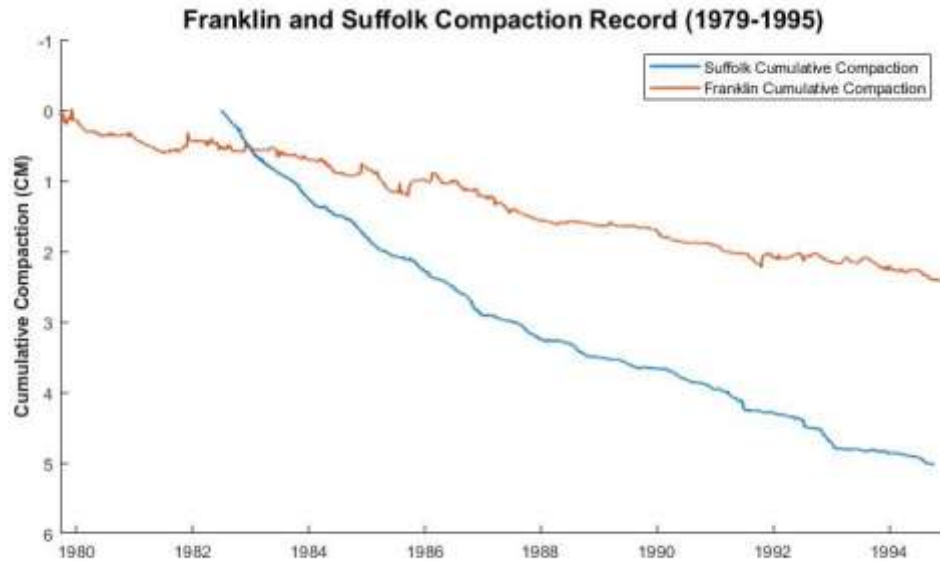


Figure 19. The observed cumulative compaction at the Franklin and Suffolk sites from 1979 to 1995 (Pope and Burbey, 2004). Suffolk experiences twice the compaction in the previous study period despite less drawdown. This is due to later development of the Potomac aquifer in Suffolk compared to Franklin as well as Suffolk's double thickness of compactible material as the wedge of unconsolidated sediment thickens from West to East.

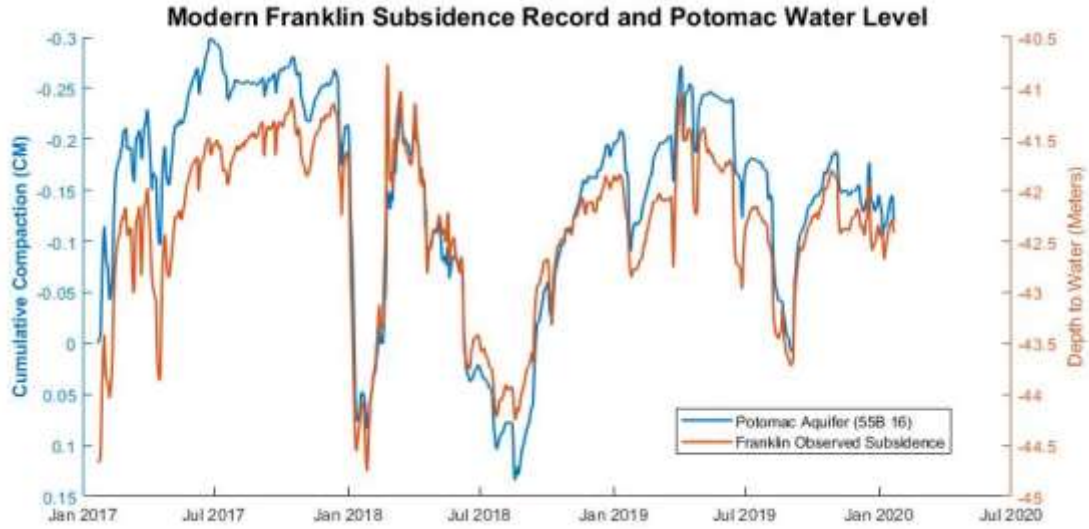


Figure 20. The modern middle Potomac water level (55B 16) and observed cumulative compaction (55B 60) at Franklin, VA.

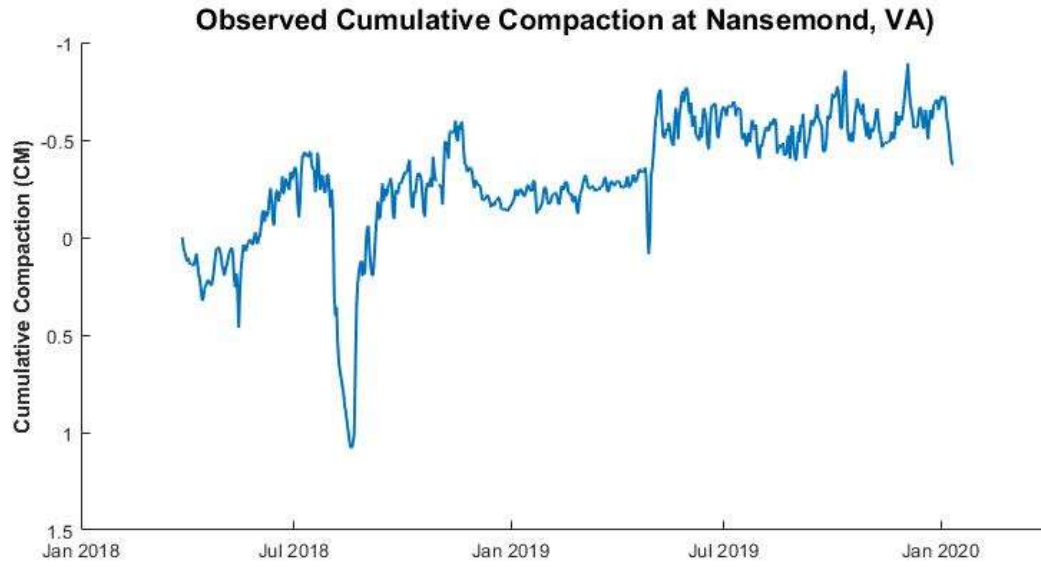


Figure 21. The observed cumulative compaction at the Nansemond site from 2018 to 2020 (USGS Well Identification 59D 39).

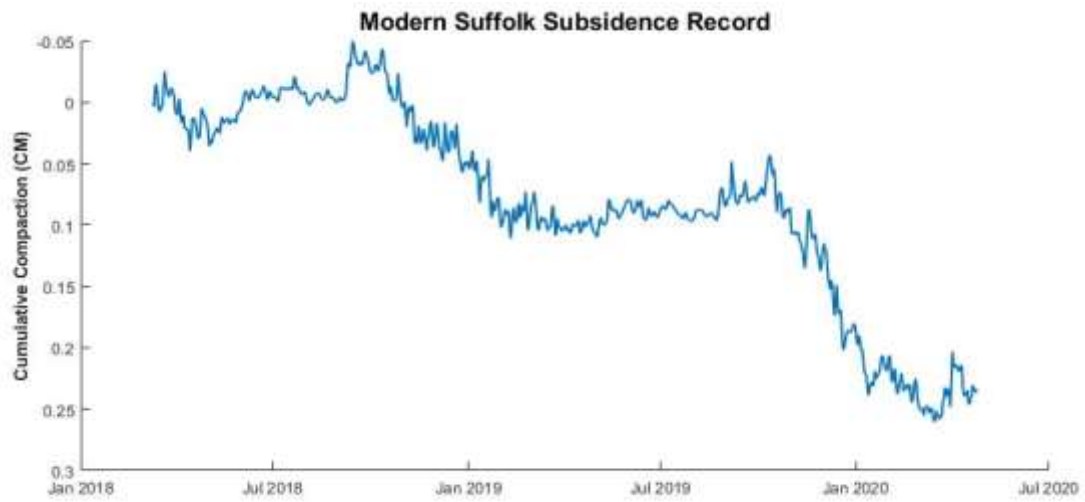


Figure 22. The observed cumulative compaction at the Suffolk extensometer site from 2018 to 2020 (USGS Well Identification 58C 52).

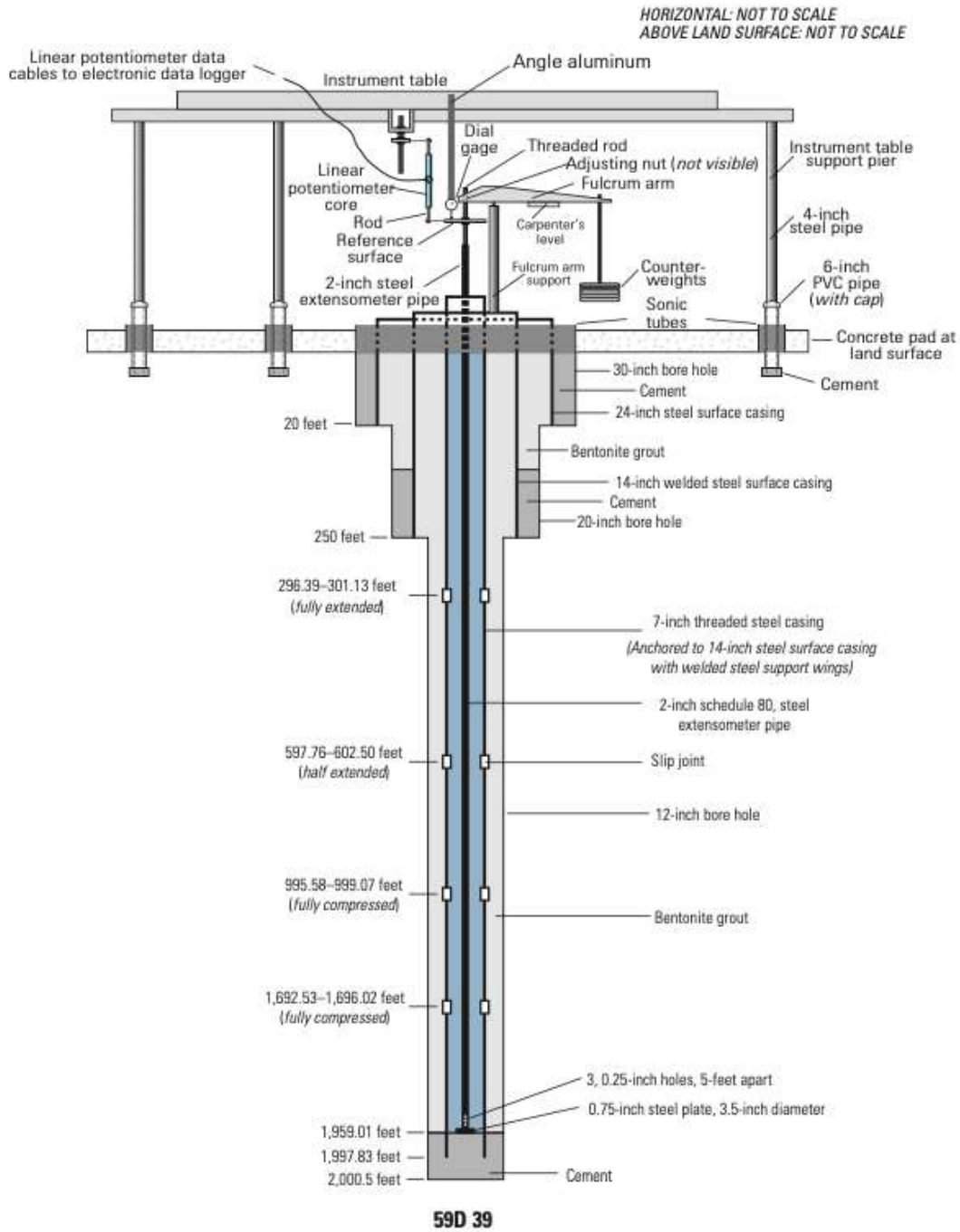


Figure 23. The measurement and construction of the borehole extensometer at Nansemond, Virginia (David Nelms, personal communication, U.S. Geological Survey, 2021).

5. One-Dimensional Simulation of Compaction

5.1 Numerical Modeling of Aquifer-System Compaction

Numerical models are used to simulate aquitard drainage through changes in effective stress and additionally to refine estimates of aquifer-system hydraulic parameters that control total compaction. Numerical models have been used since the 1970s with computers able to solve large finite-difference and finite element systems of equations. One model approach by Helm (1975) was developed to simulate one-dimensional vertical compaction by user-specified water level changes. Helm's one-dimensional approach has been used at borehole extensometer sites with detailed water level changes and compaction records (Epstein, 1987; Hanson, 1988; Hoffmann et al., 2003; Pope and Burbey, 2004). The vertical one-dimensional, finite difference models for this study were developed using MODFLOW6 and the Skeletal Storage, Compaction, and Subsidence (CSUB) package that simulates aquifer-system compaction with groundwater flow.

The CSUB package uses the same approach as the previous SUB package from MODFLOW 2000 but it is able to update material properties with each time step by calculation of changes in effective stress (Hoffman et al., 2003). The CSUB package can designate systems of interbeds as a cell fraction of an aquifer/interbed system where there is a delay in the release of water to be calculated.

While the CSUB package can typically differentiate and calculate the interbeds as delay beds within an aquifer, the interbeds here are simulated distinctly from the coarse aquifers due to a difficulty with CSUB package to appropriately simulate head equilibration between multiple delay beds and aquifers that have a large range of vertical hydraulic conductivity. The CSUB package calculates the compaction of an aggregate of all interbeds within the aquifer where the delay beds are specified. This model simulates interbeds by creating a separate layer as thick as the summation of all interbeds within an aquifer that is placed adjacent to that aquifer. The new interbed layer is discretized into three layers to simulate delayed equilibrium of heads from adjacent aquifers as they would be discretized by the delay-beds in the CSUB package as suggested by Hoffman et al., (2003).

5.2 Modeling Approach

The one-dimensional vertical model for the Virginia Coastal Plain aquifer system was divided into layers coinciding with the determined hydrogeologic layers found at each site. Pope and Burbey (2004) used an approach where individual hydrogeologic layers were grouped together into thicker units with averaged specific storage and vertical hydraulic conductivity values. The model layers for this study are confining units, aquifer units, or layers to simulate interbeds from the aquifer layers where each major hydrogeologic boundary is its own model layer during simulation to take advantage of modern computational proficiency. The approach aims to balance simplicity in the model while attempting to achieve the resolution that could be required to simulate daily submillimeter compaction. The conceptual models of the Nansemond and Suffolk sites are presented in Figure 24 and Figure 25, respectively. Figure 26 shows the hydrogeology at the Franklin site.

The simulated total compaction is the sum of the compaction within each represented hydrogeologic layer. The total simulated compaction allows for comparison to observed extensometer and leveling benchmark records. An accurate simulation of the overall compaction at each site was a goal but the ability to describe individual model layer contributions to the overall compaction to understand the dynamics of the aquifer system was an equally important goal of the modeling study.

The simulation period ranges from 1900 to 2020 in an attempt to account for the entire known history of groundwater withdrawals contributing to compaction of the aquifer system. It is important to include these long timeframes as the time constants for confining units in the aquifer system result in significant delays between when water levels decline and when the resulting compaction and land subsidence occurs.

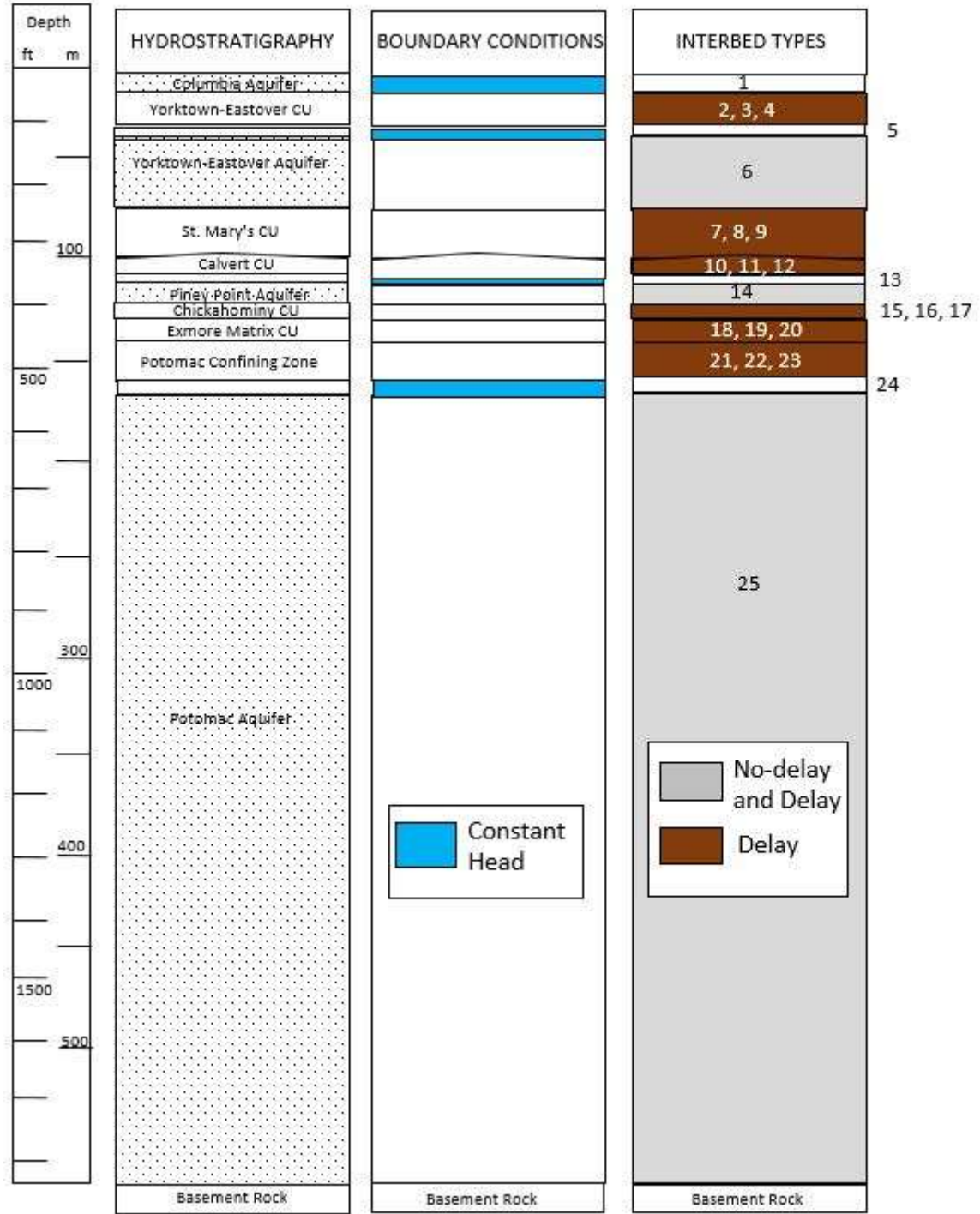


Figure 24. The one-dimensional vertical hydrogeology of the Nansemond extensometer site as interpreted by geophysical borehole logs by the U.S. Geological Survey.

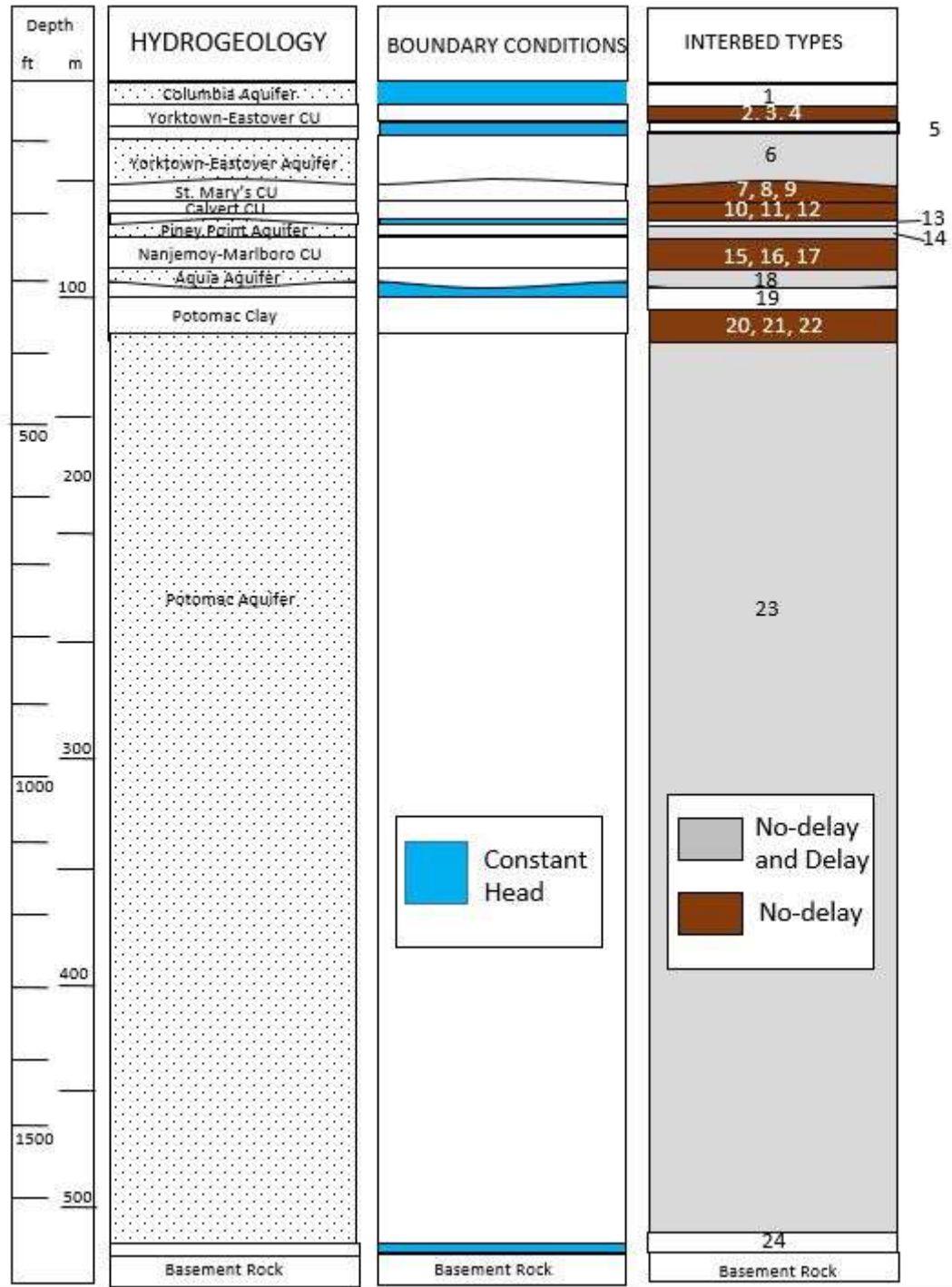


Figure 25. The one-dimensional vertical hydrogeology of the Suffolk extensometer site as interpreted by geophysical borehole logs by Pope and Burbey (2004).

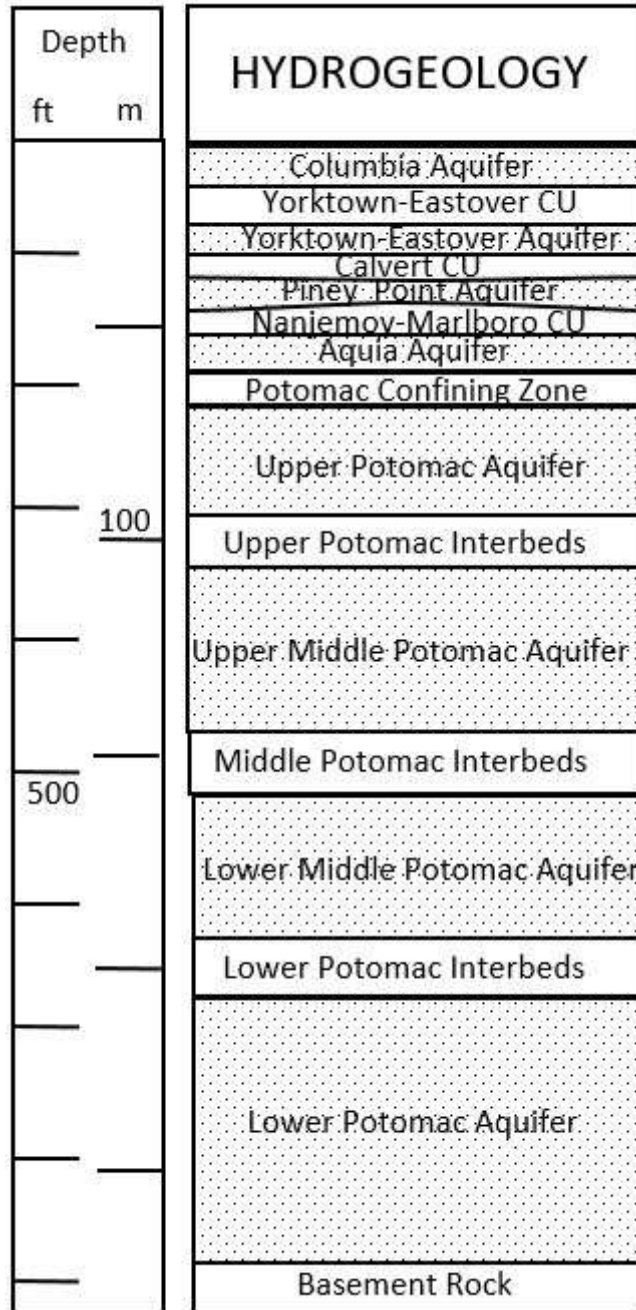


Figure 26. The one-dimensional vertical hydrogeology of the Franklin extensometer site as interpreted by geophysical borehole logs by Pope and Burbey (2004).

5.3 Model Input

The geographic and hydrogeologic similarities between the sites at Nansemond and Suffolk allow for a similar approach to discretization of model units. The conceptual model for both sites represents a simplified version of the physical aquifer system with idealized layers similar to the Lorenzi site model, Las Vegas from Pavelko (2004). The Lorenzi model uses a single lateral one-dimensional row of cells to simulate compaction and head changes that are actually vertical. Instead, this study uses a single vertical, one-dimensional column of cells. The row and column thickness are 0.328 meters by 0.328 meters (1 foot in Standard units), extending to the depth of each extensometer.

Input decisions included wells, geophysical log interpretations for model layer thicknesses, initial values of hydrogeologic properties such as porosity, elastic and inelastic specific storage, predevelopment head values, and vertical hydraulic conductivities. Tables 6 and 7 show the initial conditions used in the simulation of the two extensometer site models.

Nansemond Model Layers	Initial K'_v (m/day)	Initial S_{ske} (1/m)	Initial S'_{skv} (1/m)	Initial S'_{ske} (1/m)	Initial Preconsolidation Stress (m)
Columbia Aquifer	0.1	4.5×10^{-6}	----	----	0.03
Yorktown Confining Layer	1.2×10^{-3}	----	1.5×10^{-4}	6.0×10^{-6}	0.91
Yorktown Eastover Aquifer	2.4	4.5×10^{-6}	----	----	2.13
Yorktown Eastover Aquifer Interbeds	1.9×10^{-4}	----	1.0×10^{-4}	6.0×10^{-6}	2.13
St. Mary's Confining Layer	1.3×10^{-4}	----	1.0×10^{-4}	6.0×10^{-6}	3.05
Calvert Confining Layer	3.4×10^{-5}	----	1.0×10^{-4}	6.0×10^{-6}	5.49
Piney Point Aquifer	4.6	4.5×10^{-6}	----	----	7.62
Chickahominy Confining Layer	3.4×10^{-4}	----	1.0×10^{-4}	6.0×10^{-6}	9.15
Exmore Matrix Confining Layer	1×10^{-3}	----	1.0×10^{-4}	6.0×10^{-6}	9.76
Potomac Confining Zone	1.1×10^{-5}	----	1.0×10^{-4}	6.0×10^{-6}	10.67
Potomac Aquifer Interbeds	6.0×10^{-6}	----	1.5×10^{-5}	4.5×10^{-6}	13.72
Potomac Aquifer	15.2	4.5×10^{-6}	----	----	13.72

Table 6. Initial parameter values for each layer of the Nansemond model. Initial parameter values for each layer of the Nansemond model. Vertical hydraulic conductivities (K'_v) are from McFarland and Bruce (2006), specific storage values are from the calibrated parameters from Pope and Burbey (2004), and the initial preconsolidation stresses are from predevelopment heads estimated by Heywood and Pope (2009).

Suffolk Model Layers	Initial K'v (m/day)	Initial Sske (1/m)	Initial S'skv (1/m)	Initial S'ske (1/m)	Initial Preconsolidation Stress (m)
Columbia Aquifer	5.49	3.3×10^{-6}	----	----	3.0
Yorktown Confining Layer	4×10^{-6}	3.3×10^{-6}	3.3×10^{-5}	2×10^{-6}	7.6
Yorktown-Eastover Aquifer	3.23	3.3×10^{-6}	----	----	9.1
Yorktown-Eastover Aquifer Interbeds	3×10^{-6}	3.3×10^{-6}	3.3×10^{-5}	2×10^{-6}	9.8
St. Mary's Confining Layer	2.7×10^{-6}	3.3×10^{-6}	3.3×10^{-5}	2×10^{-6}	10.4
Calvert Confining Layer	2.8×10^{-7}	3.3×10^{-6}	3.3×10^{-5}	2×10^{-6}	10.7
Piney Point Aquifer	4	3.3×10^{-6}	----	----	10.7
Nanjemoy-Marlboro Confining Layer	9×10^{-7}	3.3×10^{-6}	3.3×10^{-5}	2×10^{-6}	12.2
Aquia Aquifer	4.6	3.3×10^{-6}	3.3×10^{-5}	2×10^{-6}	12.2
Potomac Clay	1×10^{-6}	3.3×10^{-6}	3.3×10^{-4}	2×10^{-6}	12.2
Potomac Aquifer	3×10^{-5}	3.3×10^{-6}	1.3×10^{-5}	2×10^{-6}	12.2
Potomac Interbeds	2.4	3.3×10^{-5}	----	----	12.2

Table 7. Initial parameter values for each layer of the Suffolk model. Vertical hydraulic conductivities (K'v) are from McFarland and Bruce (2006), specific storage values are from the calibrated parameters from Pope and Burbey (2004), and the initial preconsolidation stresses are from predevelopment heads estimated by Heywood and Pope (2009).

5.4 Boundary Conditions

Heads and ground water flow in both the aquifers and the aquitards are controlled by a constant head boundary or CHD package (Harbaugh et al., 2000). For this one-dimensional model, the lower, upper, and lateral boundaries of the vertical column are no flow boundaries so flow only simulates vertically within the active cells. No water enters or exits the system except as a result of head fluctuations provided by the time series head change input files within the CHD boundary layers. The compaction in the aquifer system is assumed to be only vertical and a result of the input head fluctuations. Specified constant head boundaries are in small 0.328-meter thick layers adjacent to the aquifers they represent.

All layers are assumed to have a constant porosity of 0.3. The specific yield and specific storage in the storage package (STO) are defined to be zero for all layers due to the CSUB package already using storage information that supersedes the information from the STO

package. All model layers are designated as non-convertible for hydraulic conductivity and storage properties. The default Node Property and Flow (NPF) package settings are used.

The effective stress formulation of the CSUB package is utilized to simulate compaction of the fine and coarse aquifer materials. Aquifer hydraulic conductivity is assumed to be large enough that head change results in an instant equilibration throughout all aquifer layers. The aquifers are a single layer with specified thicknesses. Aquitard hydraulic conductivity is low enough that non-linear head gradients change slowly enough to require delay in equilibration with a head change in the adjacent aquifers. Hence, fine-grained materials are represented as no-delay beds discretized into three-layer cells with low vertical hydraulic conductivity. This implicitly simulates the compaction by creating a delay in head equilibrium from surrounding aquifers as recommended by Hoffman et al. (2003). This thinning of the aquitard layers minimizes a limitation of the CSUB package to simulate residual compaction (Pavelko, 2004).

A specific gravity of 2.0 is defined for the saturated sediments. Water compressibility is simulated using a unit weight of water of 9,806.65 Newtons per cubic meter and a water compressibility of 4.6512×10^{-10} m²/Newton. The thickness of compressible materials and total porosity update after each stress period during the simulation in response to compaction.

The surficial aquifer is unsaturated but it is included in both models to calculate geostatic and effective stresses. Compaction is not simulated in the upper aquifer due to the high coarse-grained content and the slow head change that is hydrogeologically isolated from the major productive zones of the aquifer system. Compaction is not thought to be an issue in the surficial Columbia aquifer but it should be noted that compaction and storage or release of water are not simulated in cells designated as constant-head boundaries.

Interbedded aquitards are included as delay beds within the aquifers of which they are naturally a part. However, interbedded aquitards that are less than 1.5 meters thick are included with the aquifer thickness as a no-delay bed as ultimate compaction occurs within a model time step. Interbedded aquitards that are greater than 1.5 meters thick do not equilibrate within a model time step and are simulated with no-delay beds discretized into three layers in the same fashion as the confining units.

Initial preconsolidation stresses are the same as the predevelopment initial heads since the model commences at the start of groundwater pumping. Predevelopment (preconsolidation) heads represent the previous lowest heads before the model begins in 1900 taken from the three-

dimensional modeling work of Heywood and Pope (2009). Initial preconsolidation stresses for the no-delay beds are also in Tables 6 and 7. Epstein (1987) reports that errors can result from stress occurring before the start of a simulation period; however, in the Virginia Coastal Plain this was the appropriate period for estimating the initial preconsolidation stresses. This is a significantly different approach for estimating initial preconsolidation stresses than used by Pope and Burbey (2004). Calibration of these earlier models assumed 20 meters of head decline for all model layers, a value estimated by Davis (1987), to be the required drawdown for subsidence to occur in the entire Atlantic Coastal Plain based on comparing a drawdown equipotential map with an estimated land subsidence map. Therefore, the difference in the initial preconsolidation stresses between these two studies is about 20 meters and there was an expected comparative increase in resulting simulated total compaction with respect to this difference as the initial preconsolidation stress threshold is crossed almost immediately at the start of the transient simulation.

The transient models for both extensometer sites were developed with respect to availability and timeframe of well and extensometer data. Both models begin on January 1, 1900 before significant pumping out of the aquifer system commenced and well before any water levels declined below the initial preconsolidation stress value. The first stress period is steady state in order to equilibrate the heads within the aquifer system. Both monthly and daily stress periods are in the simulation while only daily time steps are used for both models from beginning to end.

5.5 Nansemond Conceptualization

The model grid for Nansemond consists of 25 layers, 1 row, and 1 column. Table 4 summarizes the model layer thicknesses. The model has an overall depth of 566.3 meters and consists of 2094 stress periods with 43,841 daily time steps for a total model duration of 120 years and 12 days. The first 1440 stress periods are monthly (30 time steps per stress period) from January 1, 1900 to March 30, 2018 and the remainder are daily stress periods from March 31, 2018 to January 12, 2020 where the observed extensometer data begins.

Initial heads in the model range from 0 to 12.2 meters and increase with depth. The interbeds within the Yorktown-Eastover aquifer are 2.7 meters thick and the interbeds within the Potomac aquifer are 122.98 meters thick. Interbeds at Nansemond that are assumed to equilibrate within one time step include those within the Piney Point aquifer, which are estimated to be

between 0.9 and 1 meter thick. As a result, the thicknesses of these interbeds are included within the thickness of the Piney Point aquifer.

5.6 Suffolk Conceptualization

The modeling approach for the Suffolk site is identical to the Nansemond site but with added complexity. Both the addition of historical compaction data that coincides with that used by Pope and Burbey (2004) at the same Suffolk site and the inability to use delay beds meant that a slightly different conceptual model had to be developed. The addition of layers at some elevations and the removal of layers at other locations was made to the Suffolk model, which made it somewhat different than the Nansemond model. Furthermore, differences in hydrogeology at Suffolk include the addition of the Nanjemoy-Marlboro clay and the Aquia aquifer along with the removal of the Exmore matrix impact-crater material and the Chickahominy confining unit.

The model grid for the Suffolk site consists of 24 layers, 1 row, and 1 column. Model layer thicknesses differ significantly from those of the Nansemond site and are summarized in Table 5. The Suffolk model has an overall depth of 514 meters. The model consists of 14,820 stress periods with 43,944 daily time steps and a total model duration of 120 years and 12 days. The first 1006 stress periods are monthly (30 time steps per stress period) from January 1, 1900 to June 29, 1982. This is followed by a period of daily stress periods beginning with stress period 1007 and extending to stress period 14,820 (June 30, 1982 to April 24, 2020). The daily stress periods coincide with the daily observed extensometer data and water level data from Pope and Burbey (2004) to modern observations.

Initial heads in the model range from 0.1 at the top of the model to 14.6 meters at the base of the model. The interbeds within the Yorktown-Eastover aquifer are 3.9 meters thick and the interbeds within the Potomac aquifer are about 30.6 meters thick. Interbeds within the Piney Point and Aquia aquifers are 0.8 meters and 0.9 meters respectively and are thus included in the aquifer model layer.

5.7 Model Simulation and Calibration

The overall aim of the model is to gain an understanding of aquifer system behavior and to reduce uncertainty of the range of plausible model parameters. It is not possible to simulate the exact hydrogeology or obtain a unique set of parameter values at the simulated sites and

decisions intentionally balanced certain aspects of the aquifer-system in order to test a hypothesis. For example, lowering the vertical hydraulic conductivity of a confining layer to ensure that observed separation of aquifers remains intact. Another example is aggregate thicknesses of one-meter thick interbeds in the Potomac aquifer are necessary for model simplicity but this will increase the time constant required for an interbed to equilibrate. Subsequent calibration to observations may have to adjust inelastic skeletal specific storage or vertical hydraulic conductivity within an inaccurate range to achieve graphical calibration.

Model simulation times generally took between five and thirty minutes for the Nansemond model and between twenty minutes and several hours for the Suffolk model on a laptop computer. Calibration of the model involved minimizing the difference between the observed water levels and total compaction to observed data, which was primarily done using trial and error methods. Minimization of the water levels and total compaction involved manipulation of both the elastic and inelastic specific storage values and K'_v of each hydrogeologic unit. An initial intention of this study was to employ inverse modeling with the Parameter ESTimation (PEST) package in a beta version of ModelMuse (Richard Winston, U.S. Geological Survey, personal commun., 2021), a free graphical user interface for MODFLOW6. PEST is one of the most commonly used calibration tools for groundwater modeling problems (Doherty and Hunt, 2010). However, significant challenges were encountered regarding successful operation of PEST with ModelMuse software and MODFLOW6 CSUB package. PEST has been successful with other packages of MODFLOW6 but the newest beta version of ModelMuse, PEST, and the CSUB package have not yet been used in conjunction successfully. For this reason, much of this work is exploratory until software issues are resolved; the use of PEST had to be abandoned for this project. The intention is to use PEST in the future for a more robust calibration of selected aquifer-system parameters with minimized uncertainty. Until that time, the property calibrations here are considered to be provisional. However, significant insights between the trial and error calibrated model and available data have been made for describing the dynamics of the aquifer system.

Trial and error methods used in this investigation include (1) selecting several model parameters that were deemed highly sensitive to imposed head variations based on inferred knowledge from available data sets, (2) adjusting the input parameters manually based on model simulation results, and (3) evaluating the model performance by time-series comparisons to

known observations and adjusting parameter values for minimization of simulated vs. observed water levels and compaction. For this study, quick graphical comparisons were made between the model-simulated time-series output of land surface motions (z-displacement) and the time-series of known observations of land subsidence. While trial and error methods are slow, the advantage is that it allows for greater understanding of the dynamics of the aquifer system and the model's sensitivities to a set of selected parameter values. Figure 27 shows a flowchart describing the method of trial and error calibration.

The CSUB package calculates compaction for each model unit separately and sums these individual compaction values of each unit to produce a total subsidence record for each extensometer site. The simulated total compaction is compared to the extensometer observed aquifer system compaction and the total cumulative compaction estimated by Pope and Burbey (2004) for validity. Pope and Burbey (2004) estimated land subsidence between 1900 and 1995, however withdrawal declined in 2008. If simulated overall compaction is in the same order of magnitude, the simulation was considered reasonable.

Initial calibration of the model focused on the Nansemond location for several reasons. First, better and more applicable water-level data are available due to having nested wells (multiple water levels at different depths) and proximity of the wells to the borehole extensometer. Additionally, the vertical discretization of the conceptual model is simpler to that of the Suffolk model. Finally, the apparent simplicity of the aquifer system response in Nansemond allowed for an approach that facilitated education in the use of ModelMuse beta software. The simpler model could then be adapted and added to as necessary for the more complex Suffolk model. The trial and error calibration of the parameter values for the model in Nansemond was applied to the Suffolk model as a baseline and differences could be identified more easily for comparison purposes. Pope and Burbey (2004) estimated parameter values that were the same for both the Suffolk and Franklin sites. These were successful at estimating the historical compaction between 1900 and 1995. However, inspection of the measured compaction at the two sites between 2017 to 2020 suggested that these parameter values in Nansemond could require adjustment. Namely, due to the lack of inelastic compaction in Nansemond and the clear seasonality of the inelastic response in Suffolk, it became clear that either the hydrogeology or the stress history was different at Nansemond from the Suffolk and Franklin sites.

The values selected for adjustment included the non-recoverable specific storage of the fine-grained interbeds (S'_{skv}), the coarse-grained recoverable specific storage (S_{ske}), the coarse-grained recoverable specific storage in the fine-grained interbeds (S'_{ske}), and the vertical hydraulic conductivity (K'_v) to match each observed borehole extensometer record.

Preconsolidation stress is important for model calibration due to the potential affect it can have on the transition between the elastic specific storage and the inelastic specific storage of the fine-grained materials (S'_{ske} to S'_{skv}). The preconsolidation stress only affects the total magnitude of compaction rather than the slope of a compaction record during the time of the active extensometer recordings. While this is useful, it is less important than those parameters that control the slope of the compaction record. S'_{skv} was the primary parameter for simulating the total magnitude of compaction. Preconsolidation stress values for this study were approximated because no available data existed to describe changes in preconsolidation stress with depth at either site. However, Pope (2002) estimates that the initial value of preconsolidation stress was exceeded in the Potomac aquifer decades before 1995. Preconsolidation stress value inputs are approximately predevelopment heads simulated by Heywood and Pope (2009). For this reason, preconsolidation stresses are exceeded from the first stress period of the model.

The values of thicknesses for each CSUB model layer have a significant effect on the simulated compaction results, especially in the fine-grained confining units and interbeds. However, the thickness and depths of model layers are not adjusted with trial and error methods assuming that the geophysical log interpretations made by the USGS are accurate.

Trial and error calibration for each model involved adjusting values for S_{ske} , S'_{skv} , S'_{ske} , K'_v for 12 layers in Nansemond and Suffolk each (4 parameters x 12 hydrogeologic layers = 48 variables). Many combinations of variables can produce the same simulated compaction record that can match the observed record. This is a problem of 'non-uniqueness' that is addressed by Helm (1975). Even when considering a single hydrogeologic unit, the problem of non-uniqueness was still significant due to the relationship between S'_{sk} and K'_v in the stress distribution equation. This report does not quantitatively solve this problem with trial and error methods but future work with inverse modeling and parameter estimation software (PEST) may further reduce uncertainty in the calibrated values provided in this investigation.

For the current investigation, a trial and error calibration approach narrows the range of acceptable parameter values. For example, values of K'_v and S'_{ske} can be constrained by geologic

conditions based on lithology and depth of burial. The trial and error process invokes a stepwise adjustment of the initial values provided by laboratory core samples and aquifer slug tests compiled by McFarland and Bruce (2006) and Pope and Burbey (2004).

Pope and Burbey (2004) used quantitative methods to solve the problem of non-uniqueness at the Suffolk site in order to refine initial parameter values for a new simulation. From these initial values, only small adjustments were made with each model run making it reasonably easy to discard unrealistic or hydrogeologically unreasonable values. For instance, an impractical value of 10^{-9} m/day for K^*v of an unconsolidated sediment. This qualitative approach to reducing uncertainty does not neglect the possibility of other reasonable combinations of parameter values that yield a calibrated model but the usefulness of these models is to achieve at least one reasonable calibration within a plausible geologic range until inverse modeling can further reduce uncertainty.

The parameter values of the calibrated Nansemond model were applied to the Suffolk model due to their close areal proximity and similar hydrogeology. However, initial inspection of the Suffolk compaction recorded suggested that additional adjustments could be necessary to explain its significantly different compaction record from that of Nansemond.

The observed compaction record at Nansemond only extends for a three-year period (2018 to 2020) but the historical total compaction is assumed to be similar to that of Suffolk and Franklin as simulated by Pope and Burbey (2004). Hence, calibration of the Nansemond model focuses primarily on the measured compaction from 2018 to 2020. The Suffolk model has two periods of time that are useful for calibration. The first period for calibration uses the same observed extensometer compaction data from Pope and Burbey (2004) spanning from 1982 to 1995 and the second time-frame is between 2018 and 2020 after the Suffolk extensometer was refurbished and reactivated by the USGS. These additional historic data for the Suffolk model proved particularly useful in the investigation of the continuing modern seasonal inelastic compaction that is so different from the clear seasonal elastic response observed in the nearby extensometers in Nansemond and Franklin, Virginia.

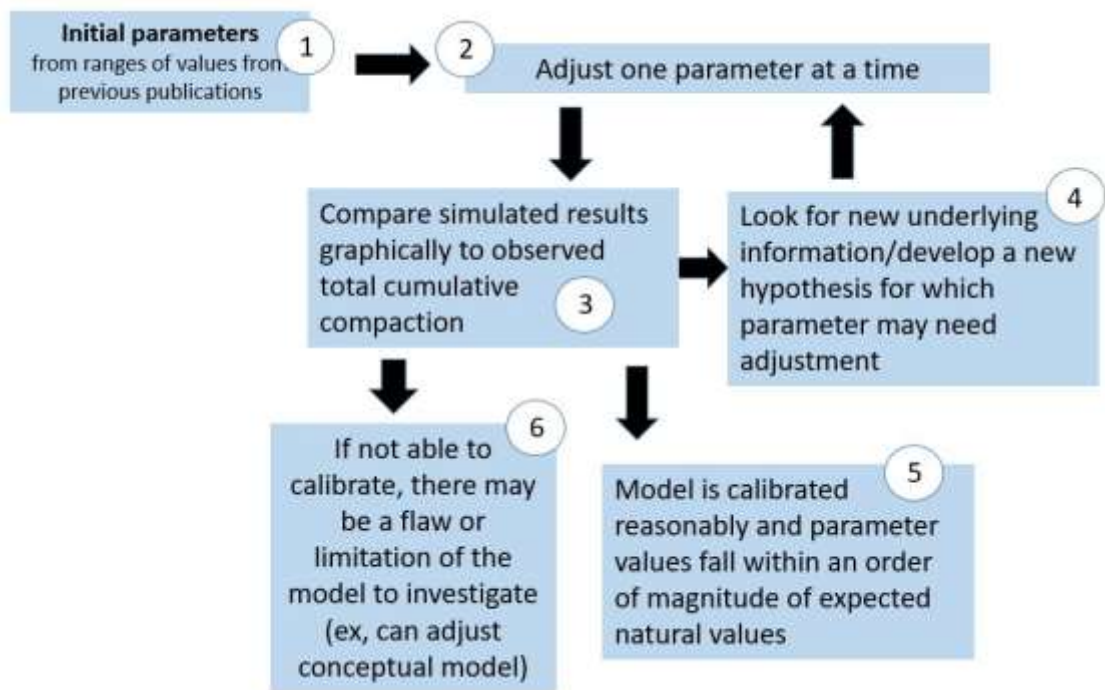


Figure 27. A flowchart describing trial and error calibration of each model to observed cumulative compaction by iterative parameter adjustment from underlying information and hypotheses.

6. Discussion of Data and Model Results

Coarse elastic specific storage (S_{ske}) values in the aquifer units were important for calibrating the short-term record; specifically with regards to the seasonal elastic response of the aquifer system to changes in stress. The short-term head changes were simple to observe in the measured compaction record and S_{ske} for the Potomac aquifer in Nansmond is calibrated with a higher level of confidence due to the dominant elastic response of the aquifer-system. However, the variations of S_{ske} in the other aquifers were not significantly large enough to be observed in the instantaneous events with short-term head changes. For this reason, identical values were used for the other aquifers and any further constraining of parameters was considered unreasonable to attempt without automated parameter estimation software (eg. PEST).

Inelastic specific storage values in the fine-grained material (S'_{skv}) were important for overall compaction. Adjustment of this property increases or decreases the linear slope of the simulated compaction record over months to decades. Vertical hydraulic conductivity (K'_v) of the confining units controlled the time for equilibration of surrounding aquifer heads within the confining units and so controlled the long-term slope of the simulated total compaction. A greater value of K'_v would allow equilibration of stress changes to occur faster in a hydrogeologic unit, thus inelastic compaction would occur sooner than a lesser K'_v . This became apparent with the two different observed records at Suffolk whereby adjustment of K'_v of a confining unit would affect the historic simulation but minimally affect the modern Suffolk compaction simulation. The timing of compaction in the fine-grained beds was controlled by K'_v . The value of the vertical hydraulic conductivity of the aquifers would either increase or decrease daily amplitudes of observed simulated compaction.

The models are insensitive to the elastic skeletal specific storage of the aquitards. These values were initially set to $3.3 \times 10^{-6} \text{ m}^{-1}$ and are not adjusted further due to the low level of sensitivity and confidence. It is likely that observed subsidence data is necessary during a more sustained period of head recovery to better estimate these values.

6.1 Time Constant Uncertainty

It is not possible to simulate the exact hydrogeology at the site and model decisions intentionally balanced certain aspects of the aquifer-system in order to test a hypothesis. A limitation of the model is that it uses aggregate thicknesses of interbeds that are known to be thin

and numerous within the Potomac aquifer system. Aggregate thicknesses of interbeds are used for model simplicity by CSUB delay beds calculation. A summation of interbeds is helpful in estimating the overall non-recoverable compaction but it increases simulated time constants beyond expected values. This method of simulating interbeds still estimates the overall compaction that would occur within the aggregate thickness if its time constant is still within the model period. However, subsequent calibration to observations has to adjust inelastic skeletal specific storage or vertical hydraulic conductivity unrealistically to achieve calibration. Interbed aggregate thickness within the Potomac aquifer is over 130 meters in the Suffolk site but the interbeds are known to be only a few meters thick at most. For this reason, the inelastic specific storage parameters, vertical hydraulic conductivities, and time-constants are not as accurate within the Potomac interbeds for these simulations as those determined in the confining layers. Even so, it appears as though the time constants of these aggregate thicknesses of interbeds are still well within the model timeframe.

6.2 Franklin Results

At Franklin, -10 mm of overall modern compaction was measured from January 2017 to January 2020 for an average rate of about -3.33 mm/yr. This site is not yet analyzed by numerical modeling but the modern observations are included in the analysis of the aquifer system. The depth of the Franklin aquifer system is 234 meters. Like Nansemond, the signal appears to be predominantly elastic and the overall cumulative subsidence record mirrors the Potomac cumulative changes in water levels. Pope (2002) notes that by 1995 a majority of the simulated compaction was occurring in the Tertiary Potomac confining zone just above the Cretaceous interbeds of the Potomac aquifer. The final consolidation of the thin Potomac interbeds likely occurred between the 1940s and 1970s. Compaction during the 1980s and 1990s was transitioning to occurring in the Potomac confining zone overlying the Potomac aquifer. The lower heads within the Potomac aquifer caused a gradient to form between the upper aquifers and the Potomac whereby leakage occurs from the fine grained clays above the Potomac. Drawdown from pumping easily exceeded the estimated initial preconsolidation stress reaching 73 meters below land surface in the Potomac aquifer.

The historical analysis of Pope (2002) suggests that while drawdown was twice the amount of drawdown in Suffolk during the 80s and 90s, the thickness of the aquifer system is

only half as deep, with half of the thickness of fine-grained sediments. The Potomac interbeds at Franklin are estimated to be 19.3 percent of the Potomac aquifer system while the Potomac aquifer system at the Suffolk site is estimated to have 26 percent fine-grained interbeds.

Figure 12 shows that water levels have since recovered to between 30.5 to 24.4 meters below land surface when withdrawals declined in Franklin from 2009 to 2010. Much of the 24 millimeters of compaction that was measured between 1979 and 1995 rebounded as water levels recovered by over 30.5 meters (effective stress decreased). Before the USGS refit the Franklin extensometer it was observed that the extensometer rod secured to the weighted tensioner was bent away from the weighted tensioner. When rebound occurs at an extensometer the distance between the recorder and the bedrock increases, resulting in the weighted tensioner being pulled by additional tension that pushes outwards on the extensometer pipe. Figures 28 and 29 show the result of land surface recovery on the extensometer pipe and the weighted tensioner at Franklin. Photographic analysis estimates that 27 mm of recovery occurred between two pictures taken between November 4, 2002 and October 26, 2015 (David Nelms, personal commun., U.S. Geological Survey, 2021). It is likely that other parts of the aquifer system on the Southern Virginia Coastal Plain would respond the same way if pumping in the Potomac aquifer were to cease. Pope (2002) estimated that 47 mm of compaction that has occurred in Franklin was due to elastic compaction of the aquifers. It is likely that if water levels recover further that 20 mm of that measured land subsidence or more can recover.

Pope (2002) estimated that the thin interbeds of the Potomac equilibrate with time constants between a few months and a few years. It is possible that the Potomac confining zone has equilibrated and that head decline may have even consolidated the (meters) upper fine-grained confining units by 2020. On this condition, a dominant elastic response of the Potomac aquifer is expected. It seems unlikely that any significant non-recoverable compaction is ongoing at Franklin from an initial inspection of the observed subsidence and water level data in Figure 20. Yet it may be possible that the fine-grained confining beds above the Potomac are not consolidated and that significant pumping beyond 73 meters below land surface could re-initiate non-recoverable compaction.



Figure 28. Photographic evidence of land surface rebound at the Franklin extensometer site as recoverable compaction happened between 2002 and 2015. Analysis of the photograph estimates 27 mm of recoverable compaction is reversed (David Nelms, personal communication, U.S. Geological Survey, 2019).



Figure 29. Photographic evidence of land surface rebound with the weighted tensioner of the Franklin extensometer site lifting upwards due to increased tension caused by an increase in distance between the land surface and the bedrock with recovery of previous compaction (David Nelms, personal communication, U.S. Geological Survey, 2019).

6.3 Nansemond Results

Current observations of the Nansemond site show -37.1 millimeters of overall compaction (rebound as negative compaction) from March 28, 2018 to January 11, of 2020 for an average rate of about -20.7 mm/yr. The modern recovery of the land surface suggests that the value of S_{ske} of the Potomac Aquifer is the most important parameter for determining the simulated total compaction. The Nansemond model results are informative but require additional explanation when comparing the results to other areas of land subsidence, particularly those commonly studied in the western United States. Knowledge of the limitations and assumptions of the model, as well as the use of underlying information allowed for a plausible understanding of the modern Potomac aquifer system. Figure 30 shows the calibrated results comparing the simulated and observed cumulative compaction. A breakdown of simulated overall compaction into non-recoverable and recoverable strain is provided in Figure 31. A simulated vertical head profile is also provided to show the equilibration of heads through time in Figure 32. The final calibrated parameters are in Table 8 and can be compared to the expected range of parameter values in Table 9. The expected ranges of vertical hydraulic conductivities is determined from published values in McFarland and Bruce (2006). Expected range of skeletal specific storages are from Sneed (2001). The simulated change of storage per model layer is provided in Table 10.

Nansemond Model Layers	K'_v (m/day)	S_{ske} (1/m)	S^1_{skv} (1/m)	S^1_{ske} (1/m)	Time Constant
Columbia Aquifer	5.5	3.3×10^{-6}	----	----	0
Yorktown Confining Layer	4×10^{-6}	3.3×10^{-6}	3.3×10^{-5}	2×10^{-6}	1731
Yorktown Eastover Aquifer	3.2	3.3×10^{-6}	----	----	0
Yorktown Eastover Aquifer Interbeds	3×10^{-6}	3.3×10^{-6}	3.3×10^{-5}	2×10^{-6}	245
St. Mary's Confining Layer	2.7×10^{-6}	3.3×10^{-6}	3.3×10^{-5}	2×10^{-6}	3528
Calvert Confining Layer	2.8×10^{-7}	3.3×10^{-6}	3.3×10^{-5}	2×10^{-6}	73478
Piney Point Aquifer	3.7	3.3×10^{-6}	----	----	0
Chickahominy Confining Layer	9×10^{-7}	3.3×10^{-6}	3.3×10^{-5}	2×10^{-6}	2016
Exmore Matrix Confining Layer	6×10^{-7}	3.3×10^{-6}	3.3×10^{-5}	2×10^{-6}	547
Potomac Confining Zone	1×10^{-6}	3.3×10^{-6}	3.3×10^{-4}	2×10^{-6}	2222
Potomac Interbeds	3×10^{-5}	3.3×10^{-6}	1.3×10^{-5}	2×10^{-6}	14933
Potomac Aquifer	2.4	3.3×10^{-5}	----	----	0

Table 8. The final calibrated parameters for the Nansemond model.

Nansemond Model Layers	Expected Range of K'_v (m/day)*	Expected Range of S_{ske} (1/m)**	Expected Range of S'_{skv} (1/m)**	Expected Range of S'_{ske} (1/m)**
Columbia Aquifer	0.1	$10^{-6} - 10^{-5}$	----	----
Yorktown Confining Layer	$1.2 \times 10^{-3} - 4 \times 10^{-6}$	----	$10^{-5} - 3 \times 10^{-4}$	$5 \times 10^{-6} - 5 \times 10^{-5}$
Yorktown Eastover Aquifer	0.21 - 110	$10^{-6} - 10^{-5}$	----	----
Yorktown Eastover Aquifer Interbeds	$1.9 \times 10^{-4} - 6.7 \times 10^{-4}$	----	$10^{-5} - 3 \times 10^{-4}$	$5 \times 10^{-6} - 5 \times 10^{-5}$
St. Mary's Confining Layer	$8.5 \times 10^{-7} - 1.3 \times 10^{-4}$	----	$10^{-5} - 3 \times 10^{-4}$	$5 \times 10^{-6} - 5 \times 10^{-5}$
Calvert Confining Layer	$2.8 \times 10^{-6} - 3.4 \times 10^{-5}$	----	$10^{-5} - 3 \times 10^{-4}$	$5 \times 10^{-6} - 5 \times 10^{-5}$
Piney Point Aquifer	0.46 - 210	$10^{-6} - 10^{-5}$	----	----
Chickahominy Confining Layer	$9.5 \times 10^{-6} - 3.4 \times 10^{-4}$	----	$10^{-5} - 3 \times 10^{-4}$	$5 \times 10^{-6} - 5 \times 10^{-5}$
Exmore Matrix Confining Layer	$1.1 \times 10^{-4} - 1 \times 10^{-3}$	----	$10^{-5} - 3 \times 10^{-4}$	$5 \times 10^{-6} - 5 \times 10^{-5}$
Potomac Confining Zone	$1.1 \times 10^{-5} - 9.1 \times 10^{-5}$	----	$10^{-5} - 3 \times 10^{-4}$	$5 \times 10^{-6} - 5 \times 10^{-5}$
Potomac Interbeds	$5.8 \times 10^{-7} - 2.5 \times 10^{-5}$	----	$10^{-5} - 3 \times 10^{-4}$	$5 \times 10^{-6} - 5 \times 10^{-5}$
Potomac Aquifer	$6.7 \times 10^{-2} - 100$	$10^{-6} - 10^{-5}$	----	----

Table 9. The expected ranges of parameter values at Nansemond from publications (*McFarland and Bruce, 2006) and (**Sneed, 2001).

Model Layer	Starting Specific Storage (1/m)	Ending Specific Storage (1/m)	Change in Specific Storage (1/m)
Yorktown-Eastover Confining Layer	3.05E-06	1.77E-06	1.28E-06
Yorktown-Eastover Aquifer	1.83E-06	-6.89E-07	2.52E-06
Yorktown-Eastover Aquifer Interbeds	3.05E-06	-1.19E-07	3.17E-06
St. Mary's Confining Layer	3.05E-06	-8.91E-08	3.14E-06
Calvert Confining Layer	3.05E-06	2.48E-05	-2.18E-05
Piney Point Aquifer	3.05E-07	2.61E-07	4.35E-08
Chickahominy Confining Layer	3.05E-06	2.62E-06	4.31E-07
Exmore Matrix Confining Layer	3.05E-06	2.74E-06	3.13E-07
Potomac Confining Zone	3.05E-05	2.59E-05	4.55E-06
Potomac Aquifer	9.30E-07	8.51E-07	7.87E-08
Potomac Interbeds	1.22E-06	7.55E-07	4.64E-07

Table 10. The simulated change in specific storage by the Nansemond model.



Figure 30. Simulated and observed cumulative compaction at Nansemond from 2018 to 2020. Observed cumulative compaction is in blue and simulated cumulative compaction is in red. The difference is a scale of millimeters.

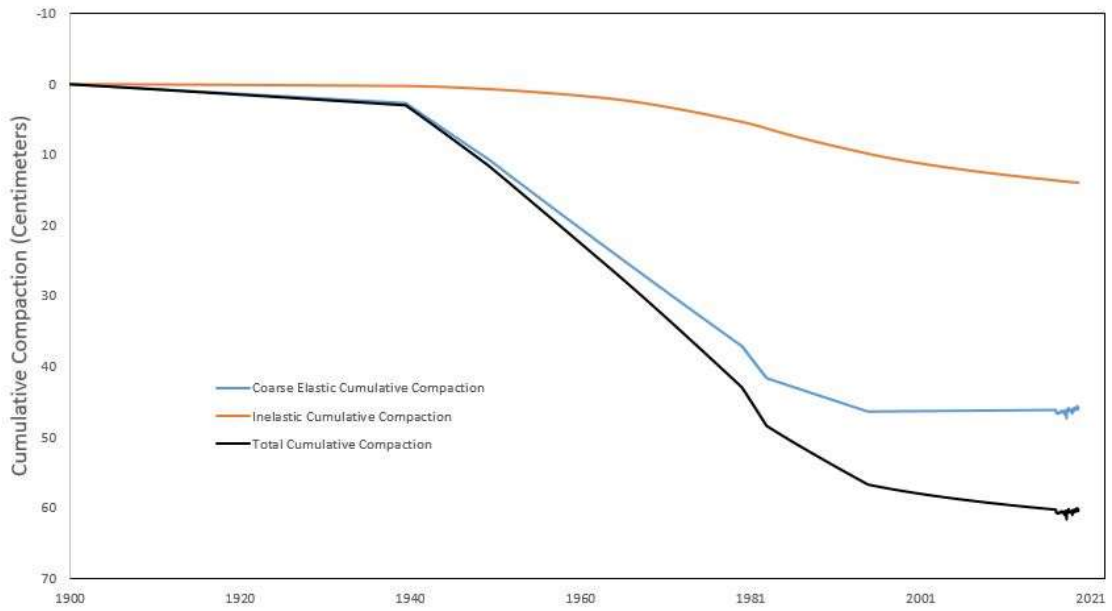


Figure 31. Comparison of simulated compaction at Nansmond for coarse elastic cumulative compaction of aquifers in blue, non-recoverable cumulative compaction in orange, and total compaction in black.

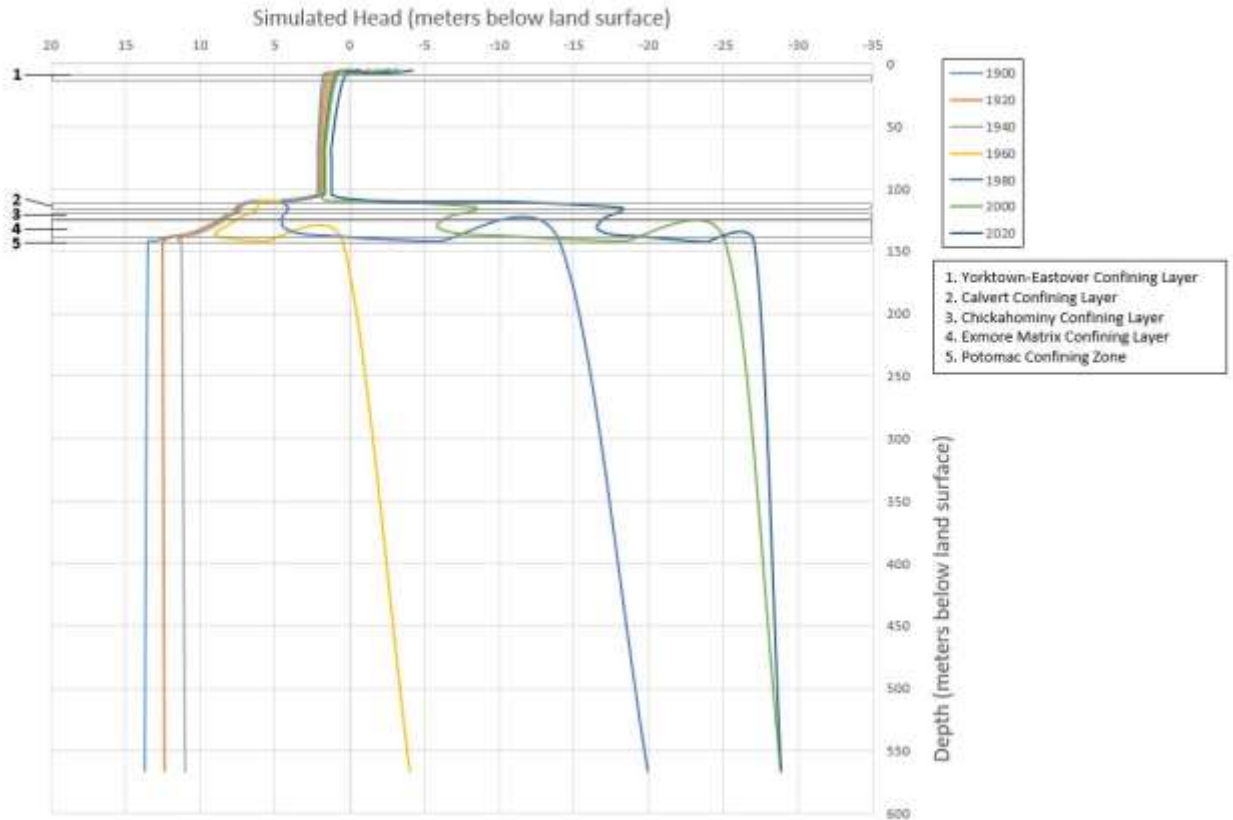


Figure 32. The simulated vertical head profile at Nansemond through time. The combined thickness of delayed beds, labeled 2, 3, 4, and 5, may separate the upper fine-grained layers from drawdown of the Potomac aquifer while also having a low compressibility to slow leakage and subsequent non-recoverable compaction. There is little drawdown simulated in the Yorktown-Eastover aquifer and adjacent St. Mary’s confining unit.

6.3.1 Analysis of Water-Level and Compaction Observations

Initial inspection of the water levels at the Nansemond site shows that effective transmission of stress occurs between the nested wells within the thick Potomac aquifer (Figure 15). Wells 59D 35 and 59D 36 are 131 meters apart vertically in depth but show the same head signal. Well 59D 34 required a saltwater conversion but it clearly shows a significantly different water record even after conversion. This different stress signal suggests that the lower Potomac confining beds are not effectively connected to the upper and middle Potomac due to a laterally continuous confining unit or aquitard that attenuates and delays equilibration. There are similar total drawdowns for all three aquifers but the sensitivity to the signals of short term pumping is less in the lower Potomac (around 541 meters in depth). This lower Potomac water level is not included in order to keep model simplicity a priority. The Upper and Middle Potomac water levels represented by well 59D 35 are sufficient to simulate the dominant seasonal elastic response of the aquifer system.

Figures 14 and 16 show the development of the Nansemond injection well screened within the Potomac aquifer, which is not observed in the Piney Point aquifer as of August 2018. This suggests that a significant disconnect occurs between the two aquifers even while there is good continuity within the upper and middle Potomac aquifer.

Comparison between the Upper and Middle Potomac water levels shows remarkable similarity to the Nansemond compaction record. This suggests that a dominant seasonal elastic response occurs through the great thickness of the Potomac aquifer. It is obvious that the model must simulate the observed seasonal elastic aquifer response that is so similar to the Potomac water levels.

In order for the Nansemond model to have an overwhelmingly elastic response to known changes in stress, with little inelastic response in the simulated modern data, two conditions are necessary. First, there must be little non-recoverable compaction occurring throughout the aquifer system and secondly there must be a strong elastic response in the Potomac aquifer. The first condition for a dominant seasonal elastic aquifer system response requires that there is little non-recoverable compaction occurring in the modern time-period of the Nansemond model. There may be a slight non-recoverable trend of subsidence still occurring at the Nansemond site but it must be small enough that it is not easily detectable in the existing three-year period of record. Calibration to the short-term modern period of observed compaction requires the inelastic

specific storage of all confining units must not be greater than $3.0 \times 10^{-6} \text{ m}^{-1}$. This value is an order of magnitude lower than the 10^{-5} m^{-1} expected for most fine-grained aquitards of similar aggregate fine-grained material thickness (Sneed, 2001; Riley, 1969). While this may not be a typical value of inelastic specific storage for the upper confining beds, it is useful in suggesting that there is not sufficient head decline within the aquitards between the Potomac aquifer and the overlying fine-grained layers to initiate non-recoverable compaction. Additionally, typical inelastic specific storage values are determined in the arid western United States where there are typically persistent head declines that allow models to calibrate the inelastic specific storage parameter with less uncertainty. In these western states, there are limited periods of elastic aquifer response that constrain the calibrated range of elastic specific storage values. The inverse appears to be true in the Virginia Coastal Plain where more confidence exists in estimating the elastic specific storage values in modern periods where the water table has recovered by as much as 30 meters in some locations and there is minimal non-recoverable compaction occurring in comparison to the western United States (Michelle Sneed, personal communication, U.S. Geological Survey, 2021). For this reason, the work of Pope and Burbey (2004) is likely better for constraining the non-recoverable specific storage values and time constants for the Virginia Coastal Plain.

The lack of shallow deformation in response to deeper stress changes in the Piney Point and Potomac aquifers suggests that there are effective confining units between the Piney Point and Potomac aquifers as well as between the Piney Point and Yorktown-Eastover aquifers. The differences in head levels suggests either long time constants of confining beds or insufficient drawdowns. Heywood and Pope (2009) use historical and modern well data to infer that no more than one meter of drawdown has occurred for the overlying Yorktown-Eastover aquifer by 2003. The Piney Point aquifer meanwhile has experienced over 20 meters of drawdown only 55 meters beneath the Yorktown-Eastover aquifer. Finally, the Potomac aquifer has experienced over 30 meters of drawdown. The head gradient across these units suggests that groundwater is leaking downwards from the upper fine-grained material towards the Potomac aquifer and causing most of the water being pumped to come from storage of the confining layers (Pope, 2002). Konikow and Neuzil (2007) estimated that almost 95 percent of water withdrawn from storage in the Virginia Coastal Plain came from the fine-grained confining layers even though water withdrawal is from the surrounding aquifers. The difference in drawdowns suggests that the

vertical hydraulic conductivities of the marine clays above the Piney point might be even less than previously estimated.

The second condition for the model simulated cumulative compaction to match the observed cumulative compaction requires a minimum elastic specific storage of $3.05 \times 10^{-5} \text{ m}^{-1}$ in the Potomac aquifer layer. This value is larger than the typical published coarse skeletal specific storage values found in similar environments, but it is still within the maximum expected range of skeletal specific storage for an aquifer in unconsolidated aquifer systems (Sneed, 2001). This large value of elastic specific storage in the Potomac aquifer also may cause the simulation to overestimate the total compaction for the 120-year simulation period.

6.3.2 Possible Consolidation of the Potomac Interbeds and Potomac Confining Zone

Total compaction of the Nansemond model was not sensitive to vertical hydraulic conductivity changes in the Potomac confining zone and the Potomac interbed layers. Adjustment of K'_v in these two layers did not increase or decrease non-recoverable strain occurring in late time and did not affect the overall compaction. Even the additional delay that a lower vertical hydraulic conductivity of $2.8 \times 10^{-7} \text{ m/day}$ simulates still allows equilibration to occur within the fine-grained material of the Potomac aquifer and Potomac confining zone within the constraints of preconsolidation stress and the 120-year period of effective stress increase due to groundwater pumping.

This suggests that the model is either (1) predicting complete consolidation of the Potomac interbeds and the Potomac confining zone, whereby no additional non-recoverable compaction can occur or (2) the decreased rate of pumping within the last 40 years has successfully decreased the effective stress sufficiently that additional drawdown is needed to restart non-recoverable compaction. The thin aquitards within the Potomac aquifer are likely consolidated due to their smaller average thickness or a few meters. Pope (2002) estimated that these interbeds were completely consolidated by 1995.

6.3.3 Time Constants and Constraining Vertical Hydraulic Conductivity

The model is able to simulate the observed lack of connection between the three aquifers with vertical hydraulic conductivities that are below the estimates compiled previously by McFarland and Bruce (2006). An inspection of the model hydrogeology for the Nansemond model shown in Table 4 indicates that the aggregate thickness of the confining units between the

Piney Point aquifer and the Yorktown-Eastover aquifer is 44.8 meters. Decreasing vertical hydraulic conductivity values to limit drawdown between the Piney Point aquifer and the upper fine-grained aquitards is effective but perhaps not realistic. McFarland and Bruce (2006) estimated that the Saint Mary's confining unit and the Calvert confining unit have some of the lowest vertical hydraulic conductivities in the Virginia Coastal Plain (between 10^{-7} and 10^{-6} m/day). The model successfully predicted a lack of non-recoverable compaction in the fine-grained material above the Piney Point by using a vertical hydraulic conductivity of 2.8×10^{-7} m/day in the Calvert confining unit that separates the large drawdowns of the Piney Point aquifer from the lesser drawdowns of those layers above it. However, this value of K'_v for the Calvert confining unit produces a time constant of over 200 years that is not likely feasible. The model approach appears limited in producing an appropriate separation of aquifers without low K'_v values. This could be attributed to the one-dimensional model constraints in a three-dimensional system.

The impact crater sediments represent the confining units between the Potomac aquifer and the Piney Point aquifer and are identified as the Exmore matrix and Chickahominy confining units. These impact crater sediments are known to have low vertical hydraulic conductivities associated with tilting that may not be observed in laboratory analysis (Jason Pope, personal communication, U.S. Geological Survey, 2021). This underlying knowledge allowed for model adjustment of the vertical hydraulic conductivities in these impact crater layers due to their impermeability laterally, especially if the beds tilt in blocks at this location as described by McFarland and Bruce (2006).

Time constants can constrain plausible vertical hydraulic conductivity values by balancing the initial observations of the subsidence records and the head observations suggesting a separation of aquifers. The published values of McFarland and Bruce (2006) would typically allow for equilibration of aquifer heads but did not simulate the observed heads in the aquifers at the end of the model period. Therefore, vertical hydraulic conductivities are lower than most published values to preserve disconnection of aquifers where necessary. The time constants and final vertical hydraulic conductivity values are in Table 8. Equation 17 illustrates that a balance exists between the vertical hydraulic conductivity and the specific storage of the aquitards when aquitard layer thicknesses remain unchanged.

The similarity between the deeper Potomac aquifer water levels, the indifference of the model to changes in K'_v in the Potomac aquifer, the elastic response, and the lack of continuing non-recoverable compaction suggests that the Potomac interbeds are consolidated within the 120-year period. The maximum time constant for the Potomac interbeds is therefore 120 years or less.

The successful use of low vertical hydraulic conductivities in the upper confining units could suggest that the dominantly seasonal elastic response may not only be associated with consolidation in the fine-grained material of the Potomac aquifer and Potomac confining zone. It is possible that the elastic response is related to longer head equilibration in the upper fine-grained material due to reduced vertical hydraulic conductivity. If this prediction is correct then there will be continued small rate of non-recoverable compaction that is not readily observed in a time-period less than the five years of modern extensometer records.

6.3.4 Coarse Elastic Compaction Overestimation and Model Limitations

The model-simulated ratio of coarse elastic strain to inelastic strain calculated by the Nansemond model also requires further explanation. Figure 30 shows that the model is simulating a majority of compaction occurring in the coarse sediments of the Potomac aquifer while normally the majority of compaction in an aquifer system comes from the non-recoverable inelastic strain of fine-grained interbeds and confining units.

The explanation likely originates from calibration of the Nansemond model to the observed modern seasonal elastic response, which requires an unusually large coarse elastic specific storage value in the Potomac aquifer over the last decade of simulation time. The thickness of the coarse sand and gravel of the Potomac aquifer unsurprisingly affects the compaction of the aquifer system by its proportionally larger ratio in comparison to fine-grained sediments. The magnitude of land subsidence predicted by the model due to the coarse compaction has not been observed. This shows a limitation of the 120-year model in calibrating to a short period of observed cumulative compaction. Parameters are chosen by trial and error to match a short five-year period of observations that are happening during a period of withdrawal declines.

The low ratio of non-recoverable compaction to recoverable compaction may also be due to the low hydraulic conductivity of the overlying impact crater layers prohibiting the expected non-recoverable compaction observed in other confined aquifer systems. The simulated vertical

head profile of the Nansemond site in Figure 31 indicates that the heads have not declined in the clays above pumped aquifers in the same way as in other environments such as that described by Pavelko (2004). The simulation of the aquifer system at the Lorenzi site in Las Vegas by Pavelko (2004) estimated 10 to 20 meters of head decline in the aquitards between pumped aquifers experiencing a similar drawdown of 90 or more meters over a period of 100 years. The Nansemond simulation estimates less than a few meters of head decline in those Tertiary layers above the Piney Point aquifer, namely the thick St. Mary's confining layer and the Yorktown-Eastover confining layer.

The parameters simulated by the model of Pope and Burbey (2004) are probably more accurate for estimating the time constants and inelastic specific storage values for the aquifer system because it was calibrated to observations during a period of persistent head decline. Modern model calibration is likely more accurate in constraining the elastic skeletal specific storage.

Future use of PEST may reduce uncertainty but it may not be as effective as trial and error methods using underlying expert information. For this modeling effort, the total land subsidence due to aquifer system compaction is not accurate. More work is necessary to confirm that the model can either update model properties in periods of head decline or head recovery.

6.4 Suffolk Results

At Suffolk, 50.2 mm of compaction was measured from April 1983 to October 1994 for an average rate of 4.39 mm/yr. Modern observations record 2.3 mm of compaction from March 2018 to April of 2020 for an average rate of 1.56 mm/yr. The decrease of compaction rate suggests that there are fine-grained delay beds that have ceased compaction, which implies that the slower rate of drawdown in the modern period has equilibrated through the fine-grained layers. The Suffolk simulation is successful in estimating the total compaction but the modern seasonal response is not simulated with the same confidence that the Nansemond site is. However, the model is useful in explaining likely dynamics of the aquifer-system. A major point of emphasis for this site is to understand why there is continuing non-recoverable compaction at this site as opposed to the other two. Figures 33 and 34 show the final calibrated simulations to observed cumulative compaction in Suffolk from 1982 to 1995 and from 2017 to 2020. The ratio

of non-recoverable and recoverable compaction at Suffolk is in Figure 35. Finally, the simulated vertical head profile through time at Suffolk is provided in Figure 36.

The final calibrated parameters are in Table 11 and can be compared to the expected range of parameter values in Table 12. The expected ranges of vertical hydraulic conductivities is determined from published values in McFarland and Bruce (2006). Expected range of skeletal specific storages are from Sneed (2001). The simulated change of storage per model layer is provided in Table 13.

Suffolk Model Layers	K'_v (m/day)	S_{ske} (1/m)	S'_{skv} (1/m)	S'_{ske} (1/m)	Time Constant (days)
Columbia Aquifer	5.5	3.3×10^{-6}	----	----	0
Yorktown Confining Layer	9.1×10^{-6}	3.3×10^{-6}	3.3×10^{-5}	3.3×10^{-6}	75
Yorktown-Eastover Aquifer	0.5	3.3×10^{-6}	----	----	0
Yorktown-Eastover Aquifer Interbeds	3×10^{-6}	3.3×10^{-6}	3.3×10^{-5}	3.3×10^{-6}	163
St. Mary's Confining Layer	7.3×10^{-5}	3.3×10^{-6}	3.3×10^{-5}	3.3×10^{-6}	12675
Calvert Confining Layer	3.5×10^{-6}	3.3×10^{-6}	1.6×10^{-4}	3.3×10^{-6}	4500
Piney Point Aquifer	0.3	3.3×10^{-6}	----	----	0
Nanjemoy-Marlboro Confining Layer	3×10^{-7}	3.3×10^{-6}	4.9×10^{-4}	3.3×10^{-6}	358681
Aquia Aquifer	4.6	3.3×10^{-6}	----	3.3×10^{-6}	0
Potomac Clay	1.8×10^{-6}	3.3×10^{-6}	4.9×10^{-5}	3.3×10^{-6}	14062
Potomac Aquifer	2.4	7×10^{-7}	----	----	0
Potomac Interbeds	3×10^{-6}	3.3×10^{-6}	3.3×10^{-6}	3.3×10^{-6}	1133

Table 11. The final calibrated parameters for the Suffolk model.

Suffolk Model Layers	Expected Range of K'v (m/day)*	Expected Range of Sske (1/m)**	Expected Range of S'skv (1/m)**	Expected Range of S'ske (1/m)**
Columbia Aquifer	0.14	10 ⁻⁶ - 10 ⁻⁵	----	----
Yorktown Confining Layer	1.2x10 ⁻³ - 4x10 ⁻⁶	----	10 ⁻⁵ - 3x10 ⁻⁴	5x10 ⁻⁶ - 5x10 ⁻⁵
Yorktown-Eastover Aquifer	0.21 - 110	10 ⁻⁶ - 10 ⁻⁵	----	----
Yorktown-Eastover Aquifer Interbeds	1.9x10 ⁻⁴ - 6.7x10 ⁻⁴	----	10 ⁻⁵ - 3x10 ⁻⁴	5x10 ⁻⁶ - 5x10 ⁻⁵
St. Mary's Confining Layer	8.5x10 ⁻⁷ - 1.3x10 ⁻⁴	----	10 ⁻⁵ - 3x10 ⁻⁴	5x10 ⁻⁶ - 5x10 ⁻⁵
Calvert Confining Layer	2.8x10 ⁻⁶ - 3.4x10 ⁻⁵	----	10 ⁻⁵ - 3x10 ⁻⁴	5x10 ⁻⁶ - 5x10 ⁻⁵
Piney Point Aquifer	0.46 - 210	10 ⁻⁶ - 10 ⁻⁵	----	----
Nanjemoy-Marlboro Confining Layer	6.7x10 ⁻⁷ - 6.1x10 ⁻⁶	----	10 ⁻⁵ - 3x10 ⁻⁴	5x10 ⁻⁶ - 5x10 ⁻⁵
Aquia Aquifer	0.5 - 91.8	----	10 ⁻⁵ - 3x10 ⁻⁴	5x10 ⁻⁶ - 5x10 ⁻⁵
Potomac Clay	1.1x10 ⁻⁵ - 9.1x10 ⁻⁵	----	10 ⁻⁵ - 3x10 ⁻⁴	5x10 ⁻⁶ - 5x10 ⁻⁵
Potomac Aquifer	6.7x10 ⁻² - 100	10 ⁻⁶ - 10 ⁻⁵	----	----
Potomac Interbeds	5.8x10 ⁻⁷ - 2.5x10 ⁻⁵	----	10 ⁻⁵ - 3x10 ⁻⁴	5x10 ⁻⁶ - 5x10 ⁻⁵

Table 12. The expected range of parameters for each Suffolk model layer as published by

*McFarland and Bruce (2006) and **Sneed (2001).

Model Layer	Starting Specific Storage (1/m)	Ending Specific Storage (1/m)	Decrease in Specific Storage (1/m)
Yorktown-Eastover Confining Unit	1.00E-06	5.71E-06	-4.71E-06
Yorktown-Eastover Aquifer	1.00E-05	2.77E-07	9.72E-06
Yorktown-Eastover Aquifer Interbeds	1.00E-05	2.91E-08	9.97E-06
St. Mary's Confining Unit	1.00E-05	-1.69E-05	2.69E-05
Calvert CU	1.00E-05	1.42E-05	-4.21E-06
Piney Point Aquifer	1.00E-06	7.75E-06	-6.75E-06
Nanjemoy-Marlboro Confining Unit	1.40E-04	2.91E-04	-1.51E-04
Aquia Aquifer	6.00E-06	8.19E-07	5.18E-06
Potomac Confining Zone	4.20E-05	9.89E-05	-5.69E-05
Potomac Aquifer	7.00E-07	6.42E-07	5.84E-08
Potomac Interbeds	1.00E-06	9.44E-07	5.65E-08

Table 13. The simulated change in specific storage in the Suffolk model.

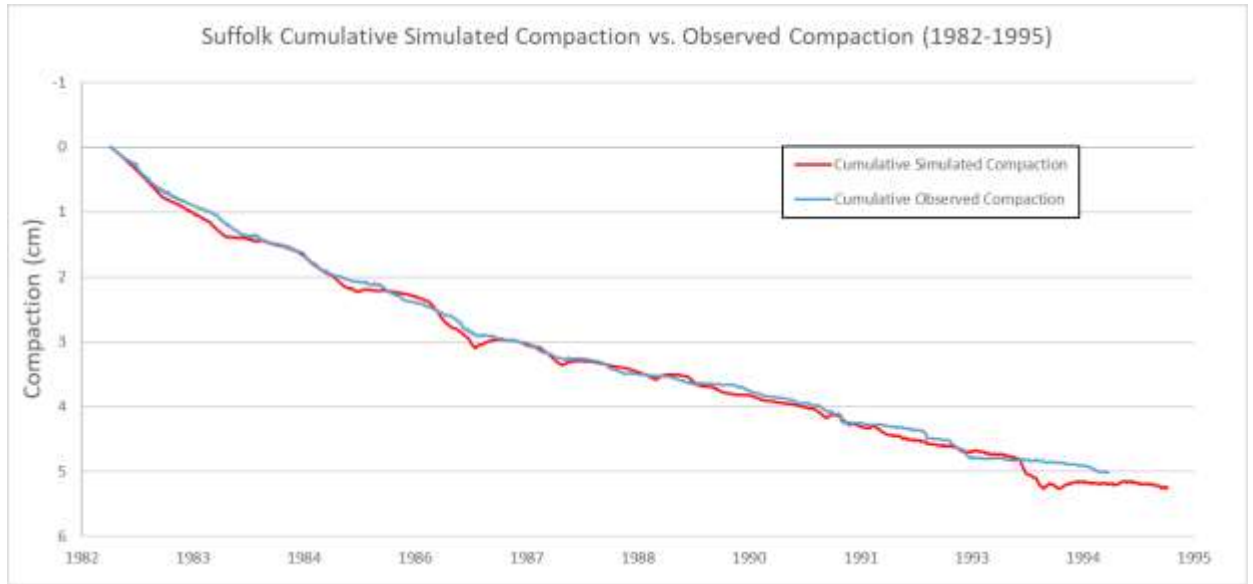


Figure 33. The simulated and observed cumulative compaction at Suffolk from 1982 to 1995.



Figure 34. The simulated and observed cumulative compaction at Suffolk from 2017 to 2020.

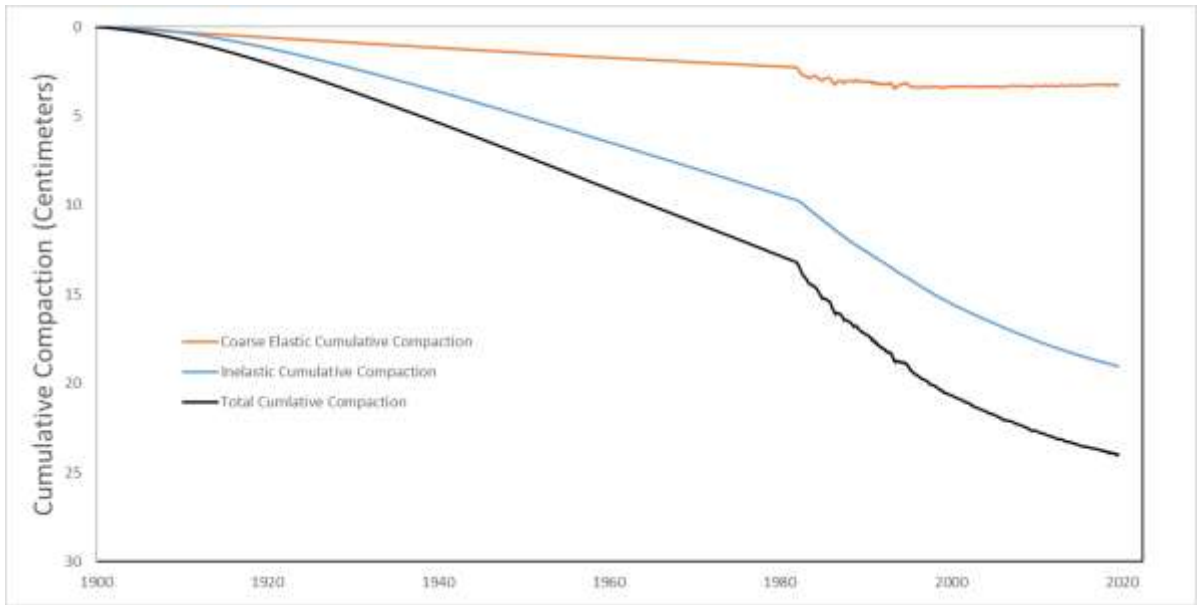


Figure 35. Comparison of simulated compaction at Suffolk for coarse elastic cumulative compaction of aquifers in blue, non-recoverable cumulative compaction in orange, and total compaction in black.

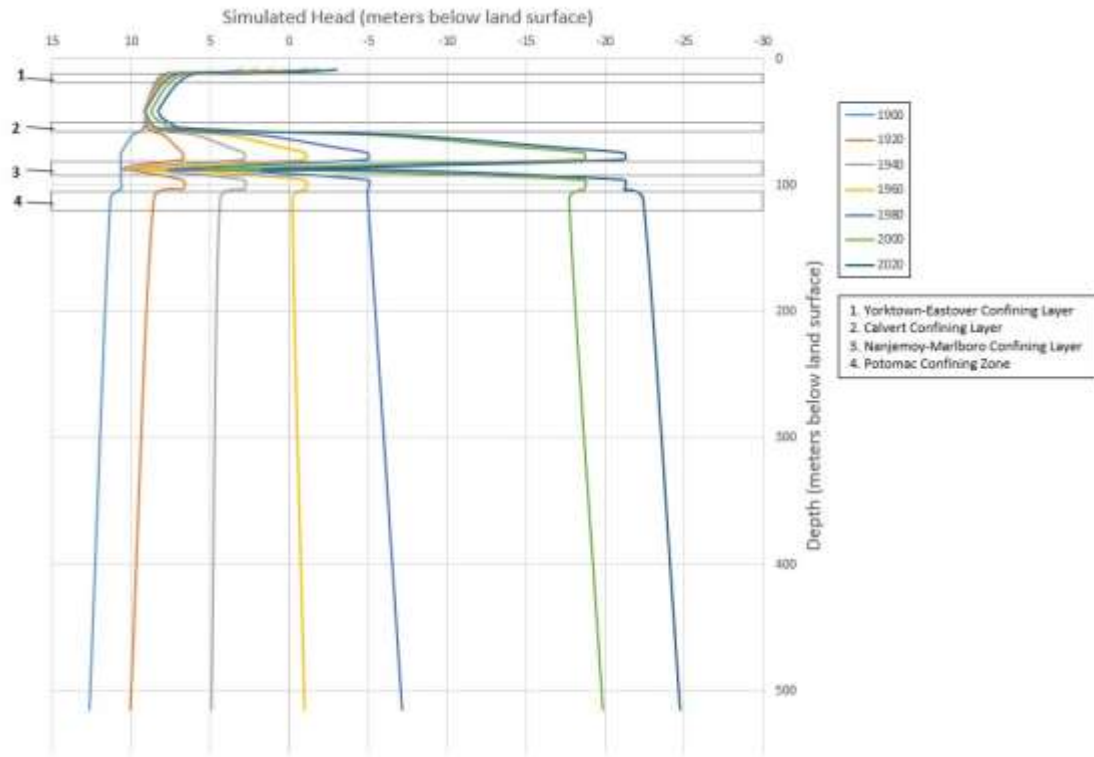


Figure 36. The simulated vertical head profile at Suffolk through time. There is little drawdown simulated in the Yorktown-Eastover aquifer and adjacent St. Mary's confining unit. The Piney Point aquifer is between the Calvert Confining Layer (2) and the Nanjemoy-Marlboro Confining Layer (3). The Aquia aquifer is between the Nanjemoy-Marlboro (3) and the Potomac Confining zone (4). The Nanjemoy-Marlboro Confining Layer has an unrealistic time-constant in the model while balancing head differences in the aquifers and timing of compaction.

6.4.1 Analysis of Water-Level and Compaction Observations

Simulated heads within each aquifer constrains where the continuing compaction may be occurring vertically within the Suffolk aquifer-system. The 2003 simulated drawdowns from Heywood and Pope (2009) within each aquifer around this site are 43 meters in the Potomac, around 15 meters in the Aquia aquifer, 11 meters in the Piney Point, and -1 meter (a meter of head increase) in the Yorktown-Eastover aquifer. This suggests that the site is still very similar to Nansemond with regard to the separation of aquifers by confining units. Large drawdowns in the Potomac aquifer, Piney Point, and Aquia aquifers are similar to the Nansemond site, suggesting that the interbeds within these aquifers have also experienced similar historical changes in stress. For this reason, it could be expected that specific storage values similar to the Nansemond would effectively result in a simulated aquifer-system response requiring a large elastic specific storage to match the modern compaction record. However, the Nansemond elastic skeletal specific storage value overestimates the elastic response of the Suffolk model by an order of magnitude. If the Potomac aquifer is responding similarly to the Potomac aquifer at Nansemond then the seasonal elastic aquifer response attenuates by a continuing long-term compaction and approximately equal inelastic aquifer-system response that may be too complex to estimate using trial and error calibration methods. Even so, the depth and timing of the seasonal inelastic compaction is the focus of the trial and error calibration efforts for Suffolk.

Analysis of the water levels and in conjunction with the hydrogeology of the conceptual models results in a plausible hypothesis to explain why the two extensometer sites located within 20 kilometers of each other could result in significantly different observed subsidence records. The model of Pope and Burbey (2004) used well 58B 269 for the Piney Point and Aquia water level between 1982 and 1995 to effectively simulate corresponding compaction. However, the modern water level data at this location appears to lack the resolution to accurately estimate the modern compaction. It became apparent that the relative change in water levels between the Piney Point at Nansemond and Suffolk is similar despite about 3.5 meters of additional drawdown occurring at the Suffolk site. Figure 37 shows the result of comparison between the modern stress histories of the two sites with an adjusted 59D 37 water level signal offset by 3.5 meters. Well 58B 269 is 5 kilometers from the Suffolk extensometer while well 59D 37 is around 20 kilometers away. However, Figure 38 shows the relative similarity between the modern observed compaction record at Suffolk and the Piney Point aquifer stress history at well

59D 37 in Nansemond. A shift of about 5 months between water levels and the observed compaction record is necessary for alignment but the similarity is significant enough to test with the model. The model was run with this adjusted Nansemond water level to see if it could accurately predict the modern observed compaction record with the thick Nanjemoy-Marlboro confining unit as the anticipated compacting bed. However, the model sensitivity to the Piney Point water level is very low. A similar pattern of stress is occurring in the correct location of the extensometer is likely a major contributor to the observed subsidence record.

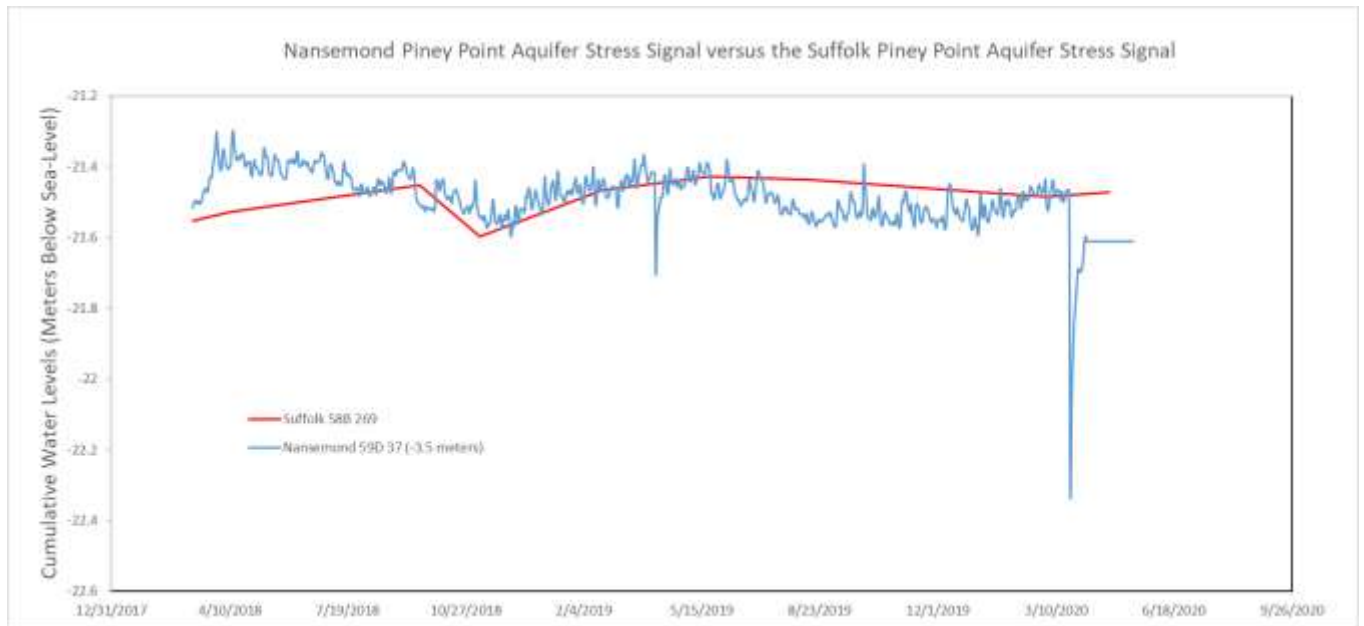


Figure 37. A comparison between the Suffolk Piney Point aquifer water levels and the Nansemond Piney Point water levels. The relative changes with time are significantly similar though the Suffolk water level is 3.5 meters lower than the Nansemond Piney Point water level. An attempt is made to simulate the compaction by artificially lowering the frequently sampled Nansemond Piney Point water level and using the cumulative Nansemond stress history in Suffolk.

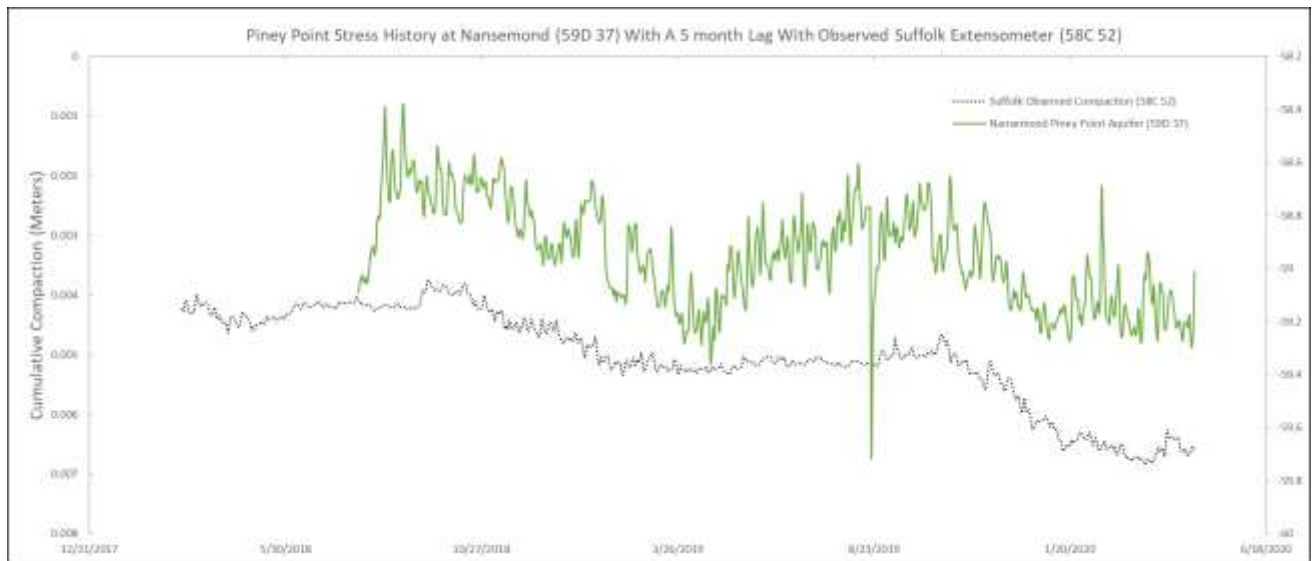


Figure 38. A comparison of the Piney Point aquifer stress history at Nansemond to the observed compaction record at Suffolk 20 kilometers away. A five-month shift in the Nansemond Piney Point aquifer water levels reveals a significant similarity.

6.4.2 Hydrogeology and Stress History Differences

There are two differences between the Nansemond and Suffolk site that may explain the difference in the modern Suffolk aquifer-system response. The first is that the hydrogeology is not the same between the two sites and second, the overall drawdown within the Suffolk aquifers is greater than those at Nansemond.

The impact crater sediments found at the Nansemond site are not found in the Suffolk site. The 15-meter thick Nanjemoy-Marlboro clay is instead located above the Potomac confining zone. The Nanjemoy-Marlboro clay is likely more compactable and leaky than the impact crater sediments found at the Nansemond site. It represents a horizontal barrier to flow but vertical leakage occurs between the Piney Point and Aquia aquifers, both of which are thin at the Suffolk site but have both experienced large drawdowns. The head gradient, however, is similar to the rest of the Virginia Coastal Plain. Hydraulic gradients are moving from the higher heads in the upper aquitards downwards to the lower heads in the Potomac aquifer. The Potomac interbeds and Potomac confining zone likely contribute most of the historical non-recoverable compaction.

Pope (2002) found that the prior simulation of the Suffolk site was insensitive to changes in vertical hydraulic conductivity due to the relatively thin fine-grained units found in the Potomac system. Trial and error adjustment of S'_{skv} in the Potomac aquifer interbeds and Potomac confining zone of this MODFLOW6 model often results in additional compaction in the 80s and 90s but has less of an effect on modern simulated compaction between 2018 and 2020. This suggests the same time constants for equilibrium of past head decline is sufficient by 2018 and the Potomac fine-grained interbeds are no longer experiencing residual compaction. The time-constants of the Potomac interbeds at the Suffolk site that were predicted by Pope (2002) are a few months to years. Additionally, it would suggest that modern compaction is occurring elsewhere, most likely in the model layers above the Potomac confining zone.

Secondly, while the timing of the drawdown in both locations is similar, the Suffolk aquifer system has undergone further drawdown. The Suffolk site is closer to the cone of depression created by the withdrawal center in Franklin. Suffolk was developed heavily in the late 1980s, decades after the heavy development in Franklin. The difference in hydrogeology and a longer period in the cone of depression may explain the difference in the aquifer system response in comparison to that at Nansemond. Additionally, the combination between the timing

of the development of the Potomac aquifer and the estimated thickness of the fine-grained units may explain the continuing non-recoverable compaction occurring in Suffolk compared to Franklin.

At Suffolk, the observed data in two different periods shows that trial changes of inelastic specific storage in the Potomac Aquifer interbeds or the Potomac clay results in changes of simulated compaction in the 1970s and 1990s but not in the modern period. Any increase in the inelastic specific storage in the Potomac Aquifer and the confining bed above it results in more rapid compaction during the 1980s and 1990s, but results in no additional compaction during the modern simulation period. However, increasing inelastic specific storage S'_{skv} in the upper layers above the Aquia aquifer increases the non-recoverable compaction occurring in modern time (2018 to 2020). This supports the idea that the Nanjemoy-Marlboro confining layer and perhaps the Calvert confining layer have begun to equilibrate and compact as they release water downwards into the Aquia or Potomac aquifers. Inelastic specific storage values of $4.9 \times 10^{-4} \text{ m}^{-1}$ in the Nanjemoy-Marlboro confining layer and $1.8 \times 10^{-4} \text{ m}^{-1}$ in the Calvert confining layer are sufficient to cause the simulated average slope to mimic the observed compaction slope of compaction in the modern period. However, the estimated inelastic specific storage values are not accurate for simulating the non-recoverable compaction from 2017 to 2020. The merit of the modern simulated inelastic specific storage values in these upper confining layers is that it shows these layers are likely causing the current modern non-recoverable compaction at Suffolk. The slope of the simulated non-recoverable compaction is an average rate but do not reflect the more accelerated short seasonal declines in land surface between late 2018 and early 2019 or between late 2019 and early 2020. Calibration to these shorter seasonal cycles of non-recoverable compaction was deemed to be too complex and time consuming for trial and error estimation. PEST will likely be helpful for reducing uncertainty in estimating the value of these inelastic specific storage values.

Increasing the coarse elastic storage increases the total compaction, as well as the daily modern elastic response to the stress changes in the aquifers. A coarse elastic specific storage value of $2.3 \times 10^{-6} \text{ m}^{-1}$ was necessary in the Potomac aquifer layer to keep the Potomac water level from dominating the simulated compaction in late time. Larger values of coarse elastic specific storage create a dominant elastic response similar to what was necessary to calibrate the Nansmond model to the observations. It is unlikely that the coarse elastic specific storage

values are low in comparison to the Nansemond site. There are two plausible explanations for the limitation of the Suffolk model in simulating the observations. Firstly, the coarse elastic response of the Potomac aquifer is either not represented accurately in the modern period or secondly an equally strong inelastic response is occurring that is attenuating the seasonal elastic response. Both situations are beyond the ability of trial and error calibration techniques for this report.

The distance between observation wells used for the stress history of the nearby Potomac aquifer has been noted to introduce additional uncertainty to the simulation. Additionally, the subsidence for the 1970s to 1990s is noted by Pope (2002) to lack sensitivity to neighboring water level changes. The expected short-term elastic compaction and expansion of coarse-grained units was not observed. Pope (2002) notes that with deep aquifer systems with limited head data, it is less likely for head screened in short 3-meter intervals to accurately represent the short-term head fluctuations in the rest of the aquifer. If head is not actually transmitted instantly throughout the vertical thickness of coarse aquifers, the simulated compaction will differ from observed subsidence. This limitation may explain the difficulty of simulating the short-term elastic head fluctuations. While this report provides a plausible explanation for the subsidence record at Suffolk, there may be missing stress information within the aquifers that can better explain the observed strain.

7. Conclusions

Over the past 120 years, there has been a prolonged period of groundwater withdrawal from the confined aquifers within the Virginia Coastal Plain that has resulted in declines in hydraulic heads. These head declines contributed to tens of centimeters of total land subsidence since the initial development of the confined aquifers in the 1940s, namely the coarse-grained, thick interbedded Potomac aquifer. The rate of land subsidence in the region is smaller than many other areas experiencing land subsidence due to groundwater withdrawal. However, while the rate of land subsidence has only been millimeters per year, the combined rate of land subsidence and sea-level rise in the Virginia Coastal Plain may be cause for concern. Significant damage is attributed to sea level rise by nuisance flooding in coastal cities like Norfolk, Virginia if there is delayed compaction of fine-grained beds due to past increases of effective stress.

Rates of withdrawal have decreased in the past few decades, causing significant head recovery in the confined aquifers, especially in the Potomac aquifer at Franklin, Virginia. The land surface at Franklin appears to have responded elastically with the increases in head around 2008. However, the Suffolk extensometer observes continued non-recoverable compaction despite the modern decrease in groundwater withdrawal at Franklin. This could be due to delayed release of water from fine-grained confining layers or a slow lateral change in head outwards from the cone of depression at Franklin.

The model of Pope and Burbey (2004) increased understanding of how head decline in confined aquifers resulted in land subsidence by aquifer compaction in the region. The hydrogeology is complex and the modern refitting and installation of a new extensometer at Nansemond provides a good opportunity to reexamine the aquifer system over 20 years later.

The Franklin extensometer is located near the center of the cone of depression. By 1995, it seemed likely that the Potomac aquifer interbeds had equilibrated and consolidated with the overlying Potomac confining zone contributing a major portion of the overall compaction of the system as the withdrawal from the lowermost Potomac aquifer creating a head gradient that makes the overlying fine-grained beds drain downwards. Modern observed land subsidence data shows predominantly elastic compaction that responds to the Middle Potomac head. Image analysis of the extensometer after the head recovery from 2002 to 2015 estimates up to 27 mm or more compaction was reversed. If any continuing non-recoverable compaction is happening it is too small to observe in a short 3 year period of modern subsidence observations. This suggests

that the overlying fine-grained beds have either (1) equilibrated and consolidated or (2) that the recent recovery of heads have ceased non-recoverable compaction until heads decline past the previous minimum. It is uncertain if modern heads in the confined aquifers return to previous observed minimums if non-recoverable compaction will continue.

The Suffolk extensometer is within 20 km to the east of the Franklin extensometer and the cone of depression. Development of the Potomac aquifer was a few decades behind the development around Franklin, Virginia and the aquifer system is twice as thick, with twice the thickness of compactable sediments. A seasonal non-recoverable response is observed with a steady rate of compaction of about 1.5 cm/year. A major focus of this study was to find a plausible explanation for continuing non-recoverable compaction when both Nansemond and Franklin were responding elastically to stress in the Potomac aquifer within 20 kilometers of each other. One-dimensional numerical modeling and analysis of time-series head data in the confined aquifers suggests that the Potomac confining zone and Potomac aquifer interbeds are likely consolidated and the overlying Nanjemoy-Marlboro confining bed or Calvert confining bed are now experiencing non-recoverable compaction between the Aquia and Piney Point aquifers. Time constant calculation is uncertain due to the need to estimate low vertical hydraulic conductivities in the Nanjemoy-Marlboro and Calvert confining beds to simulate the observed separation of aquifers. The difficulty the model has in simulating aquifer separation may be due to a limitation of one-dimensional modeling of a three-dimensional problem. For this reason, it is not certain how long non-recoverable compaction could continue in Suffolk until PEST is utilized to reduce uncertainty.

The observed compaction at the Nansemond site also predominantly elastically responding to the time-series head changes within the Potomac aquifer. There is a separation of aquifers similar to Suffolk where little to no drawdown has happened in the Yorktown-Eastover aquifer while there has been consistent head decline in the Piney Point aquifer for decades. Both the elastic response of the aquifer and the separation of aquifers can be explained and supported by low vertical hydraulic conductivities of the fine-grained Calvert and Saint Mary's confining beds. Likewise, the separation between the heads of the Potomac aquifer and Piney Point aquifer is explained by the presence of impact crater sediments, the Exmore matrix confining bed and the Chickahominy confining bed. It is possible that the impact crater sediments are the primary difference between the Nansemond and Suffolk sites that have prevented Nansemond from

experiencing non-recoverable compaction. At Suffolk, there are perhaps more compactable sediments between the Piney Point and Potomac aquifer in the Nanjemoy-Marlboro confining unit that are draining downwards towards the lower heads of the Potomac aquifer, following the head gradient.

Trial and error calibration is limited in calibrating the parameters of a complex aquifer system with limited subsidence data throughout time. The modeling effort describes dynamics of the aquifer system but realistic parameter values of the hydrogeologic layers are still considered unfinished without having extended modern land subsidence observations or the use of parameter estimation (PEST) to reduce uncertainty.

There are uncertainties in the modeling effort related to (1) simulating a three-dimensional system in one-dimension, (2) attempting to calibrate the models to short-term modern observations, and (3) calibrating a subsidence model to periods of elastic land recovery rather than compaction. The lack of simulated lateral distance for confining units may decrease the effectiveness of confining units, leading to a need for longer time constants and low hydraulic conductivities in the model simulation than may be realistic. Alternatively, the anticipated storage values and vertical hydraulic conductivities for unconsolidated fine-grained beds may not be valid as these properties may have decreased to the point of consolidation lower in the vertical profile.

Attempting to calibrate 120 years of the aquifer system to only three years of observed land subsidence also causes difficulty in calibrating the model appropriately. Most subsidence models are calibrated to longer periods of observed subsidence data and in environments with predominantly non-recoverable compaction. The Nansemond simulation required a large elastic specific storage value in the Potomac aquifer to estimate the observed elastic cumulative compaction at the extensometer; however, this large elastic response applied to the entire 120-year period simulates an amount of total compaction that is an order of magnitude greater than that. The Nansemond model is calibrating to millimeters of observed cumulative compaction in an aquifer system that is 560 meters thick, which is problematic over a short period. Additionally, the inelastic specific storage values of the confining layers are uncertain in the modern simulation of Nansemond due to the lack of observed non-recoverable compaction. Likewise, the coarse elastic specific storage value of the Potomac aquifer in Suffolk is uncertain due to the lack of an elastic response in the Suffolk land subsidence observations. For this

reason, the inelastic specific storage values of the model of Pope and Burbey (2004) are considered less uncertain because the simulation was done during a period of persistent non-recoverable compaction. It is likely that these models are less uncertain in calibrating the parameters of coarse elastic specific storage because the modern observations are within a period of head recovery and are responding to elastic changes in stress. The model is sensitive and dependent on the data set that it is being calibrated to. Despite the limitations of these models, they are useful in explaining which layers may be contributing modern compaction or separating aquifers but longer modern records of land subsidence may be necessary to reduce uncertainty in the aquifer system parameters.

Ongoing efforts include, but are not limited to, modeling the Franklin site and simulating an aquifer system response to proposed simulated injection by SWIFT. Modeling the Franklin site can be useful to see if the calculation of 27 mm of land surface recovery can be supported. Modeling Franklin would also provide an opportunity to calibrate a model to a historical period of persistent inelastic compaction and a modern period of elastic compaction in the same simulation.

8. Bibliography

- Bawden, G.W., Johnson, M.R., Kasmarek, M.C., Brandt, J.T. and Middleton, C.S., 2012, Investigation of land subsidence in the Houston-Galveston region of Texas by using the global positioning system and interferometric synthetic aperture radar, 1993-2000, Report 2328-0328, US Geological Survey
- Brown, P.M., Miller, J.A. and Swain, F.M., 1972, Structural and stratigraphic framework and spatial distribution of permeability of the Atlantic Coastal Plain, North Carolina to New York, Report 2330-7102, US Govt. Print. Off.
- Burbey, T.J., 2001, Storage coefficient revisited: Is purely vertical strain a good assumption? *Groundwater*, 39: 458-464.
- Cederstrom, D., 1939, Geology and artesian water resources of a part of the southern Virginia coastal plain: *Virginia Geol. Survey Bull*, 51: 123-136.
- Cederstrom, D.J., 1941, Ground-water resources of the southeastern Virginia Coastal Plain
- Cederstrom, D.J., 1945a, Selected well logs in the Virginia coastal plain north of James River. Division of Purchase and Printing
- Cederstrom, D.J., 1945b, Geology and ground-water resources of the Coastal Plain in southeastern Virginia. Commonwealth of Virginia, Virginia Conservation Commission, *Virginia Geological Survey Bull*, 63.
- Cederstrom, D.J., 1957, Geology and ground-water resources of the York-James Peninsula, Virginia. U.S. Geological Survey Water-Supply Paper, 1361: 237.
- Clark, W.B. and Miller, B.L., 1912, The physiography and geology of the Coastal Plain province of Virginia. University of Virginia.
- Cooper Jr, H.H., 1966, The equation of groundwater flow in fixed and deforming coordinates. *Journal of Geophysical Research*, 71: 4785-4790.
- Davis, G.H., 1987, Land subsidence and sea level rise on the Atlantic Coastal Plain of the United States. *Environmental Geology and Water Sciences*, 10: 67-80.
- Doherty, J.E. and Hunt, R.J., 2010, Approaches to highly parameterized inversion: a guide to using PEST for groundwater-model calibration. US Department of the Interior, US Geological Survey Reston
- Eggleston, J. and Pope, J., 2013, Land subsidence and relative sea-level rise in the southern Chesapeake Bay region. US Geological Survey Circular, 1392: 30.
- Epstein, V.J., 1987, Hydrologic and geologic factors affecting land subsidence near Eloy, Arizona. Department of the Interior, US Geological Survey Water-Resources Investigations Report 87-4143.

- Fetter, C.W., 2018, Applied hydrogeology. Waveland Press
- Galloway, D.L., Jones, D.R. and Ingebritsen, S.E., 1999, Land subsidence in the United States. US Geological Survey Circular 1182.
- Galloway, D.L. and Burbey, T.J., 2011, Regional land subsidence accompanying groundwater extraction. *Hydrogeology Journal*, 19: 1459-1486.
- Hamilton, P.A. and Larson, J.D., 1988, Hydrogeology and analysis of the ground-water flow system in the Coastal Plain of southeastern Virginia. Department of the Interior, US Geological Survey Water Resources Investigations Report 87-4240.
- Hammond, E.C. and Focazio, M.J., 1995, Water Use in Virginia Surface-Water and Ground-Water Withdrawals During 1992 Fact Sheet FS-057-94. 2.
- Hampton Roads Sanitation District, n.d., The Potomac Aquifer: A Diminishing Resource.
- Hanson, R.T., 1988, Aquifer-system compaction, Tucson Basin and Avra Valley, Arizona. U.S. Geological Survey Water Investigations Report 88-4172.
- Harbaugh, A.W., Banta, E.R., Hill, M.C. and McDonald, M.G., 2000, Modflow-2000, the U. S. Geological Survey modular ground-water model-user guide to modularization concepts and the ground-water flow process. Open-file report. U. S. Geological Survey 2000-92.
- Harsh, J.F. and Lacznik, R.J., 1990, Conceptualization and analysis of ground-water flow system in the Coastal Plain of Virginia and adjacent parts of Maryland and North Carolina. US Government Printing Office. U.S. Geological Survey Professional Paper 1404-F.
- Helm, D.C., 1975, One-dimensional simulation of aquifer system compaction near Pixley, California: 1. Constant parameters. *Water Resources Research*, 11: 465-478.
- Herrera-García, G., Ezquerro, P., Tomás, R., Béjar-Pizarro, M., López-Vinielles, J., Rossi, M., Mateos, R.M., Carreón-Freyre, D., Lambert, J. and Teatini, P., 2021, Mapping the global threat of land subsidence. *Science*, 371: 34-36.
- Heywood, C.E., 2003, Influence of the Chesapeake Bay impact structure on ground-water flow and salinity in the Atlantic Coastal Plain aquifer system of Virginia in MODFLOW and More 2003: Understanding Through Modeling, International Ground Water Modeling Center.
- Heywood, C.E. and Pope, J.P., 2009, Simulation of groundwater flow in the Coastal Plain aquifer system of Virginia. US Geological Survey Scientific Investigations Report 2009-5039.
- Hoffmann, J., Leake, S.A., Galloway, D.L. and Wilson, A.M., 2003, MODFLOW-2000 ground-water model--User guide to the subsidence and aquifer-system compaction (SUB) package, U.S. Geological Survey Open-File Report 03-233.

- Holdahl, S.R. and Morrison, N.L., 1974, Regional investigations of vertical crustal movements in the US, using precise relevelings and mareograph data. *Tectonophysics*, 23: 373-390.
- Jacob, C.E., 1940, On the flow of water in an elastic artesian aquifer. *Eos, Transactions American Geophysical Union*, 21: 574-586.
- Jacob, C.E., 1950, Flow of groundwater in *Engineering Hydraulics*, edited by H. Rouse. John Wiley and Sons, New York.
- Keys, W., 1990, Borehole geophysics applied to ground-water investigations: US Geological Survey Techniques of Water-Resources Investigations, book 2, chap. Chapter E2.
- Konikow, L.F. and Neuzil, C.E., 2007, A method to estimate groundwater depletion from confining layers. *Water Resources Research*, 43.
- Kull, T.K. and Laczniaak, R.J., 1987, Ground-water withdrawals from the confined aquifers in the Coastal Plain of Virginia, 1891-1983, U.S. Geological Survey Water Resources Investigations Report 87-4049.
- Laczniaak, R.J. and Meng, A.A., 1988, Ground-water resources of the York-James Peninsula of Virginia. U.S. Geological Survey Water Resources Investigations Report 88-4059.
- Lofgren, B., 1968, Analysis of stresses causing land subsidence. *Geological Survey Research: B219-B225*.
- McFarland, E.R., 1999, Hydrogeologic framework and ground-water flow in the Fall Zone of Virginia. U.S. Geological Survey Water Resources Investigations Report 99-4093.
- McFarland, R.E. and Bruce, S.T., 2006, The Virginia coastal plain hydrogeologic framework. U.S. Geological Survey Professional Paper 1731.
- Meng, A.A. and Harsh, J.F., 1988, Hydrogeologic framework of the Virginia coastal plain. U.S. Geological Survey Professional Paper 1404-C.
- Pavelko, M.T., 2004, Estimates of hydraulic properties from a one-dimensional numerical model of vertical aquifer-system deformation, Lorenzi Site, Las Vegas, Nevada. US Department of the Interior, U.S. Geological Survey Water-Resources Investigations Report 03-4083.
- Poland, J.F., Lofgren, B.E. and Riley, F.S., 1972, Glossary of selected terms useful in studies of the mechanics of aquifer systems and land subsidence due to fluid withdrawal. U.S. Geological Survey Water Supply Paper 2025.
- Poland, J.F., 1984, Guidebook to studies of land subsidence due to ground-water withdrawal.
- Pope, J.P., 2002, Characterization and modeling of land subsidence due to groundwater withdrawals from the confined aquifers of the Virginia Coastal Plain, Virginia Tech

- Pope, J.P. and Burbey, T.J., 2004, Multiple-aquifer characterization from single borehole extensometer records. *Groundwater*, 42: 45-58.
- Powars, D.S. and Bruce, T.S., 1999, The effects of the Chesapeake Bay impact crater on the geological framework and correlation of hydrogeologic units of the lower York-James Peninsula, Virginia. U.S. Geological Survey Professional Paper 1612.
- Richardson, D.L., 1994, Hydrogeology and analysis of the ground-water-flow system of the Eastern Shore, Virginia. US Department of the Interior, US Geological Survey Water Supply Paper 2401.
- Riley, F.S., 1969, Analysis of borehole extensometer data from central California. *Land subsidence*, 2: 423-431.
- Sanford, S., Clark, W.B. and Miller, B.L., 1912, The underground water resources of the Coastal Plain province of Virginia. University of Virginia
- Sneed, M. and Galloway, D.L., 2000, Aquifer-system compaction and land subsidence: measurements, analyses, and simulations: the Holly site, Edwards Air Force Base, Antelope Valley, California. US Department of the Interior, US Geological Survey Water Resources Investigations Report 2000-4015.
- Sneed, M., 2001, Hydraulic and mechanical properties affecting ground-water flow and aquifer-system compaction, San Joaquin Valley, California. US Department of the Interior, US Geological Survey Open File Report 2001-35.
- Terzaghi, K., 1925, Principles of soil mechanics, IV—Settlement and consolidation of clay. *Engineering News-Record*, 95: 874-878.
- Terzaghi, K. and Peck, R.B., 1948, *Soil mechanics in engineering practice*. John Wiley and Sons, Inc., New York.
- Tiefke, R., 1973, Stratigraphic units of the Lower Cretaceous through Miocene Series, Part 1; Geological Studies, Coastal Plain of Virginia: Virginia Division of Mineral Resources. *Bulletin*, 83: 78.
- Tolman, C.F. and Poland, J.F., 1940, Ground-water, salt-water infiltration, and ground-surface recession in Santa Clara Valley, Santa Clara County, California. *Eos, Transactions American Geophysical Union*, 21: 23-35.